TECHNISCHE UNIVERSITÄT MÜNCHEN

II. Medizinische Klinik und Poliklinik des
Klinikums rechts der Isar

The Role of Insulin Receptor and Insulin-like Growth Factor I Receptor in GEMM-driven Pancreatic Ductal Adenocarcinoma

Evdokia Kalideris

Zusammenfassung

Ziel dieser Arbeit war es, mittels verschiedener Mausmodelle die genaue Rolle des insulinähnlichen Wachstumsfaktor I Rezeptors (Igf1R) und des Insulin Rezeptors (IR) sowie der beteiligten Signalwege in der Initiation und Progression des duktalen Adenokarzinoms des Pankreas (PDAC) zu analysieren. PDAC ist nach wie vor eines der tödlichsten Malignome und um die systematische Therapie zu verbessern ist die Identifizierung neuer Zielstrukturen erforderlich. Rezeptor-Tyrosinkinasen übernehmen eine zentrale Rolle in der Pankreas Karzinogenese. Die Igf1R Tyrosinkinase ist ein wichtiger Mediator der protumorigenen Effekte von IGF-I/II und Inhibitoren des Igf1R Signalweges werden derzeit in zahlreichen klinischen Therapiestudien getestet, allerdings mit limitiertem Erfolg. Des Weiteren sprechen immer mehr Hinweise für eine Assoziation zwischen dem hoch homologen IR und Tumorgenese wie zum Beispiel Hyperinsulinämie als bedeutender Risikofaktor. Um die Funktion beider Rezeptoren in PDAC genauer zu charakterisieren, wurden verschiedene genetisch veränderte Mausmodelle (GEMM) mit pankreas-spezifischer Deletion von IR und Igf1R generiert. Mittels gut etablierten GEMMs, wie z.B. mit einer pankreas-spezifischen Aktivierung des *Kras* Onkogens, können alle Stadien des PDAC, frühe präneoplastische Läsionen bis Karzinome im Endstadium untersucht werden. Die genetische Ablation von Igf1R oder IR im Pankreas von *Kras*^{G12D} Mäusen verursachte interessanterweise eine deutlich Reduktion der Formation von präneoplastischen Läsionen und keine Progression zum invasiven PDAC. Ursache dafür ist eine Notwendigkeit der beiden Rezeptoren für die Proliferation der Läsionen in den frühen Stadien der Tumorgenese. Onkogenes KRAS aktiviert eine Vielzahl von Signalwegen, darunter auch den Raf/MEK/ERK und den PI3K/AKT Signalweg. Analysen dieser nachgeschalteten Signalwege und Expressionsstudien zeigten eine starke Regulation der PI3K Signalkaskade durch Igf1R/IR Hybridrezeptoren. Zusätzlich bestätigen weitere genetische Modelle die Abhängigkeit des PI3K/AKT Pfades von diesen beiden Tyrosinkinasen für die Progression zu PDAC, wobei der Raf/MEK/ERK Signalweg wahrscheinlich eher für die Initiation zuständig ist. Diese Studie trägt daher zur weiteren Charakterisierung des Zusammenhangs der relevanten Signalwege des PDAC bei.

Parts of this thesis were presented on national and international symposia.

Oral presentations

1. "The role of insulin receptor and insulin-like growth factor I receptor in pancreatic ductal adenocarcinoma"
Z Gastroenterol 2013; 51 - K205
DOI: 10.1055/s-0033-1352845
(Annual meeting of the German society for general and visceral surgery (DGAV), September 19-22, 2012, Hamburg, Germany)

2. "Igf1R/IR hybrid receptors regulate PI3K signalling and thus pancreatic carcinogenesis"
 (EMBO Workshop on Liver and pancreas development, function and disease, May 26-30, 2013, Athens, Greece)

3. "Igf1R/IR hybrid receptors regulate PI3K signalling and thus pancreatic carcinogenesis"
(Biochemical Society focused meeting: Signalling and Acquired Resistance to Targeted Cancer Therapeutics, January 05-07, 2014, Cambridge, UK)

Poster presentations

1. "The Role of Insulin receptor and Insulin-like growth factor I receptor in Pancreatic ductal adenocarcinoma"
(AACR conference: Pancreatic Cancer: Progress and Challenges, June 18-21, 2012, Lake Tahoe, USA)

2. "The Role of Insulin receptor and Insulin-like growth factor I receptor in GEMM-driven Pancreatic Ductal Adenocarcinoma"
(2nd international Meeting on Molecular-Based Treatment of GI-Cancer, March 01-02, 2013, Gottingen, Germany)

Own publications

1. The role of insulin and IGF system in pancreatic cancer.
Trajkovic-Arsic M, **Kalideris E**, Siveke JT.
J Mol Endocrinol. 2013 Apr 23;50(3):R67-74.

2. Multimodal Molecular Imaging of Integrin αvβ3 for In Vivo Detection of Pancreatic Cancer.
Trajkovic-Arsic M, Mohajerani P, Sarantopoulos A, **Kalideris E**, Steiger K, Esposito I, Ma X, Themelis G, Burton N, Michalski CW, Kleeff J, Stangl S, Beer AJ, Pohle K, Wester HJ, Schmid RM, Braren R, Ntziachristos V, Siveke JT.
J Nucl Med. 2014 Mar;55(3):446-51.

3. MALDI imaging mass spectrometry for in situ proteomic analysis of preneoplastic lesions in pancreatic cancer.
Grüner BM, Hahne H, Mazur PK, Trajkovic-Arsic M, Maier S, Esposito I, **Kalideris E**, Michalski CW, Kleeff J, Rauser S, Schmid RM, Küster B, Walch A, Siveke JT.
PLoS One. 2012;7(6):e39424.

4. Spatial tissue distribution of erlotinib correlates with survival in GEMM-based pancreatic cancer.
Barbara M. Grüner, Isabel Winkelmann, Annette Feuchtinger, Benjamin Balluff, Nicole Teichmann, Alexander Herner, **Evdokia Kalideris**, Katja Steiger, Irene Esposito, Roland M. Schmid, Axel Walch, Jens T. Siveke
(Manuscript submitted)

5. Igf1R/IR Hybrid Receptors regulate PI3K Signalling and Progression to PDAC
Evdokia Kaliders, Pawel K. Mazur, Barbara M. Grüner, Marija Trajkovic-Arsic, Bence Sipos, Roland M. Schmid, Jens T. Siveke
(Manuscript in preparation)

Table of contents

1. Introduction

1.1 Anatomy and physiology of the pancreas

The pancreas is located in the upper half of the abdomen, between the stomach and the spine. The head of the organ lies in the curve of the duodenum and the tail ends near the spleen (Fig. 1.1 A). The pancreas is composed of two functionally different compartments, the exocrine and the endocrine compartment. The exocrine compartment (acinar) forms grape like structures, which are producing digestive enzymes. These enzymes are secreted into a network of ducts and are transported through it into the duodenum (Fig. 1.1 B and C). The endocrine compartment consists of five different cell types: glucagon secreting α-cells, insulin secreting β-cells, somatostatin releasing δ-cells, ghrelin producing ε-cells and the pancreatic polypeptide secreting PP-cells, which all-together group into islets, the islets of Langerhans (Fig. 1.1 D). The produced hormones are all participating in the regulation of glucose homeostasis and nutrient metabolism [1] [2].
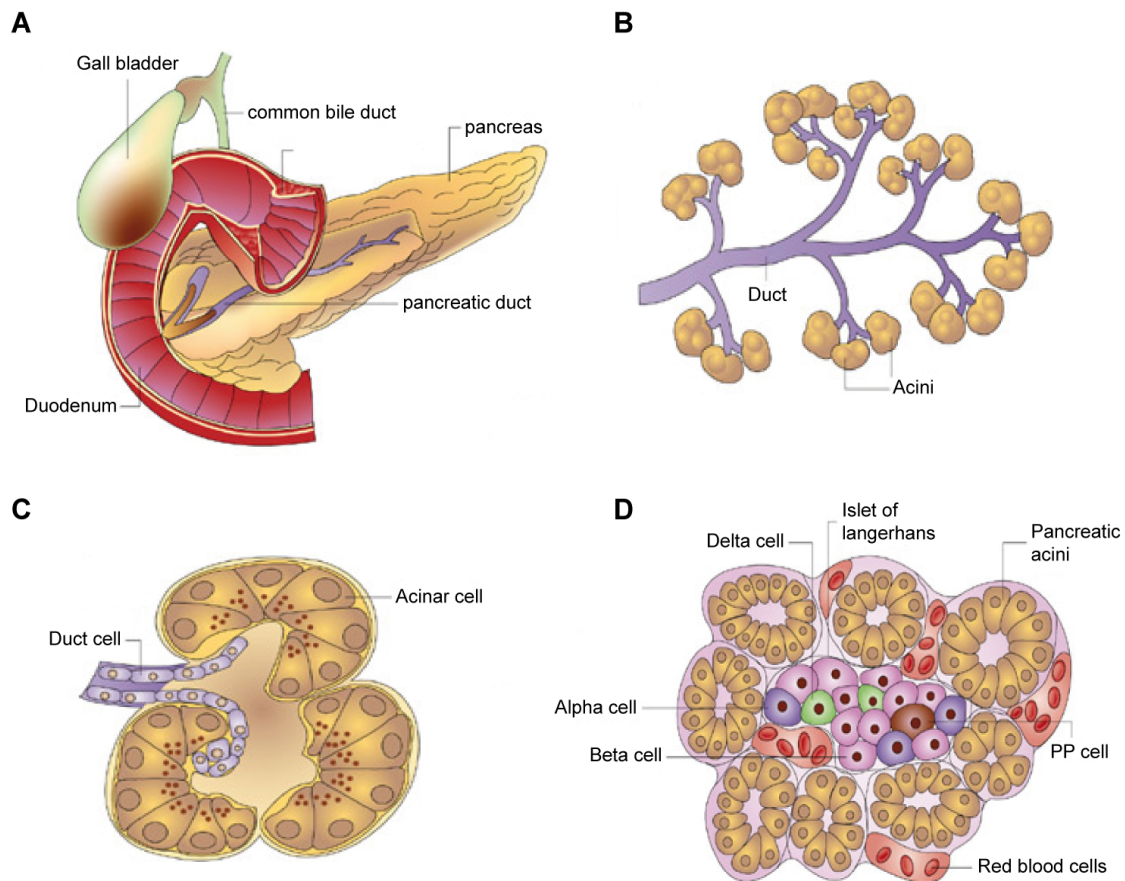
Figure 1.1: Anatomy of the pancreas. Adapted from Bardeesy et al [1].
(A) Gross anatomy and morphological elements of the pancreas.
(B) The exocrine pancreas with the islands of Langerhans.
(C) A single acinus.
(D) A pancreatic islet embedded in exocrine tissue.

1.2 Development of the pancreas

In the mouse, development of the pancreas begins between embryonic day (E) 8.5 and 9.5. At that time point to birth, the cells of the pancreatic epithelium execute a complex program of proliferation, branching, and differentiation that results in the formation of three primary structures: the endocrine pancreas, the exocrine pancreas, and the ductal network [3]. The first pancreatic epithelium specific transcriptions factors that can be detected are Pdx1 and Ptf1a. Both are required to form the dorsal and ventral buds, Pdx1 and Ptf1a knockout mice are unable to develop a matured pancreas [4] [5]. Additionally to these two factors, distinct sets of transcriptional regulators and signalling molecules get stepwise activated and control the progression of the arising organ [6].

Cancer can arise in the head, body or tail of the pancreas. In more than 70% of cases the pancreatic head is the site of origin. A second parameter is the cell compartment, depending on whether the cancer began in the exocrine or endocrine component. Depending on that, several types of pancreatic cancers have been defined [7]. The most frequent types are pancreatic ductal adenocarcinoma (PDAC), endocrine neoplasms and acinar cell carcinoma.

1.3.1   Acinar cell carcinoma

Acinar cell carcinoma is a rare exocrine tumour, accounting only 1-2% of all malignancies of the pancreas. Despite the high rarity of this cancer, affected patients have a poor prognosis, with a 5-year survival rate of 10% and a metastasis rate of 50% at the time of diagnosis. Characteristic for this malignant epithelial neoplasm is an acinar morphology with evidence of pancreatic exocrine enzyme production. Next to a prominent acinar formation without lobular arrangements, the presence of single remarkable nuclei is very typical for that malignancy (Fig. 1.2). All other pancreatic components, like ducts, islets and cytoplasm are absent [8].

1.3.2   Endocrine neoplasm carcinoma

Pancreatic endocrine tumours (PETs) can be ordered in functional or non-functional. While functional tumours produce extra amounts of endocrine hormones, non-functional tumours are not able to do so and cause symptoms by spreading and growing. Due to this, most non-functional PETs are malignant, however PETs are more often functional and have thus a better prognosis. Depending on the endocrine hormones produced, they can be classified in different types, like gastrinoma, insulinoma and glucagoma. Morphological these tumours reflect in shape islets cell characteristics and are very solid (Fig. 1.2) [7].

1.3.3   Pancreatic Ductal Adenocarcinoma (PDAC)

PDAC originates from the exocrine compartments and is by far the most common type of pancreatic malignancy. It is an aggressive and highly lethal malignancy with a 5 year overall survival rate lower than 5% [9]. Although PDAC represents only 3% of new cancer cases, it is the fourth leading cause of malignancy related deaths in humans [10]. Furthermore, it is expected to be the second most cancer-related death in the western world by 2020 due to the extraordinarily high therapeutic resistance, early metastasis and a late possible detection. Almost 80% of PDAC cases have metastasis at the time of diagnosis while only the remaining 20% are resectable and thus potentially curable [11]. This fatal diagnosis has basically not changed during the last 20 years; the only opportunity for improved survival is complete surgical resection for those with localized disease [12]. As opposite to this, intensive research efforts in investigating pancreatic carcinogenesis has broadened our knowledge and many molecular mechanisms essential for PDAC carcinogenesis and its maintenance have been described [13, 14]. However, efficient therapies are missing despite great academic and industrial efforts.

Histologically, PDAC is characterized by the presence of a dense stroma of fibroblast and inflammatory cells, termed desmoplasia. It exhibits a glandular pattern with duct-like structures and varying degrees of cellular atypia and differentiation (Fig. 1.2) [15]. Aggressiveness correlate with the level of differentiation and undifferentiated types offer the worst prognosis. PDAC occurs with high frequency in association with different types of preneoplastic lesions although the cell of origin is unknown. Several studies using experimental animal models suggest that it may derive from acinar cells undergoing ductal reprogramming processes [16] [14].
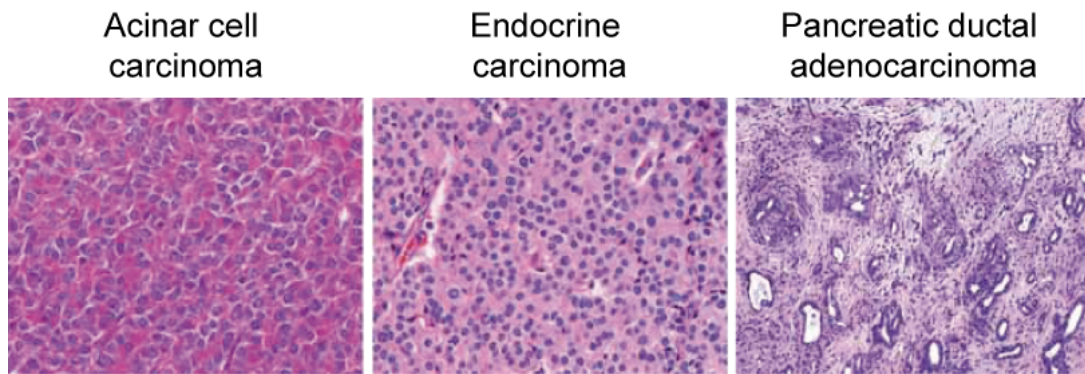
Figure 1.2: Histology of main pancreatic cancer subtypes.

1.3.4 Preneoplastic pancreatic lesions

As already mentioned, PDAC does not develop de novo; it is a multistep progression from precursor lesions to PDAC. The histopathological features and accompanying molecular profiles of these different preneoplastic lesions are well defined. Less common precursor lesions are mucinous cystic neoplasms (MCN) and intraductal papillary mucinous neoplasms (IPMN), while pancreatic intraepithelial neoplasms (PanIN) represent more than 90% of all pancreatic preneoplastic lesions [17] [18].

Several recent lineage tracing studies suggest that premalignant lesions may arise from differentiated acinar cells and/or centroacinar cells in part through a reprogramming mechanism named acino-ductal metaplasia (ADM) [19-21]. Along this process acinar cells react to various stimuli thereby reducing expression of exocrine markers and developing into tubular structures with ductal properties. Thus, centroacinar and/or mature acinar cell may harbor unique properties, leading to pancreatic precursor lesion formation (Fig. 1.3 A).

MCNs are large epithelial cystic lesions that produce mucin and harbour a variable degree of epithelial dysplasia and focal regions of invasion. Characteristic for MCNs is an ovarian-like stroma, expressing progesterone and estrogene receptors. The lesions are usually located in body to tail, and show no communication with the pancreatic ductal system.

IPMNs are non-invasive, predominantly papillary or rarely flat epithelial neoplasms with mucin hyper secretion. They arise from the main pancreatic duct or branch ducts, with varying degrees of ductal dilatation. The clinical

outcome of these precursors shows two subtypes of invasive cancer, typical PDAC and a colloid type [22].

PanINs are by far the most common preneoplastic lesions and associated with high risk PDAC. They are classified into three histologic grades of PanIN1, PanIN2, and PanIN3, depending on the degree of atypia. The early stages exhibit a typical columnar, mucinous epithelium, whereas higher-grade stages are associated with increasing nuclear atypia and architectural disorganization. PanIN1 is a proliferative lesion without nuclear abnormality and subclassified into PanIN1-A and PanIN1-B. PanIN1-A is a flat epithelial lesion composed of tall columnar cells with basally located nuclei and abundant supra nuclear mucins. The small, oval nuclei are oriented perpendicular to the basement membrane. PanIN1-B has papillary architecture, but is otherwise identical to PanIN1-A. First architectural and cytonuclear abnormalities can be detected in PanIN2. These abnormalities may include loss of polarity, nuclear crowding, enlarged nuclei and hyperchromatism. During progression to PanIN3 they obtain increasing amounts of those anomalies and they show cells budding into the lumen of the duct. PanIN3 are considered as so called carcinoma in situ which is the last precursor before PDAC (Fig. 1.3 B) [15] [23]. Next to morphological changes a growing number of genetic alterations of oncogenes and tumour suppressor genes are observed with increasing stage.

1.4 Therapy of pancreatic cancer

Treatment of PDAC suffers from late diagnosis and high treatment resistance. The overall resectability rate is only about 20% and even in these cases the median survival is 17 months due to a high rate of recurrence [24]. For the majority of patients the tumour is too far progressed or metastasized and thus inoperable.

Gemcitabine was the first chemotherapy that has been found to improve the disease-related symptoms and double the survival rate for no more than 18% of the patients [25]. Today's most active protocols are FOLFIRINOX and Gemcitabine/nab-Paclitaxel, which prolong overall survival in patients with metastatic PDAC to 11 and 8.5 months respectively [26] [26].

While these newer protocols over some advantage compared to gemcitabine monotherapy, they are less well tolerated and do not lead to sustained responses. Given this limited efficacy, there is an urgent need for new therapeutic strategies for this disease. Due to the improved understandings of the molecular mechanisms underlying PDAC development, numerous targeted therapies are currently in clinical trials, among them inhibitors for tyrosinkinase receptors.
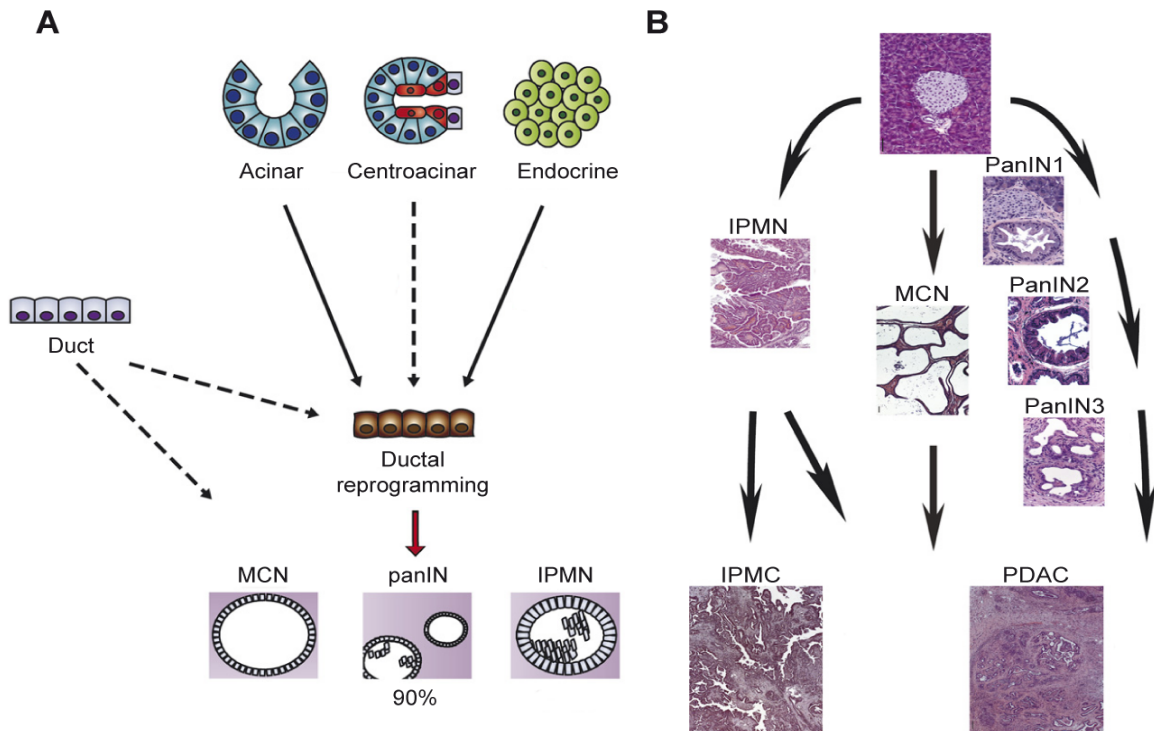
Figure 1.3: Routes to pancreatic ductal adenocarcinoma (PDAC). Adapted from Mazur et al. 2012 [14].
(A) Distinct pancreatic cell lineages can progress to different preneoplastic lesions by KRAS-induced ductal reprogramming. Different subtypes of non-invasive precursors of PDAC have been identified: microscopic pancreatic intraepithelial neoplasia (PanIN), intraductal papillary mucinous neoplasm (IPMN) and mucinous cystic neoplasm (MCN).
(B) A classification system (grades 1-3) for PanINs, which is by far the most common precursor lesion, is based on morphological features including the degree of cell architecture abnormalities and nuclear atypia. Macroscopic (cystic) precursor lesions, IPMN and MCN, are cystic mucinous lesions, of which IPMNs can give rise to invasive IPMN (intraductal papillary mucinous carcinoma (IPMC)), whereas it is thought that all lesions can progress to invasive and metastatic PDAC.

1.5 Molecular signalling pathways in pancreatic cancer

The development of pancreatic cancer is progressive, starting from early preneoplastic lesions and concluding with invasive carcinoma. The various stages of these lesions have been shown to harbour distinct, specific alterations in signalling pathways that remain throughout this tumourigenesis process to have a

cumulative effect. Genome-wide sequencing studies have evolved a molecular landscape with only very common genetic alterations including *Kras* mutations and deletion or inactivation of *INK4a/ARF*, *p53* and *SMAD4* (Fig. 1.4 A). Besides these common alterations, a myriad of additional alterations have been identified in individual cases, leaving a picture of high heterogeneity as a likely cause for the high intrinsic resistance to therapeutic approaches. Furthermore, increased growth factor receptor signalling, activation of developmental signalling pathways, telomere dysfunction and epigenetic silencing are characteristics of invasive PDAC (reviews covering the topic [15] [1] [27] [16]). In the next chapter a small overview and description of the most prominent mutations underlying PDAC development will follow.

1.5.1 P16 and p19

INK4a and *ARF* are two tumour suppressor genes, encoded on the same chromosomal locus via distinct first exons and alternative reading frames. Many pancreatic cancers harbour a homozygous deletion of this locus and its respective protein products p16^{INK4a} and p19^{ARF}. Especially loss of p16^{INK4a} function, through mutation, deletion or promoter hypermethylation occurs in 80-95% of PDAC [28]. P16^{INK4a} inhibits phosphorylation of the retinoblastoma protein (Rb), thereby blocking entry into the S phase of the cell cycle. P19^{ARF} stabilizes p53 by inhibiting its MDM2 dependent proteolysis. Under normal conditions *INK4a* is regulated by environmental stress, age and aberrant proliferative signals associated with senescence. Cooperation between activated *Kras* and the loss of *INK4a* has been observed in PDAC animal models, so there must be a selective pressure after KRAS activations for mutation in the *INK4a/ARF* locus [29].

1.5.2 P53

In more than 50% of PDACs the *p53* tumour suppressor gene is mutated, mostly by a missense alteration of the DNA-binding domain [30]. P53 is the guardian of the genome, conserving stability by preventing genome mutations

and consequently implicated in diverse types of human tumours. On the one side it functions as transcription factor for specific genes and on the other side as inhibitor of transcription of certain genes. The outcomes of *p53* expression and regulation are G_1 arrest and apoptosis. Thus, loss of *p53* function could serve to enable the growth and survival of cells harbouring procarcinogenic chromosomal aberrations as it is usually seen in PDAC. *P53* mutation appears in higher grade PanINs, where the selective pressure to eliminate *p53* is enormous and may stem in part from a collective accumulation of genetic damage [31].

1.5.3   SMAD4

SMAD4 inactivating mutations are far more common in PDAC than in other cancer types, with more than 50% incidence [32]. This tumour suppressor gene encodes a transcription factor that is a central effector of the transforming growth factor-β (TGF-β) signalling pathway. It is well known that TGF-β signalling has growth and survival inhibitory effects on epithelial cells through modulation of expression of cell cycle regulator and activation of apoptosis [33]. The tumour suppressor role of TGF-β signalling is underscored by presence of inactivating TGF-β receptor mutations in several cancers. To the contrary, TGF-β can enhance the malignant growth in later stages, promoting tumour cell proliferation, migration and epithelial-to-mensenchymal transition (EMT) [34]. Together, it inhibits carcinoma initiation while promoting the higher-grade advancement and dissemination of established tumours.

1.5.4   KRAS

One of the earliest events in pancreatic tumourigenesis are mutations of the oncogene *Kras,* which is found in 20% of PanIN1 lesion and the incidence increases with progression reaching nearly 100% in PDAC. It has been confirmed by mouse models that *Kras* mutations are an initiating step in pancreatic carcinogenesis. Moreover RNA interference knockdown studies offered also a crucial role of mutated *Kras* for PDAC maintenance [35]. In

healthy cells this GTP-binding protein is responsible for cellular functions like proliferation, differentiation and survival [36]. Activating *Kras* point mutations at codon 12 make the molecule insensitive to GTPase activating proteins and results in a decrease of the intrinsic rate of GTP hydrolysis. Subsequently the oncogenic mutation of *Kras* inhibits its enzymatic activity and results in a constitutively activated molecule that is essentially independent of growth factor stimulations. KRAS activates several downstream effector pathways, which contribute essentially to proliferation, differentiation and cell survival of tumourigenic cells. The two most prominent affected pathways on which oncogenic *Kras* mutations drive tumour dependency are the Raf-mitogen-activated kinase (MAPK) and Phosphoinositide 3-kinase (PI3K) signalling pathways (Fig. 1.4 B).

The MAPK pathway consists of a protein kinase cascade linking growth and differentiation signals with transcription in the nucleus. After activation through different growth factors and tyrosinkinases the MAPK translocate to the nucleus and activates multiple transcription factors by phosphorylation. The most influential of the three MAPK pathways in PDAC is the ERK pathway. It consists of the Raf protein (MAP3K) that phosphorylates MEK (MAP2K), which in turn phosphorylates ERK (MAP1K), which activates multiple cellular functions.

The PI3Ks are a family of proteins involved in the regulations of cell survival, growth, metabolism and glucose homeostasis. AKT is the major downstream effector of the PI3K and phosphorylates numerous enzymes, kinases and transcription factors, producing a wide variety of immediate and delayed effects on cell function. The two most important downstream targets of AKT are the mammalian target of rapamycin (mTOR) and NF-κB. Hyperactivation and misregulation of the MAPK and/or the PI3K pathways are required for malignant transformation. The interaction between those two signalling cascades and the upstream and downstream factors are of central importance for targeted therapeutic strategies [37].

1.5.5 Receptor tyrosine kinases

Receptor tyrosine kinases (RTK) are playing at least a contributively role in all of the previous listed signalling pathways (Fig. 1.4 B). Above that, increasing

evidence points to the involvement of the RTK pathways as major effectors in pancreatic cancer development and as potential targets for intervention. 20 different subfamilies of RTKs are described, which regulate a wide range of functions in normal cells like development, cell and tissue growth, differentiation and interaction. Although the activity of RTKs is tightly regulated in normal cells, malignant cells frequently harbour gain of function alterations in RTKs, leading to the aberrant and excessive activation of downstream pathways [38]. Dysregulation of RTKs is a common feature of numerous cancers and it has been shown to correlate with the development and progression of the different malignancies [39] [40]. While recently the role of EGFR in PDAC development and preclinical therapy has been defined [41], the role of other RTK is less clear. Many RTK inhibitors have been investigated in large clinical trials, however, no clear benefit has been reached with the exception of erlotinib, a small molecule kinase inhibitor directed against the EGFR. Erlotinib has been shown to have a significant albeit limited and thus clinically not relevant benefit in PDAC patients [42]. Obviously, we are still missing essential parts of the tumour's biology.
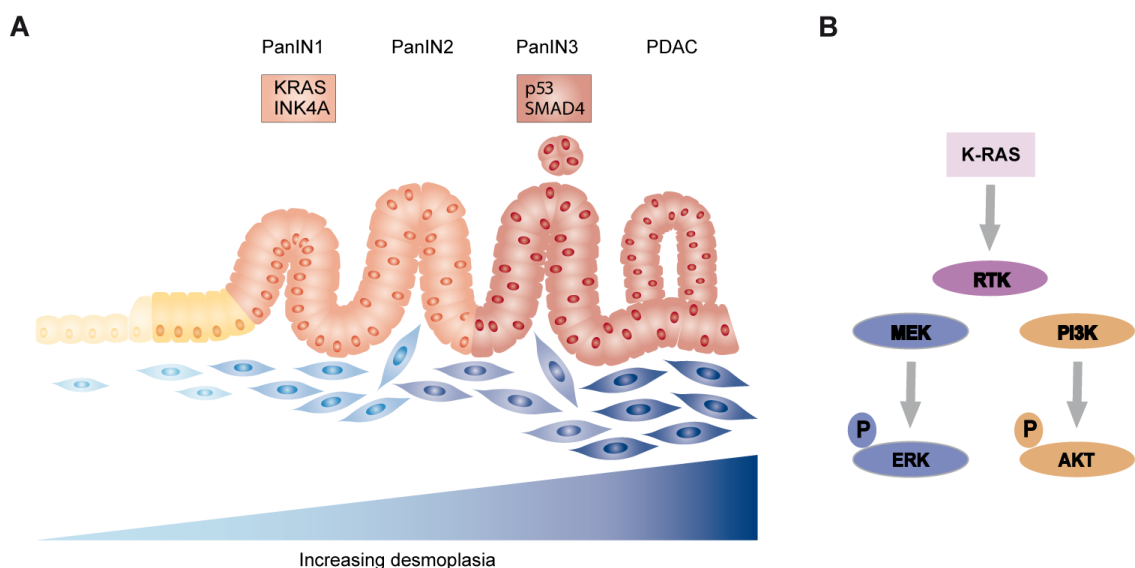
Figure 1.4: Progression model of PDAC. Adapted from Morris et al. 2010 [16].
(A) Constitutively active KRAS is sufficient to initiate the development of PanIN and PDAC. PanINs are classified into three stages of increasing cellular atypia and have been found to possess increasing numbers of mutations (common mutations are indicated in boxes).
(B) KRAS as master regulator of various oncogenic signalling cascades via receptor tyrosine kinases.

1.6 Mouse models of pancreatic cancer

The identification of innovative therapeutic strategies for PDAC heavily relies on the availability of relevant and predictive preclinical models recapitulating the essential features of human PDAC. Numerous in vitro methods and in vivo approaches with xenografts have been used to evaluate novel therapeutic agents, but none of these studies has led to improvement in pharmacological treatment of patients with PDAC. A possible explanation could be the lack of numerous key features of PDAC in these systems, including intratumoural genetic heterogeneity, desmoplasia and spontaneous metastasis. To circumvent many of these disadvantages, molecular cornerstones of pancreatic carcinogenesis have been used to generate a genetically engineered mouse model (GEMM) of PDAC.

A major breakthrough in the research field of PDAC emerged from the development of a GEMM with a conditional Cre/loxP based activation of endogenous mutant *Kras* in pancreatic progenitor cells by Tuveson and colleagues [43]. They used *Pdx1* and *Ptf1a* transcription factors that are expressed in the developing pancreas (see chapter 1.2) to drive expression of Cre recombinase. A stop cassette flanked by loxP sites is silencing the mutated *Kras* allele to prevent ubiquitous expression of the oncogene (*LSL-Kras^{G12D}*). Consequently, this stop cassette can be excised only in cells expressing the Cre recombinase thereby activating permanent expression of oncogenic KRAS in these recombined cells. With this strategy mice recapitulate human PDAC with PanIN lesion development and progression to invasive and metastatic PDAC with increasing age. Negative side effects using the described Cre/loxP approach are the timing and the targeted cellular compartment. The crossing of *Pdx1-Cre* transgenic strains with *Kras^{G12D}* mice results in an activation of mutant KRAS in the pancreas, as well as in organs of the developed foregut (duodenum, stomach) and the epidermis [44]. PTF1a, on the other hand, is expressed in the nervous system including brain, spine and retina. Thus, tumour development can occur in extra pancreatic organs, potentially affecting pancreatic carcinogenesis and responses to therapeutic approaches as well as the life span of respective mice. Moreover *Pdx1-Cre;Kras^{G12D}* and *Ptf1a$^{+/Cre}$;Kras^{G12D}* mice express mutated KRAS during embryogenesis which does not reflect the acquisition of sporadic mutations in adult cells in humans [14]. Nevertheless, as in humans, PDAC develops at an

advanced age of these mice, typically not before 12 months of age despite occurrence of early-grade PanIN lesions starting a few weeks after birth. To analyse additional genetic alterations, several groups generated follow up models with conditional inactivation of established tumour suppressor genes (see chapter 1.5) (Fig. 1.5 C). Conditional loss of the *INK4a/ARF locus* in *Pdx1-Cre*;*Kras*^{G12D} mice led to acceleration of PanIN and tumour development. Characteristic for this mouse model is an aggressive, poorly differentiated and anaplastic PDAC with micro metastasis to liver and lung [29]. Another acceleration of the *Kras*^{G12D} model was achieved by conditional deletion or dominant negative mutation in the *p53* tumour suppressor gene (*p53*^{R172H}) (Fig. 1.5 A). Here, *Pdx1-Cre*;*Kras*^{G12D};*p53*$^{loxP/loxP}$ mice show a more aggressive disease than *Pdx1-Cre*;*Kras*^{G12D};*p53*^{R172H} animals [45] [31]. Inactivation of SMAD4 in a *Kras*^{G12D} mediated background showed a phenotype of cystic lesion development with similarity to human IPMN and MCN [46] [47].

Analysis of these GEMM demonstrated activation of a wide range of effector pathways including the highly activated MEK/ERK and PI3K/AKT signalling cascades [48]. The next step was the use of GEMM to analyse the specific function of these effector pathways of oncogenic *Kras.* Mouse strains with conditional activation of constitutively active MEK1-DD [49] and of PI3K (active p110a^{H1047R} subunit of the PI3K) [50] were generated. These GEMMs show highly consistent development of PanIN and ADM lesions progressing to PDAC, thus photocopying the *Kras*^{G12D} model (Fig. 1.5 B).

Overall, targeting of key genes altered during pancreatic carcinogenesis leads to the formation of various preneoplastic lesions and PDAC, demonstrating the importance of the distinct genes for tumour initiation and formation.
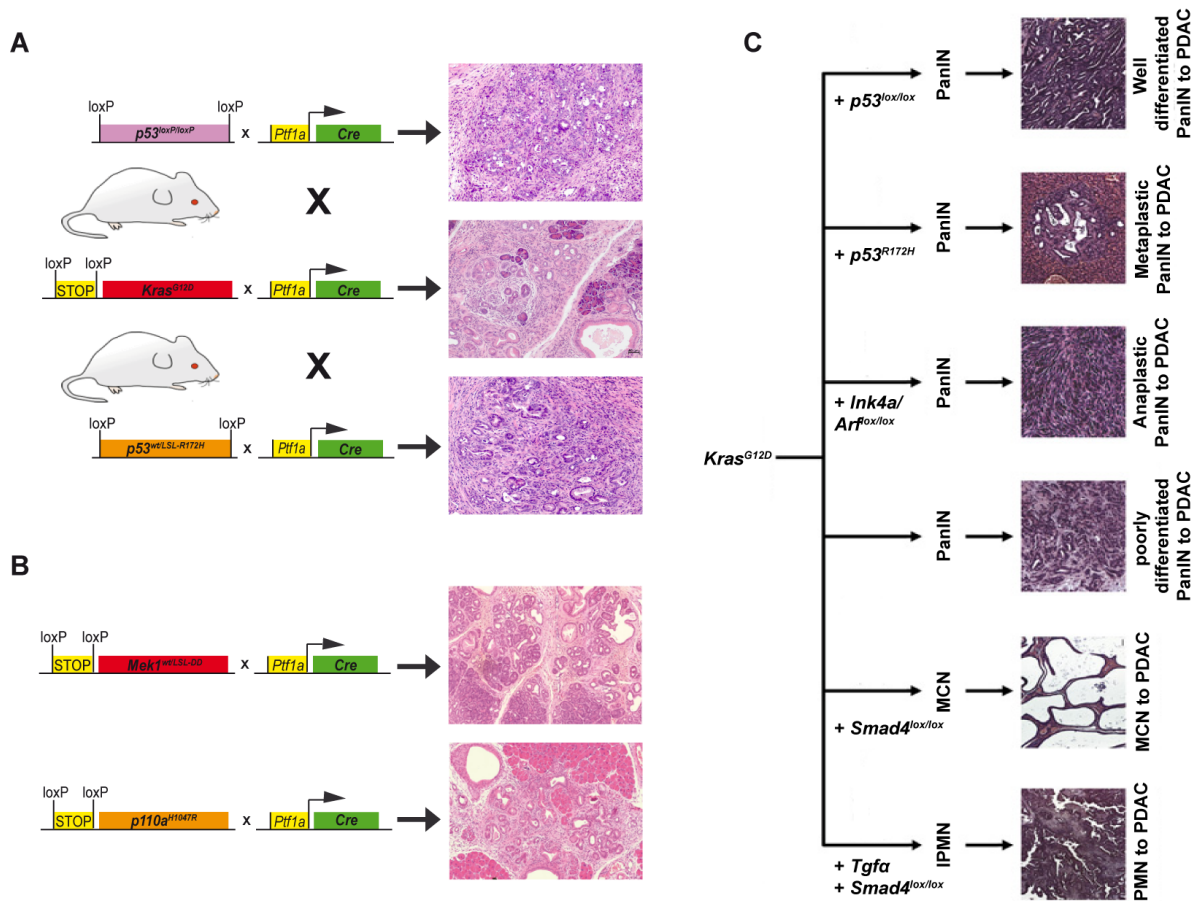
Figure 1.5: Cre/loxP mediated recombination and histological appearance of main murine pancreatic lesions and PDAC.
(A) Schematic representation of Cre/loxP target Kras^{G12D} recombination. Cre/loxP mediated conditional activation or inactivation of genes can be used for targeting oncogenes and tumour suppressors in the pancreas.
(B) Cre/loxP recombination and activation of mutated Mek and p110.
(C) GEMMs develop tumours that resemble different types of human preneoplastic lesions and PDAC with varying latency depending on the induced genetic alterations and cancer evolution. Adapted from Mazur et al. 2012 [14].

1.7 The insulin and insulin-like growth factor I receptor (IR and Igf1R) system

Insulin-like growth factors, IGF-I and IGF-II, and their receptors, Igf1R and Igf2R, have been acknowledged as important players in a variety of cancers. Already twenty years ago the connection between circulating IGF-I levels and risk of cancer was demonstrated [51] [52]. Igf1R is a tyrosine kinase that activates intracellular signalling cascades responsible for cell survival and proliferation, implicating that deregulation of such signalling might lead to establishment of non-regulated cell growth and cancer [53] [54]. Interestingly, Igf1R is found to be overexpressed in many cancers and is thus very appealing as a drugable target

[55] [56]. Despite the initial enthusiasm, virtually all clinical trials with antibodies targeting the Igf1R in many different cancers have failed as no significant clinical improvement was observed upon blocking of Igf1R [57]. One of the potential reasons for failure of Igf1R targeted therapies is the co-existence of the structurally and functionally related insulin receptor (IR). Two insulin receptors exist: IR-B responsible for metabolic actions of insulin and IR-A that is usually found in fetal tissues and interestingly is re-expressed in cancer [58]. IRs and Igf1Rs are members of the same family of transmembrane receptor tyrosine kinases. A high degree of homology is reflected especially in their tyrosine kinase domains that share up to 85% of similarity in amino acids [59].

1.7.1   Structure and function of the IR and the Igf1R

Igf1R and IR have evolved from a common parental family member in primitive organisms and probably the need to regulate cellular glucose uptake independently of cell survival and proliferation led to the evolution of distinct receptors in more complex animals [60]. Both are widely expressed on normal tissues on the cell surface. Both types of receptors have tetrameric structures, characterized by two half receptors, each of which in turn compromises an extracellular α-chain and a transmembrane β-chain. The two half receptors form holoreceptors with a ligand binding α-subunit and an intracellular β-subunit that includes the tyrosine kinase domain. Once their ligands are bound, the receptor tyrosine kinase domains of the holoreceptors are auto-phosphorylated and further promote phosphorylation and activation of downstream effectors [61]. Cells that co-express the two receptor genes offer not only holoreceptors but also hybrid receptors formed by an insulin half receptor and an Igf1 half receptor (Fig. 1.6 B).

Under physiological conditions, IGFs are peptides synthesized mainly by the liver and are major stimulators of tissue and cellular growth [62]. In general, IGFs stimulate proliferation and inhibit apoptosis in target tissues. But it is thought that IGF-II is more important for the early fetal development [63] while IGF-I is necessary for achieving maximal growth [64]. It is generally accepted that IGF-I signalling through Igf1R is responsible for cell growth regulating

actions while Igf2R does not seem to activate intracellular signalling pathways and works rather as a scavenger receptor for IGF-II [65].

Insulin is produced by the Beta cells in the Langerhans islets of the pancreas, is secreted into the blood and regulates cellular glucose uptake as well as uptake of amino and fatty acids. This function of insulin is initiated by binding of an insulin molecule to its prospective insulin receptor on the cell surface resulting in intracellular signalling and membrane expression of glucose transporters. Glucose molecules are then transported into the cell and used for catabolic or anabolic processes with decreasing blood glucose levels being one major effect. In the insulin-secreting organ, the pancreas itself, IR-B is also expressed and, even more importantly, is involved in the autocrine regulation of insulin secretion. Early mouse studies demonstrated that a beta cell specific IR knockout leads to development of progressive glucose intolerance, smaller islets and decreased insulin content as well as a delay in acute insulin secretion from the islets [66]. Insulin however, not only regulates glucose homeostasis in the body but also acts as a growth-promoting factor and as such can contribute to carcinogenesis in many cancers including PDAC [67] [68].

1.7.2   Igf1R system in PDAC

Evidence suggests that insulin and the IGF-I receptor system is intimately involved in development and progression of pancreatic cancer. In PDAC patients, studies have reported an increased expression of Igf1R in the cancer [69] and this has been associated with higher tumour grade and poor survival [70]. Furthermore, increased amounts of IGF-I and IGF binding proteins have also been detected in serum and tissues of PDAC patients [71]. The screening of single nucleotide polymorphisms among the members of the IGF axis in humans results in significant associations between IGF axis gene variants and haplotypes and risk as well as clinical outcome in PDAC patients [72]. *In vitro* experiments showed that exogenously added IGF-I increases the growth of PDAC cancer cell lines and this effect can be blocked by an Igf1R specific antibody [73]. Igf1R exerts antiapoptotic effects and plays a role in proliferation and motility of cancer cells supporting the mitogenic and metastatic role of this molecule [74]. As both IGF-I and Igf1R mRNAs have been found on pancreatic

23

cancer cells in human PDAC tissues, it is also suggested that IGF-I upregulates expression of its own receptor by autocrine or paracrine mechanisms thus enhancing its own growth promoting effects [73].

1.7.3 Insulin receptor system in PDAC

Pancreatic ductal adenocarcinoma (PDAC) develops from the exocrine part of the pancreas, yet the cell of origin is still not known [15]. Exocrine cells are in vicinity of the islets of Langerhans and are thus directly exposed to high insulin concentrations. A complex "insulo-acinar portal system" supplies the exocrine part of the pancreas with blood coming from the islets and thus rich in insulin but also in glucagon, somatostatin and other molecules secreted by the endocrine pancreas [75]. This imposes that the hormones of the endocrine pancreas may regulate functions of the exocrine pancreas. Evidence suggests that insulin regulates both growth and function of the exocrine pancreas as well [76]. Many potential actions of the insulin system in pancreatic cancer have been discovered. In humans with type 2 diabetes, an increase in ductal replication rate that precedes PDAC has been reported [77]. Overexpression of docking peptides that transmit the intracellular activation of the IR, IR substrate 1 and 2, has been observed in human PDAC tissues and cells [78]. It has also been shown that IR crosstalks with G-protein coupled receptors and stimulates DNA synthesis and proliferation of cancer cells in PDAC [79]. Also, PDAC cells kept in culture increase their proliferation rate in direct response to addition of insulin into the medium [80].

1.7.4 IR and Igf1R signalling in PDAC

Actions of both IRs and Igf1Rs are mainly performed via two major signalling cascades: MAPK and PI3K [56]. MAPK pathway activation mainly results in proliferation, while PI3K activation results in glucose uptake regulation, inhibition of apoptosis and stimulation of protein synthesis (Fig. 1.6 A) [53]. In case of PDAC, both PI3K and MAPK signalling pathways are suggested to be central signalling cascades (see chapter 1.5.4). Additionally it has been shown,

that there is a direct connection between Igf1R, MAPK and PI3K signalling in pancreatic cancer. Mutated *Kras* and downstream MAPK signalling as well as autocrine activation of Igf1R by IGF-II ligand are necessary for activation of PI3K signalling and proliferation of pancreatic ductal epithelial cells [81]. It was also shown that even in the presence of mutated KRAS, epithelial cells require functional Igf1R for formation of pancreatic cancer and that only combined inactivation of both Igf1R and MAPK reduced survival of pancreatic ductal epithelial cells. In pancreatic cancer cell lines AKT signalling induces expression of Igf1R and the inhibition of the respective signalling pathway leads to a decrease in Igf1R expression [82]. They suggest that this relationship between Igf1R and AKT is one of the mechanisms that promote invasiveness of pancreatic cancer.

Taken together, exposure of the exocrine pancreas to higher insulin concentrations as well as presence of the tyrosine kinases IRs and Igf1Rs in the exocrine pancreas might lead to the idea that exocrine cells are exposed to high mitogenic challenge that can be of crucial importance for cancer development and its progression. Indeed, only lately the role of tyrosine kinase receptors in PDAC carcinogenesis has been emphasized and experiments showed that functional receptors upstream of mutated KRAS are necessary to provide permissive environment for KRAS transforming actions [41]. Namely, murine pancreas specific knockout of epidermal growth factor receptor (EGFR) with activation of oncogenic KRAS blocked development of PDAC suggesting that EGFR-dependent signalling is necessary to allow initiation of PDAC development through the Ras/Raf/MEK/ERK cascade. IR and Igf1R belong to the same family as EGFR and trigger similar cascades. Analysis of human PDAC samples showed existence of a potential crosstalk of Igf1R with EGFR that can be relevant for progression and metastasis of cancer and to predict the outcome in patients [70].

1.7.5   IR and Igf1R targeted therapies in treatment of pancreatic cancer

Three different strategies are applied for blocking IGF and insulin signalling in cancers: receptor blockade via monoclonal antibodies, kinase inhibition with small molecular inhibitors and ligand sequestration.

There are several obstacles limiting successful therapeutic targeting of insulin and the IGF system in cancers. Especially targeting IR can cause adverse metabolic effects and undesired effects as hyperglycaemia [83]. Another issue is that due to high structural and functional homology of Igf1R and IR, if one is blocked, the other receptor may redundantly take over the function as a resistance mechanism [84]. Even more, expression of the non-targeted receptor might increase. Furthermore, if hybrid Igf1R/IR-A receptors are the dominating species in cancer, specific blocking of only Igf1R or IR would be of no benefit as the hybrid receptor is not targeted and will continue signalling.

Clinical trials of Igf1R blocking antibodies on PDAC patients are either terminated without success (AMGEN) or still active (www.clinicaltrials.gov, IMC-A12, MK0646). Boehringer Ingelheim has recently launched a phase 1 clinical trial for treatment of solid tumours, including PDAC, with IGF neutralizing antibody BI836845. In comparison to Igf1R blocking antibodies, a potential of this strategy lies in the fact that BI836845 shows high affinity towards ligands IGF-I and IGF-II but not insulin and should decrease the signalling of Igf1R homodimers in cancers but also of the hybrid receptors and IR-A in cancer. It would allow normal function of metabolic regulator IR-B and blocking of proliferative signalling from IGF-I and IGF-II with any of their receptors.
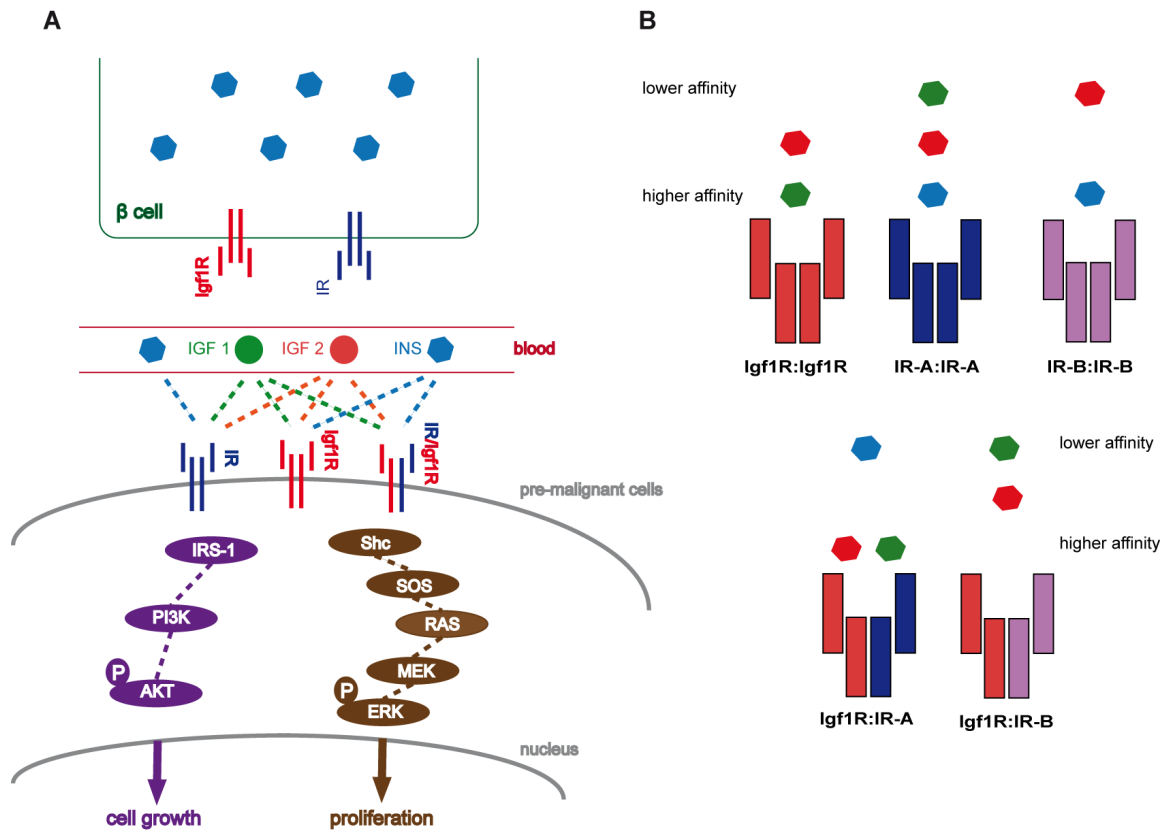
Figure 1.6: Igf1R and IR signalling and affinities. Adapted from Trajkovic-Arsic, Kalideris et al. 2013 [59].
(A) Signalling cascades of insulin and IGF in the pancreas and pancreatic cancer.
(B) Insulin and IGF homodimeric and hybrid receptors and their ligands.

1.8 Aim of this thesis

Aim of this thesis was to analyse the contribution of the Igf1R and IR in PDAC formation and progression and decipher their strongly branched signalling network using different genetically engineered mouse models (GEMMs). Understanding the underlying molecular mechanism can create new hypothesis about potential therapeutic targeting of these signalling systems.

2. Material and methods

2.1 Mice

$Kras^{LSL\text{-}G12D/+}$, $Ptf1a^{Cre/+}$, $Trp53^{R172H}$, $Trp53^{\Delta/\Delta}$, $Igf1R^{\Delta/\Delta}$, $IR^{\Delta/\Delta}$, $p110a^{wt/LSL\text{-}H1047R}$ and $Mek^{wt/LSL\text{-}DD}$ strains have been described previously [43] [85] [86] [87] [88] [89] [50] [90]. Experiments were conducted in accordance with the German Federal Animal Protection Laws and approved by the Institutional Animal Care and Use Committees at the Technical University of Munich. Mice were intercrossed to obtain the indicated genotypes. For genotyping, mice were tailed between three and four weeks of age and DNA isolation and PCR was performed as described in 2.4.1 and 2.4.2. Littermates without *Cre* expression served as wild type controls (*wt*). The genotypes and abbreviations used are listed in table 2.1.

Table 2.1: Abbreviations used for genotypes of GEM as referred to in the text

Genotype	Abbreviation
$Ptf1a^{wt/Cre};Igf1R^{loxP/loxP}$	$Igf1R^{\Delta/\Delta}$
$Ptf1a^{wt/Cre};IR^{loxP/loxP}$	$IR^{\Delta/\Delta}$
$Ptf1a^{wt/Cre};Kras^{wt/LSL\text{-}G12D}$	$Kras^{G12D}$
$Ptf1a^{wt/Cre};Kras^{wt/LSL\text{-}G12D};Igf1R^{loxP/loxP};IR^{wt/loxP}$	$Kras^{G12D};Igf1R^{\Delta/\Delta}$
$Ptf1a^{wt/Cre};Kras^{wt/LSL\text{-}G12D};IR^{loxP/loxP};Igf1R^{wt/loxP}$	$Kras^{G12D};IR^{\Delta/\Delta}$
$Ptf1a^{wt/Cre};Kras^{wt/LSL\text{-}G12D};p53^{wt/LSL\text{-}R172H}$	$Kras^{G12D},p53^{R172H}$
$Ptf1a^{wt/Cre};Kras^{wt/LSL\text{-}G12D};p53^{wt/LSL\text{-}R172H};Igf1R^{loxP/loxP};IR^{wt/loxP}$	$Kras^{G12D};p53^{R172H};Igf1R^{\Delta/\Delta}$
$Ptf1a^{wt/Cre};Kras^{wt/LSL\text{-}G12D};p53^{wt/LSL\text{-}R172H};IR^{loxP/loxP};Igf1R^{wt/loxP}$	$Kras^{G12D};p53^{R172H};IR^{\Delta/\Delta}$
$Ptf1a^{wt/Cre};Kras^{wt/LSL\text{-}G12D};p53^{loxP/loxP}$	$Kras^{G12D};p53^{\Delta/\Delta}$
$Ptf1a^{wt/Cre};Kras^{wt/LSL\text{-}G12D};p53^{loxP/loxP};Igf1R^{loxP/loxP};IR^{wt/loxP}$	$Kras^{G12D};p53^{\Delta/\Delta};Igf1R^{\Delta/\Delta}$
$Ptf1a^{wt/Cre};Kras^{wt/LSL\text{-}G12D};p53^{loxP/loxP};IR^{loxP/loxP};Igf1R^{wt/loxP}$	$Kras^{G12D};p53^{\Delta/\Delta};IR^{\Delta/\Delta}$
$Ptf1a^{wt/Cre}; p110a^{wt/LSL\text{-}H1047R}$	$p110^{H1047R}$
$Ptf1a^{wt/Cre}; p110a^{wt/LSL\text{-}H1047R};Igf1R^{loxP/loxP};IR^{wt/loxP}$	$p110^{H1047R};Igf1R^{\Delta/\Delta}$
$Ptf1a^{wt/Cre}; p110a^{wt/LSL\text{-}H1047R};IR^{loxP/loxP};Igf1R^{wt/loxP}$	$p110^{H1047R};IR^{\Delta/\Delta}$
$Ptf1a^{wt/Cre}; Mek1^{wt/LSL\text{-}DD}$	$Mek1^{DD}$
$Ptf1a^{wt/Cre}; Mek1^{wt/LSL\text{-}DD};Igf1R^{loxP/loxP};IR^{wt/loxP}$	$Mek1^{DD};Igf1R^{\Delta/\Delta}$
$Ptf1a^{wt/Cre}; Mek1^{wt/LSL\text{-}DD};IR^{loxP/loxP};Igf1R^{wt/loxP}$	$Mek1^{DD};IR^{\Delta/\Delta}$

2.1.1   Glucose Tolerance Test

Glucose tolerance test (GTT) was performed on mice after 12 hours overnight fasting. Glucose was injected i.p. (2 g/kg, using 20% glucose solution). Blood glucose levels were assessed by collecting tail blood and glucose level data were recorded at indicated time points.

2.2 Cell culture

2.2.1   Isolation and culture of primary murine tumour cells

For the isolation of primary murine pancreatic tumour cells, different parts of the developed tumour were resected into small pieces and placed into a 10 cm cell culture plate. Next a sterile one replaced the plate and the tumour pieces were cut as small as possible under sterile conditions. Then cell culture medium was added (DMEM high glucose with 10% FCS, 1% Penicillin/Streptomycin, 1 x non-essential amino acids, all Invitrogen) and cells incubated in a 37 °C incubator with 5% CO_2. During the next two days tumour cells got attached and grew on the plate. Afterwards the medium was changed and the cells were split at least three times with 0.25% Trypsin EDTA (Invitrogen) and reseeded to ensure no contamination with fibroblasts before using them for further experiments.

2.2.2   Cell viability assay

For the cell viability assay, 5000 primary murine pancreatic tumour cells ($Kras^{G12D}$) were seeded in a well of 96-well plates and were allowed to attach over night. On the next day the cells were treated with different concentrations of BMS-754807 (Selleckchem) for 72 hours. After this incubation time, 10 µl MTT reagent (Roche) and after 4 hours 100 µl of lysisbuffer was added to each well and incubated over night at 37°C according to kit instructions (Cell Proliferation Kit I from Roche). Only living cells are able to cleave the MTT and

to produce thereby formazan dye, which can be quantitated using a scanning multi-well ELISA reader at 580 nm (Anthos reader 2001, from Anthos).

2.3 Histological analysis

Mice were killed, either upon indicated time points or notable symptoms of disease by an overdose of isoflurane anaesthesia. Pancreas and other tissues were rapidly removed, immediately fixed in 4% formalin for 24 hours at 4°C and then dehydrated with increasing concentrations of ethanol, xylol and paraffin in a Leica S300 tissue processing unit. All dehydrated organs of the mouse were embedded in liquid paraffin and then cooled to harden. The formalin-fixed, paraffin-embedded (FFPE) blocks were stored at room temperature. For histological analyses FFPE-blocks were cut to 2 µm on a microtome (Thermo Scientific, HM 3559), transferred to a 50 °C water bath for stretching and collected on microscopic glass slides (Thermo Scientific, Superfrost plus). Sections were allowed to dry overnight.

2.3.1   H&E

H&E contains the two dyes haematoxylin and eosin. Haematoxylin is a basic dye and used to stain acidic structures, like nuclei in a purple blue. Whereby eosin an acidic dye is and stains basic structures in pink like the cytoplasm. For an H&E staining paraffin sections were deparaffinised with xylol (Roti-Histol, Roth) in 2 changes, 3 minutes each. A rehydration followed in 2 changes of descending alcohol steps of 100%, 96% and 70% ethanol for 3 minutes each. The slides were than washed briefly in distilled water. After washing, slides were stained with haematoxylin (Mayer's hemalaun, Merck) for 5 minutes and immediately washed in running tap water for 10 minutes. To turn the nucleus into a deep purplish blue colour the slides were plunged shortly into ammonia water (500 ml tap water with 40 drops ammonia). After a brief washing step with distilled water the slides were dipped two times into HCl-water (500 ml distilled water with 2,5 ml 37% HCl) to decolorize the cytoplasm (differentiation) and to remove excess haematoxylin from chromatin. Afterwards the slides were washed with running tap water and plunged again shortly into ammonia water.

A quick bath with distilled water and 70% alcohol followed before counterstaining the slides with ethanolic eosin (diluted 1:5 with 96% ethanol) for 2 minutes. At the end slides were dehydrated using 70%, 96% and 100% ethanol steps and cleared with xylol, again 2 changes and 3 minutes each. Mounting medium (pertex, Medite GmbH) and coverslips were placed and microscopic pictures were taken on Zeiss Axiovert Imager.

2.3.2   Immunhistochemistry

For immunhistochemical stainings FFFPE-slides were deparaffinised and rehydrated as described in 2.3.1. After a washing step with distilled water for 5 minutes the slides were boiled in citric acid based buffer (Vector Laboratories) for 15 minutes to retrieve the antigen. Again a washing step followed with distilled water and the slides were afterwards shaken for 10 minutes in 3% Hydrogen Peroxidase (Merck) to block the endogenous peroxidase. The slides were rocked 3 times for 5 minutes, once with water and twice with PBS (Fluka). After washing, unspecific antibody binding was blocked with 5% serum (Vector Laboratories) from the species of which the secondary antibody was derived, for one hour at room temperature. Then the slides were incubated over night at 4 °C with the respective primary antibody (Table 2.2) diluted in blocking solution. Blocking and incubation occurred in a wet chamber.

On the next day the slides were washed three times for 5 minutes with PBS and incubated for one hour with the specific biotinylated secondary antibody (all Vector Laboratories) diluted 1:1000 in blocking solution at room temperature. In the meanwhile the ABC solution (Vector Laboratories) was prepared (5ml of PBS and 2 drops of A and 2 drops of B) and stored for 30 minutes at 4 °C. After washing once with PBS the slides were incubated for at least 30 minutes with the ABC reagent and then rocked three times, once with PBS and twice with distilled water for 5 minutes each. Signal detection was performed with the DAB kit (Vector Laboratories), 5 ml distilled water were mixed with 2 drops of buffer pH 7.5 plus 4 drops of DAB plus 2 drops of H_2O_2. The DAB solution was added to the slides under the microscope to monitor the staining and as soon as the sections developed they were immersed in distilled water. Slides were

counterstained with haematoxylin for 30 seconds and dehydrated and mounted as described in 2.3.1.

2.3.3 Histological quantification

For quantification of Ki67-positive nuclei or MUC5AC-positive PanIN lesions two representative slides per mouse were chosen and pictures from the whole pancreas were taken from each slide and calculated using the AxioVision 4.8 software (n = 7 to 8 mice per group)

Table 2.2: Primary antibodies for immunohistochemistry

Antigen	Species	Dilution	Company
Amylase	Rabbit	1:1000	Sigma
Insulin	Guinea pic	1:500	Dako
MUC5AC	Mouse	1:200	Neomarkers
Ki67	Rabbit	1:2500	Abcam
Stat3 pTyr705	Rabbit	1:100	Cell Signalling
Akt pSer473	Rabbit	1:50	Cell Signalling
Erk pThr202/Tyr204	Rabbit	1:100	Cell Signalling
Igf1Rβ	Rabbit	1:500	Cell Signalling
InsRβ	Rabbit	1:500	Cell Signalling
Igf1R/InsR pTyr 1135/11336	Rabbit	1:500	Cell Signalling

2.4 RNA/DNA analyses

2.4.1 DNA isolation from mouse tails for genotyping

DNA was isolated from mice tails using 100µl tail and tissue lysis buffer from Peqlab with adding 10 µl 5% Proteinase K (Roche) for each sample. The tails were incubated over night at 56°C and on the next day the enzyme was inactivated at 95°C for 60 minutes. 1 µl of the lysate was used as template for PCR.

2.4.2 Genotyping PCR

The isolated tail DNA was used to genotype the respective mice by PCR with the RedTaq Ready Mix from Sigma and the accordingly primer in an end concentration of 10 pM. Primers were purchased from MWG Biotech AG. The following conditions were applied for amplification: Denaturation 95°C 30 sec, annealing 58°C 30 sec, elongation 72°C 1 min for 35 cycles. Genotyping results were visualized on 2 % agarose gels.

The following genotyping primers were used and gave the indicated band sizes:

Ptf1a$^{+/Cre}$ wt 324 bp   lox 199 bp
ACCAGCCAGCTATCAACTCG/TTACATTGGTCCAGCCACC/CTAGGCCACA
GAATTGAAAGATCT/GTAGGTGGAAATTCTAGCATCATCC

Kras$^{+/LSL-G12D}$ wt 300 bp   lox 200 bp
CACCAGCTTCGGCTTCCTATT/AGCTAATGGCTCTCAAAGGAATGTA/CCAT
GGCTTGAGTAAGTCTGC

Trp53$^{Δ/Δ}$ wt 250 bp   lox 350 bp
CACAAAAACAGGTTAAACCCA/AGCACATAGGAGGCAGAGAC

Trp53^{R172H}   wt 565 bp   lox 270 bp
AGCCTTAGACATAACACACGAACT/GCCACCATGGCTTGAGTAA/CTTGGAG
ACATAGCCACACTG

Igf1R$^{Δ/Δ}$ wt 300 bp   lox 350 bp
TCCCTCAGGCTTCATCCGCAA/CTTCAGCTTTGCAGGTGCACG

IR$^{Δ/Δ}$ wt 200 bp   lox 250 bp
GATGTGCACCCCATGTCTG/CTGAATAGCTGAGACCACAG

p110a$^{wt/LSL-H1047R}$ wt 600 bp   lox 410 bp
AAAGTCGCTCTGAGTTGTTAT/GCGAAGAGTTTGTCCTCAACC/GGAGCGG
GA GAAATGGATATG

Mek$^{wt/LSL-DD}$ wt 297 bp   lox 347 bp
TTGTTCGGATCCATAACTTCG/AAGGGAGCTGCAGTGGAGTA/CCGAAAATC
TGTGGGAAGTC

2.4.3   RNA Isolation

For RT-PCR experiments, shock-frozen pancreatic tissue of at least three different regions was homogenized in RLT-buffer (Promega) including 1% β-Mercaptoethanol (Roth). Total RNA was extracted from these lysates with the Maxwell 16 LEV simplyRNA Tissue Kit from Promega according to manufacturer´s protocol. RNA concentration was measured on a Nano-Drop 2000 spectrophotometer (Thermo Scientific) and quality was checked on a 1% agarose gel.

2.4.4   cDNA Synthesis

For cDNA synthesis 1 µg of RNA was incubated with 0,5 µg random primers and 1 µl of 10 mM dNTPs Mix (both Promega) in a volume of 12 µl for 5 minutes at 65°C. To the mixture 4 µl of 5x first-strand buffer, 2 µl of 0.1 M DTT (both Invitrogen) and 40 units RNaseOUT (Ambion) was add and incubated for 2 minutes at 25°C. Subsequently 1 µl (200 units) of Superscript II (Invitrogen) were added and mixed. The mixture was incubated at 25°C for 10 minutes, at 42°C for 50 minutes and the reaction was inactivated at 70 °C for 15 min.

2.4.5   Quantitative RT-PCR

Quantitative RT-PCR was performed on the Lightcycler480 system using the SYBR Green master mix (both from Roche). The applied RT-PCR program was 40 cycles of 95°C for 10 seconds, 58°C for 20 seconds and 72°C for 10 seconds. 100 ng cDNA were used as template and Cyclophilin was used for normalization of the measured target gene. Melting Curve analysis was performed to verify primer specificity. Values were calculated with the following exponential equation: $2^{DeltaCT(Cyclophilin) - DeltaCT(target\ gene)}$. P values were calculated using the GraphPad statistic software Prism 5 and the Mann-Whitney-test for non-normally distribution.

The following primers (final concentration 10 pM) were used:

Cyclophilin-Forward-Reverse

ATGGTCAACCCCACCGTGT/TTCTGCTGTCTTTGGAACTTTGTC

IGF-I-Forward-Reverse

TGGATGCTCTTCAGTTCGTG/GCAACACTCATCCACAATGC

IGF-II-Forward-Reverse

AAGTCGATGTTGGTGCTTCTCATCT /CCCCTCCGCACAGAGTCTCT

Insulin-Forward-Reverse

AAACCCACCCAGGCTTTTGT /ATCCACAATGCCACGCTTCT

Igf1R-Forward-Reverse

CCTCGGAGTTGGAGAACTTC /GAGTAGTTCCCTTCCAGCTGC

IR-A-Forward-Reverse

TCCTGAAGGAGCTGGAGGAGT /CTTTCGGGATGGCCTGG

IR-B-Forward-Reverse

TCCTGAAGGAGCTGGAGGAGT /TTCGGGATGGCCTACTGTC

2.5 Protein biochemistry

2.5.1 Isolation of protein from cells or tissue

To isolate whole protein tissue lysates of the pancreas, three pieces from different regions were resected as fast as possible after sacrificing the mice and immediately snap frozen in liquid nitrogen and stored at -80 °C. For generating the lysates, frozen pieces were put in non-denaturing lysis buffer (NDLB: 20 mM Tris HCl pH 8 (Sigma), 137 mM NaCl (Sigma), 10 % Glycerol (Roth), 1 % NP-40 (Sigma), 2 mM EDTA pH 8 (Sigma)) provided with Protease- and Phosphatase inhibitors (both Roche) and directly homogenized using an electric tissue homogenizer (silentCrusherM from Heidolph). The frozen state of the tissue facilitates the homogenization process. To isolate protein lysates from mammalian cells, cells were plated on a 10 cm cell culture dish and grown to approximately 80% confluence. Thereafter the medium was removed and they were washed with ice cold PBS. 1,5 ml NDLB (ice cold) with protease and phosphatase inhibitor provided was added directly to the cells and they were

scraped with a cell scraper (Sarstedt). Next both types of lysates (tissue or cell) were sonicated (Sonopuls from Bandelin) for 10 seconds and incubated on ice for 30 minutes to let the lysis buffer work. Afterwards the lysates were centrifuged at 4 °C for 10 min at 13200 rpm and the supernatants were transferred to new vials. Protein concentrations were determined using the BCA kit from Thermo Scientific according to manufacturer´s instructions. Linear absorbance was measured at 580 nm on an ELISA microplate reader (Anthos reader 2001, from Anthos). For further experiments the lysates were stored for short term in -20 °C and for long term in -80 °C.

2.5.2 SDS polyacrylamide electrophoresis (SDS PAGE) and Western Blot

50-100 µg protein lysate (depending on target expression and antibody quality) were supplemented with 5x Laemmli buffer (SDS 10% (Sigma), TRIS-Base 300 mM (Sigma), bromphenolblue 0.05 % (Sigma), Glycerol 50% (Roth) and β-mercaptoethanol 5% (Sigma)) and denatured at 95 °C for 5 min. Protein separation was performed with a SDS-PAGE gel (for proteins around 50 kDa 12% was used and for proteins around 100 kDa 8% was used) in SDS running buffer at 100 Volt in BioRad Mini Protean Gel System chambers. Gels consisted of two fractions, a stacking gel (upper part of the gel) and a running gel (lower part). After gel separation of the proteins they were transferred to a PDVF membrane (Immobilon-PSQ from Milipore). The PDVF membranes were activated shortly in methanol and the Western Blot protein transfer was performed at 100 Volt for 2 hours. The membrane and the gel were clamped between a sponge and two Whatman papers on each side and the blotting chamber was cooled with an ice pack for the time of the transfer. After transfer, membranes were incubated for 30 minutes in 5% skim milk powder (Fluka) diluted in TBS-T, to block any unspecific antibody binding. Then the milk was removed, the membrane washed shortly with TBS-T and incubated over night at 4°C with the primary antibody (Table 2.3) diluted in 5% BSA/TBS-T. On the next day the membrane was washed 3 times with TBS-T for 20 minutes and incubated with the species-specific HRP-coupled antibody in 5% skim milk in TBS-T for 1h at room temperature. After 2 washing steps with TBS-T and one

with TBS for 10 minutes each, the protein band was visualized using the ECL Western Blotting Detection Reagents and Amersham Hyperfilms (both GE Healthcare)

10 x TBS
80g NaCl (Sigma),
31.5g Tris-HCl (Sigma)
add 1l dH$_2$O pH 7.6

TBS-T
1l of 1 x TBS (Sigma)
1 ml Tween20 (Sigma)

10 x running buffer
10 g SDS (Sigma)
30 g Tris-Base (Sigma)
144 g Glycin (Sigma)
add 1 l dH$_2$O.

10 x transfer buffer for wet transfer
144 g Glycin (Sigma)
30 g Tris-Base (Sigma)
add 1 l dH$_2$O.

1 x transfer buffer for wet transfer
100 ml 10 x transfer buffer
200 ml Methanol (Merck)
700 ml dH$_2$O.

<u>5% stacking gel (5 ml for 2 gels)</u>

3,4 ml dH$_2$O

830 µl 30% acrylamide mix (Roth)

630 µl 1.0 M Tris (pH 6.8) (Sigma)

50 µl 10% SDS (Sigma)

50 µl ammonium persulfate (Sigma)

5 µl TEMED (Sigma)

<u>8% running gel (25 ml for 2 gels)</u>

11,5 ml dH$_2$O

6,7 ml 30% acrylamide mix (Roth)

6,3 ml 1.0 M Tris (pH 6.8) (Sigma)

250 µl 10% SDS (Sigma)

250 µl ammonium persulfate (Sigma)

15 µl TEMED (Sigma)

<u>12% running gel (25 ml for 2 gels)</u>

8,2 ml dH$_2$O

10 ml 30% acrylamide mix (Roth)

6,3 ml 1.0 M Tris (pH 6.8) (Sigma)

250 µl 10% SDS (Sigma)

250 µl ammonium persulfate (Sigma)

15 µl TEMED (Sigma)

<u>Secondary antibodies used:</u>

HRP-coupled α-rabbit IgG 1:10000 (GE Healthcare)

HRP-coupled α-goat 1:5000 (Santa Cruz)

Table 2.3: Primary antibodies for immunoblot analysis

Antigen	Species	Dilution	Company
Hsp90	Rabbit	1:2500	Santa Cruz
Akt pThr308	Rabbit	1:100	Cell Signalling
Akt pSer473	Rabbit	1:1000	Cell Signalling
Akt 1/2	Goat	1:500	Santa Cruz
Erk pThr202/Tyr204	Rabbit	1:1000	Cell Signalling
Erk 1/2	Rabbit	1:1000	Santa Cruz
Igf1Rβ	Rabbit	1:500	Cell Signalling
InsRβ	Rabbit	1:500	Cell Signalling
Igf1R/InsR pTyr 1135/11336	Rabbit	1:500	Cell Signalling

2.5.3   Immunoprecipitation

For the immunoprecipitation primary murine $Kras^{G12D}$ cell lines were lysed in NDLB (see 2.5.1). 500 µg protein were incubated with 4 µg primary antibody (Table 2.3) under gentle rotation for 2 hours at 4 °C. Afterwards, immunoprecipitates were pulled down with 100 µl A/G agarose (Thermo Scientific) for 1 hour at 4 °C with gentle rotation. After washing the beads three times with NDLB to remove unbound protein, they were resuspended in 20 µl NDLB and mixed with 10 µl 5 x Laemli. The lysate were denaturated at 95°C for 5 minutes and separated on a SDS-PAGE gel. Co-immunoprecipitated proteins were detected with standard Western Blot (2.5.2).

2.5.4   ELISA – Enzymed linked immunosorbent assay

To analyse the amount of Igf1 and Insulin in the blood of different GEM, blood was taken from the aorta of the respective mice immediately after sacrification. The serum was isolated through centrifugation of the blood in serum tubules (Microvette from Sarstedt). The ELISA kit for quantitative determination of IGF-I concentrations in serum was obtained from abcam and that for insulin from Merck. ELISA was performed according to the manufacturer´s protocol. The principle of the test is based on a competitive reaction between the free antigen

in the sample and the immobilized antigen on the microplate. Standards or samples are transferred directly to the pre-coated plate together with the primary antibody against Igf1 or Insulin. The antigen of the sample competes with the immobilized antigen of the plate for the free binding side of the antibody. Detection and quantitation are effected by the means of a peroxidase-labelled secondary antibody and the respective substrate reaction. In parallel, a standard curve, consisting of the optical density at 450 nm versus the standard concentrations, is compiled to determine the concentration in the sample.

3. Results

3.1 Overexpression of Igf1R and IR in early PDAC precursor lesions

The Igf1R signalling system is implicated in autocrine-paracrine stimulation of a variety of cancers, including PDAC [69]. For the IR a very similar action has been reported under malignant conditions, despite its metabolic function in healthy tissues [80]. This and the fact that the two receptors share a high homology [91] lead to the assumption that the IR can convey resistance to Igf1R targeted therapies. To better understand the specific implication of both receptors in PDAC initiation and progression and thus the effectiveness of therapeutic strategies, the expression of Igf1R and IR in human and murine precursor lesions and cancer was tested. The highest presence of both receptors could be seen in early stages, so called PanIN1 of human PDAC. In higher-grade lesions and carcinoma the signal of Igf1R and IR decreased (Fig. 3.7 A), whereas in normal human pancreatic tissue the expression was nearly absent. To assess Igf1R and IR expression in murine $Kras^{G12D}$-induced PDAC, $Kras^{wt/LSL-G12D}$ mice were crossed to $Ptf1a^{wt/Cre}$ mice (referred to as $Kras^{G12D}$) as previously described [92]. $Kras^{G12D}$ mice have been shown to recapitulate the morphological and molecular features of the human disease, with metaplasia, mPanIN formation and progression to PDAC at around 1 year of age [43]. Similar to the human phenotype, there was an overexpression of the Igf1R in PanIN1 of $Kras^{G12D}$ mice and the appearance of the receptor decreased with higher stages (Fig. 3.7 B). Immunhistochemical (IHC) analysis of the IR expression in $Kras^{G12D}$ mice showed also a stronger upregulation in earlier stages, but reappeared in PDAC (Fig. 3.7 B). The data suggest a higher requirement of the Igf1R and the IR in early stages of PDAC, although there is a consistent presence of both receptors and their precursors in human and murine $Kras^{G12D}$ driven pancreatic cancer cell lines (Fig. 3.7 C and D). Thus, the expression of these two tyrosine kinase receptors is increased in pancreatic carcinogenesis *in vivo*, especially in earlier stages and remains definitely detectable in higher stages and *in vitro*.
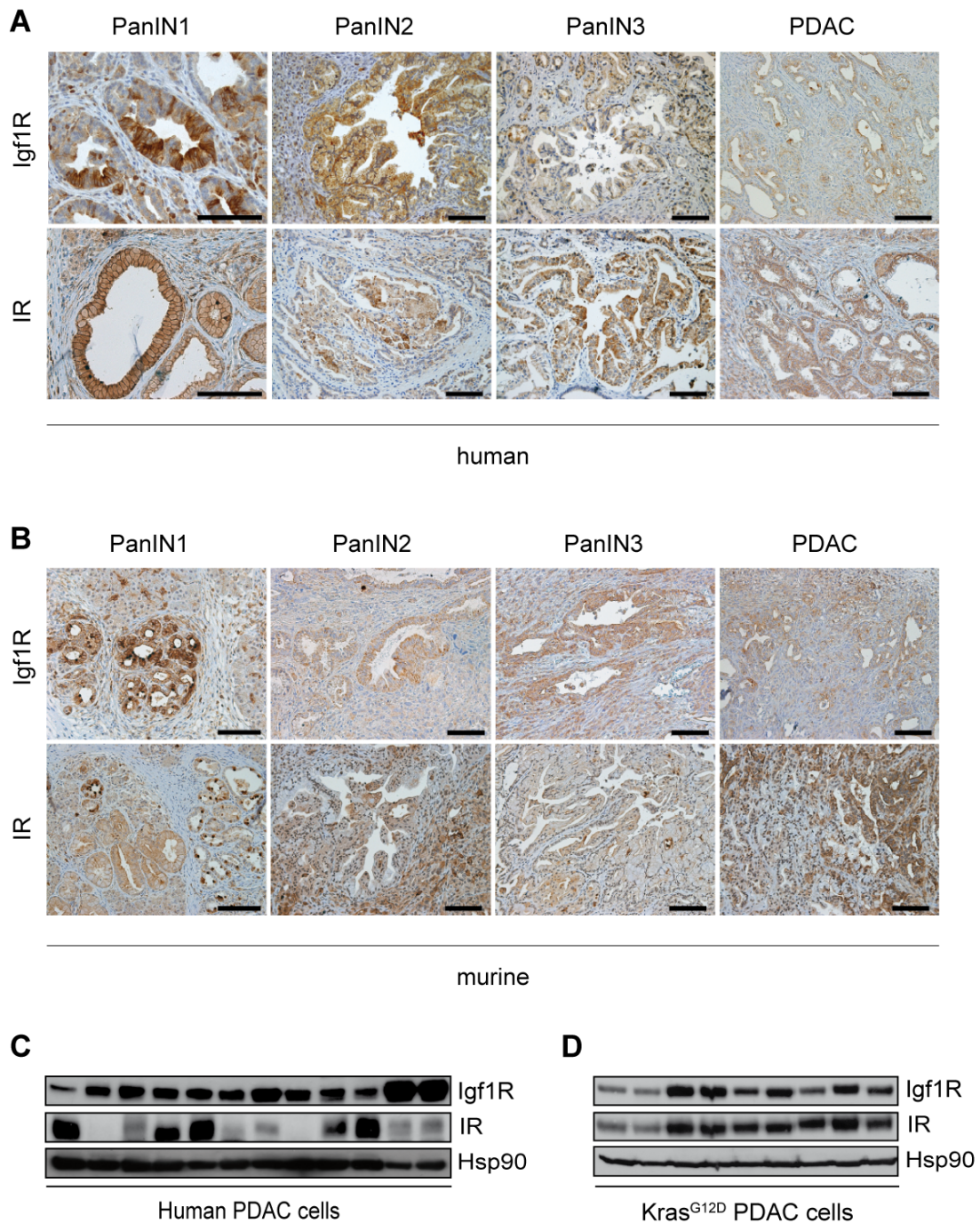
Figure 3.7: Igf1R and IR expression in different PDAC stages.
(A) Staining for Igf1R and IR in different human PanIN lesions and PDAC displayed a strong expression of both receptors in early PanIN1 stages and a decrease of this expression with increasing stages and in PDAC. Scale bar = 50 µm.
(B) Staining for Igf1R and IR in different stages of murine PanIN lesions and PDAC displayed a strong expression of both receptors in early PanIN1 and a decrease of this expression with increasing preneoplastic stages. In contrast to the human PDAC tissue, the IR signal strengthened again in murine PDAC. Scale bar = 50 µm.
(C and D) Detectable Igf1R and IR expression by Western Blot analysis in human and murine PDAC cell lines.

3.2 Pancreatic loss of Igf1R but not of IR gives rise to a metabolic impairment in mice

3.2.1   Genetic deletion of the Igf1R and the IR in the pancreas

Most organs and tissues express the Igf1R with very high levels in the brain and extremely low levels in the liver [93]. In contrast, the insulin receptor exists in two isoforms, IR-B is mostly expressed on metabolically active tissue and IR-A is usually highly present in fetal tissues [58]. To ascertain that a pancreas specific deletion of either of these receptors has no effect on pancreatic development and function, previously described $Igf1R^{aP2Cre}$ [88] and $IR^{flox/flox}$ [89] mice were crossed with the $Ptf1a^{wt/Cre}$ line to generate mice with pancreatic $Igf1R$ or IR deficiency (referred to as $Igf1R^{\Delta/\Delta}$ and $IR^{\Delta/\Delta}$). Upon Cre recombination exon 3 of the Igf1R and exon 4 of the IR allele, both flanked with loxP sites were cut out (Fig. 3.8 A). The consequence thereof is a shift of the reading frame of the respective gen and a following induced stop codon so that the protein product cannot be completely generated. Polymerase chain reaction and Western Blot analysis revealed successful generation of mice with homozygous Cre-mediated recombination of the IR and $Igf1R$ locus (Fig. 3.8 B and C).
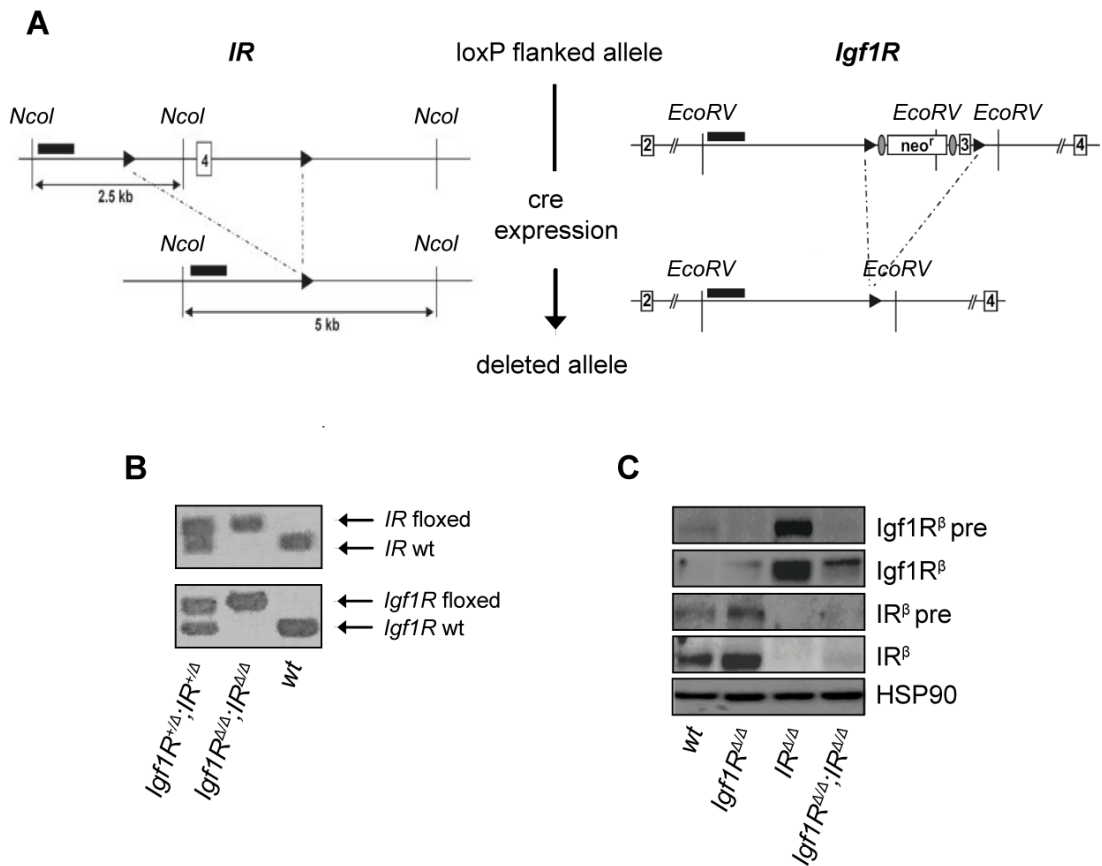
Figure 3.8: Conditional *Igf1R*- and *IR*- knockout.
(A) For conditional knockout of *IR* and *Igf1R*, exon 4 and exon 3 of the respective receptor genes were flanked *by loxP* sites. Upon *Cre*-mediated recombination these parts of the *Igf1R* and *IR* genes get deleted resulting in an ablation of the protein; black triangles represent the *loxP* sites (adapted from [88, 89]).
(B) PCR for correct recombination of *loxP* sites depicted specific deletion of *IR* and *Igf1R* in the pancreas of *Igf1R*$^{\Delta/\Delta}$, *IR*$^{\Delta/\Delta}$ and *Igf1R*$^{+/\Delta}$;*IR*$^{+/\Delta}$ mice.
(C) Western Blot analysis of whole pancreatic lysates from *Igf1R*$^{\Delta/\Delta}$, *IR*$^{\Delta/\Delta}$ and *Igf1R*$^{\Delta/\Delta}$;*IR*$^{\Delta/\Delta}$ mice showed loss of the protein in the pancreas in comparison to *wildtype* controls.

3.2.2 Developmental charachterisation of *Igf1R*$^{\Delta/\Delta}$ and *IR*$^{\Delta/\Delta}$ mice

Igf1R$^{\Delta/\Delta}$ and *IR*$^{\Delta/\Delta}$ mice were born at the expected Mendelian ratio, viable and fertile. While single receptor knockout mice showed a normal development and body growth similar to wildtype littermates at an age of 8 weeks, mice lacking both receptors in the pancreas had an impaired pancreas development and died within 2 months (Fig. 3.9 A). Histological analysis displayed no gross pancreatic abnormalities of *Igf1R*$^{\Delta/\Delta}$ or *IR*$^{\Delta/\Delta}$ mice but a hypomorphic pancreas in *Igf1R*$^{\Delta/\Delta}$;*IR*$^{\Delta/\Delta}$ mice, emphasizing the importance of the presence of at least one of these two receptors for organ growth. Functionality of the endocrine and exocrine compartments of the pancreas have been investigated on the one hand by immunhistochemical stainings for amylase and insulin and on the other

hand by a Glucose tolerance test. The exocrine and endocrine secrets were present both in the single knockout as well as in the double knockout mice (Fig. 3.9 C). But whereas $IR^{\Delta/\Delta}$ mice in the glucose tolerance test behaved very similar to $Igf1R^{+/\Delta};IR^{+/\Delta}$ littermates with only a slight delay in glucose uptake compared to wildtype animals, $Igf1R^{\Delta/\Delta}$ mice showed a significantly higher disturbance in glucose metabolism and were unable to reach the initial values (Fig. 3.9 B).
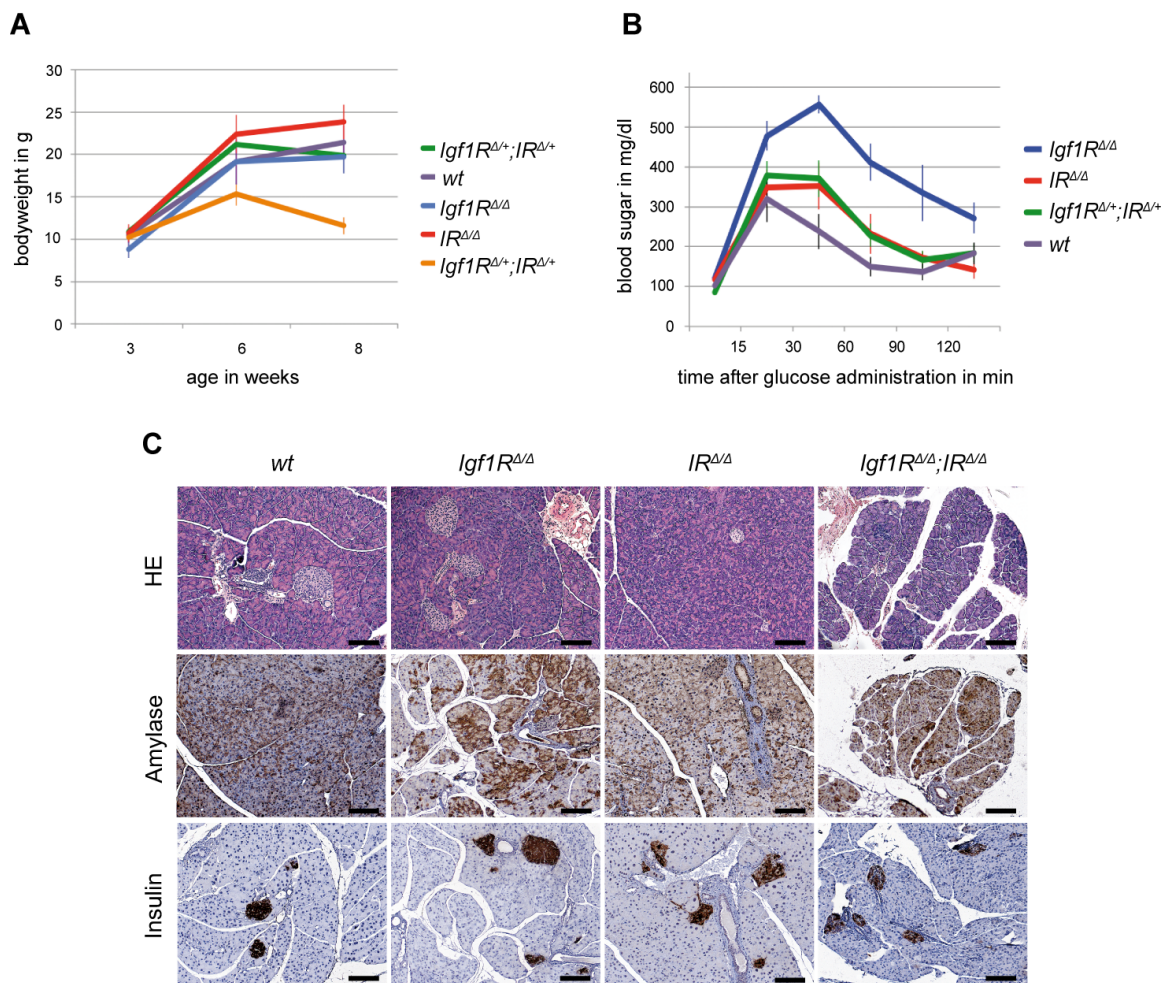
Figure 3.9: Developmental impairment of $Igf1R^{\Delta/\Delta};IR^{\Delta/\Delta}$ mice and disturbed glucose uptake in $Igf1R^{\Delta/\Delta}$ mice.
(A) Heterozygous or homozygous knockout of only one receptor in the pancreas resulted in a normal development, double knockout of both receptors showed an impaired development (bodygrowth) of the respective mice (n = 6, p = 0,04 (wildtype vs. $Igf1R^{\Delta/\Delta};IR^{\Delta/\Delta}$ mice)).
(B) $IR^{\Delta/\Delta}$ and $Igf1R^{+/\Delta};IR^{+/\Delta}$ mice exhibited a slight delay in glucose uptake compared to wildtype controls. An abnormal glucose tolerance was seen in $Igf1R^{\Delta/\Delta}$ mice, they were not able to reach the initial values (n = 6, p = 0,0085 (wildtype vs. $Igf1R^{\Delta/\Delta}$)).
(C) Histological analysis displayed pancreatic abnormalities only in $Igf1R^{\Delta/\Delta};IR^{\Delta/\Delta}$ mice, not in $Igf1R^{\Delta/\Delta}$ and $IR^{\Delta/\Delta}$ animals. All knockout models showed a normal expression of exocrine and endocrine markers (amylase and insulin). Scale bar = 50 µm.

Furthermore, despite no developmental abnormalities in size and weight, the life expectancy of $Igf1R^{\Delta/\Delta}$ mice was significantly shorter than for $IR^{\Delta/\Delta}$ and *wildtype* littermates (Fig. 3.10) likely due to their metabolic imbalance. On the contrary, $IR^{\Delta/\Delta}$ mice lived significantly longer than wildtype controls, supporting the hypothesis of insulin as life reducing factor. The median survival of $Igf1R^{\Delta/\Delta};IR^{\Delta/\Delta}$ mice was only 55 days, most probably caused by their hypomorphic pancreas and the associated exocrine and endocrine insufficiency. Thus, as foundation for the forward experiments a wildtype phenotype of $IR^{\Delta/\Delta}$, a late in life increasing metabolic disturbed phenotype of $Igf1R^{\Delta/\Delta}$ and an early and severely disturbed phenotype of $Igf1R^{\Delta/\Delta};IR^{\Delta/\Delta}$ mice can be concluded.
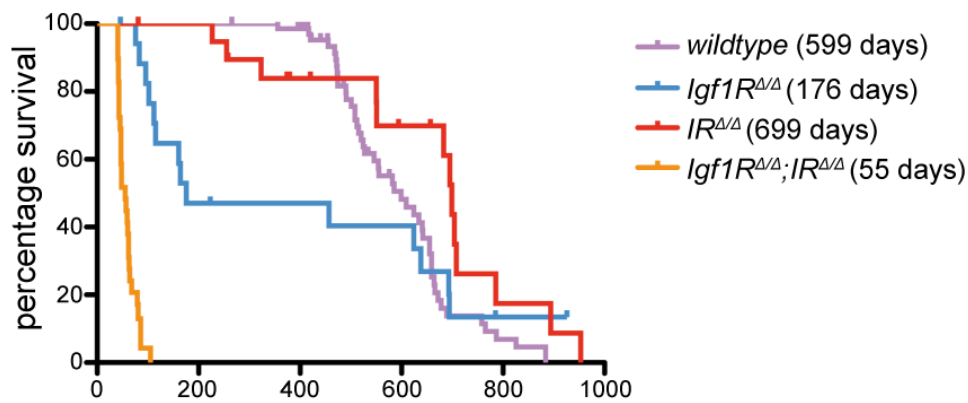
**Figure 3.10: Survival analysis of $Igf1R^{\Delta/\Delta}$ and $IR^{\Delta/\Delta}$ mice.**
Pancreas specific deletion of Igf1R but not IR shortened the survival of $Igf1R^{\Delta/\Delta}$ mice compared to wildtype mice. Prolonging survival effect could be observed in $IR^{\Delta/\Delta}$ mice. Survival analysis of wildtype (n= 47, median 599 days) versus $Igf1R^{\Delta/\Delta}$ (n= 14, median 176 days, p < 0.0001 (wildtype vs. $Igf1R^{\Delta/\Delta}$)) versus $IR^{\Delta/\Delta}$ (n= 13, median 699 days, p = 0,0292 (wildtype vs. $IR^{\Delta/\Delta}$)) versus $Igf1R^{\Delta/\Delta};IR^{\Delta/\Delta}$ mice (n= 28, median 55 days, p < 0.0001 (wildtype vs. $Igf1R^{\Delta/\Delta};IR^{\Delta/\Delta}$)).

3.3 Ablation of *Igf1R* and *IR* reduces PanIN burden and prevents PDAC development in *Kras^G12D* mice

3.3.1 Generation of *Kras^G12D;Igf1R^{\Delta/\Delta}* and *Kras^G12D;IR^{\Delta/\Delta}* mice

To test the requirement of IR and Igf1R during carcinogenesis, $Igf1R^{\Delta/\Delta}$ and $IR^{\Delta/\Delta}$ mice were crossed to $Kras^{G12D}$ mice ($Kras^{G12D};Igf1R^{\Delta/\Delta}$ and $Kras^{G12D};IR^{\Delta/\Delta}$). IHC for both receptors on $Kras^{G12D}$, $Kras^{G12D};Igf1R^{\Delta/\Delta}$ and $Kras^{G12D};IR^{\Delta/\Delta}$ murine pancreatic tissue was performed to confirm the deletion of the specific protein. An increase of Igf1R and IR in $Kras^{G12D}$ preneoplastic lesions and a lack of expression of the receptor protein in lesions of the respective knockout mice

could be shown (Fig. 3.11 A). These results were additionally confirmed by qRT-PCR, furthermore a significant decrease of *IR* mRNA expression in *Kras*^{G12D};*Igf1R*$^{Δ/Δ}$ and of *Igf1R* mRNA expression in *Kras*^{G12D};*IR*$^{Δ/Δ}$ mice was observed (Fig. 3.11 B), indicating a possible interaction of expression of the two receptors.

A

| *Kras*^{G12D} | *Kras*^{G12D};*IR*$^{Δ/Δ}$ | *Kras*^{G12D} | *Kras*^{G12D};*Igf1R*$^{Δ/Δ}$ |

B
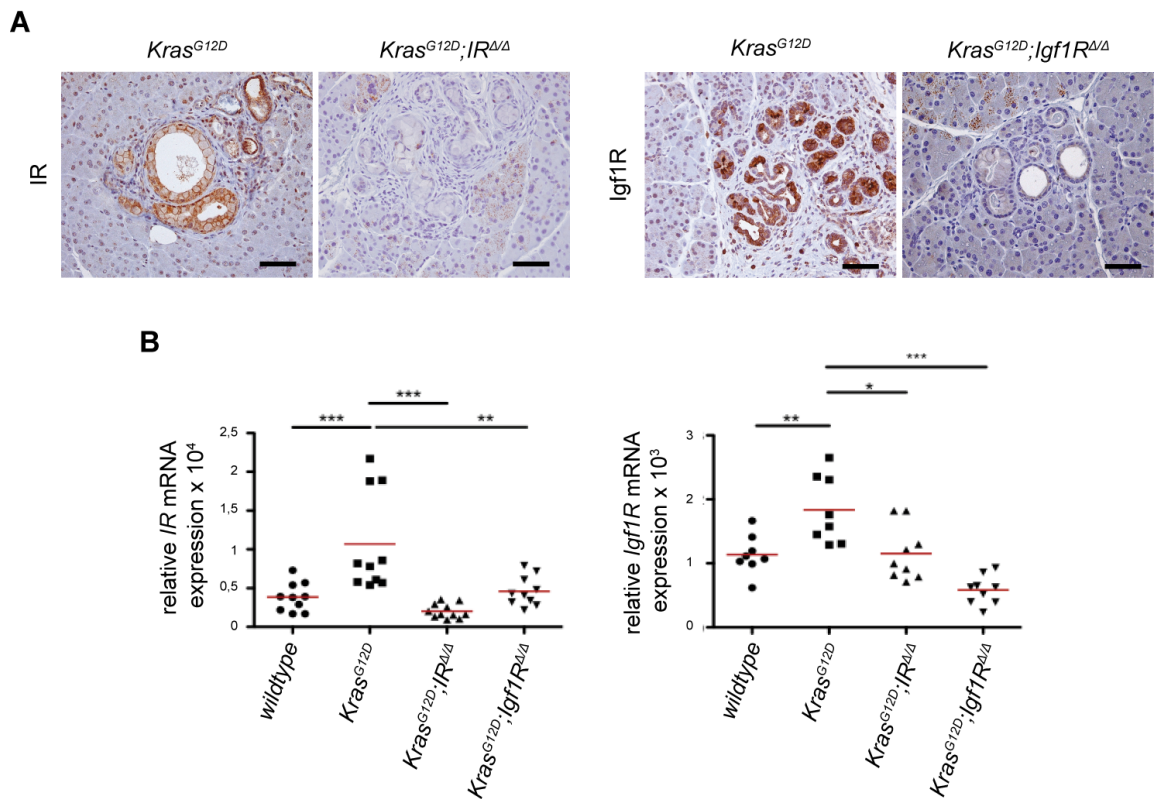
Figure 3.11: Igf1R and IR ablation in *Kras*^{G12D} mice.
(A) IHC analyses showed an increase Igf1R and IR expression in precursor lesions of *Kras*^{G12D} mice and the lost expression of these proteins in the respective knockout mice. Scale bar = 50 µm.
(B) Enhanced mRNA expression of *Igf1R* and *IR* in *Kras*^{G12D} mice compared to wildtype littermates was observed and a decrease of this expression in both knockout animals (n = 8-10, * p < 0.1, ** p < 0.01, *** p < 0.001).

3.3.2 Igf1R or IR ablation diminishes PanIN burden in *Kras*^{G12D} mice

Bodyweight comparison of 6 months old wildtype mice with *Kras*^{G12D}, *Kras*^{G12D};*Igf1R*$^{Δ/Δ}$, *Kras*^{G12D};*IR*$^{Δ/Δ}$ and *Kras*^{G12D};*Igf1R*$^{Δ/Δ}$;*IR*$^{Δ/Δ}$ animals revealed, similar to the findings without the Kras^{G12D} mutation an impaired development of the double knockout mice, but no differences between single knockout and control animals. The pancreas/body weight index of *Kras*^{G12D};*Igf1R*$^{Δ/Δ}$ and *Kras*^{G12D};*IR*$^{Δ/Δ}$ animals dropped to levels of wildtype littermates, however that of

heterozygous $Kras^{G12D}$;$Igf1R^{\Delta/+}$;$IR^{\Delta/+}$ mice was comparable to the $Kras^{G12D}$ controls. In $Kras^{G12D}$;$Igf1R^{\Delta/\Delta}$;$IR^{\Delta/\Delta}$ nearly no pancreas was detectable and again a life expectancy of only 2 months was observed (Fig. 3.12).
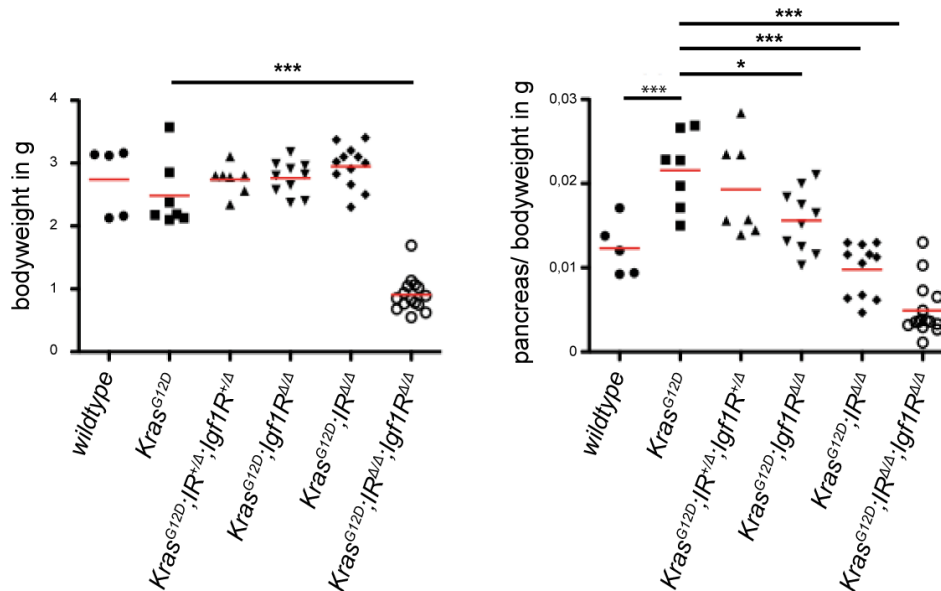
**Figure 3.12: Body and pancreas weight correlation of the different $Kras^{G12D}$ models.**
Comparable bodygrowth is shown for 6 months old wildtype, $Kras^{G12D}$, $Kras^{G12D}$;$Igf1R^{\Delta/\Delta}$, $Kras^{G12D}$;$IR^{\Delta/\Delta}$ and $Kras^{G12D}$;$Igf1R^{+/\Delta}$;$IR^{+/\Delta}$ mice. $Kras^{G12D}$;$Igf1R^{\Delta/\Delta}$;$IR^{\Delta/\Delta}$ animals exhibited an impairment of pancreas and body development. $Kras^{G12D}$ mice lacking one of the two receptors showed a wildtype like pancreas weight, whereas $Kras^{G12D}$ and $Kras^{G12D}$;$Igf1R^{+/\Delta}$;$IR^{+/\Delta}$ animals revealed an increase of pancreatic mass compared to wildtype littermates (n = 5-12, * p < 0.1, ** p < 0.01, *** p < 0.001).

Most surprisingly, both 6 months old $Kras^{G12D}$;$Igf1R^{\Delta/\Delta}$ and $Kras^{G12D}$;$IR^{\Delta/\Delta}$ mice showed already macroscopically unexpected distinctions compared to the controls. A macroscopic enlarged and cystic pancreas is frequent for $Kras^{G12D}$ animals at this age, whereas the pancreas of $Kras^{G12D}$;$Igf1R^{\Delta/\Delta}$ mice as well as $Kras^{G12D}$;$IR^{\Delta/\Delta}$ mice appeared smaller and similar to that of wildtype mice. The pancreas of $Kras^{G12D}$;$Igf1R^{+/\Delta}$;$IR^{+/\Delta}$ mice resembled the $Kras^{G12D}$ phenotype and as previously mentioned $Kras^{G12D}$;$Igf1R^{\Delta/\Delta}$;$IR^{\Delta/\Delta}$ animals displayed nearly no pancreas and did not reach the age of 6 months (Fig. 3.13). H&E staining of tissue from these mice including pancreas, liver, spleen, duodenum and lung (data not shown) was performed to figure out the underlying mechanism. The $Igf1R$ and IR heterozygous control mice showed the same morphological features as $Kras^{G12D}$ mice, larger areas of the pancreas were replaced by acinar-to-ductal metaplasia (ADM) and PanIN1-2 surrounded by abundant stroma, high quantity of inflammatory infiltrates and fibrosis everywhere. In

contrast to this, the $Kras^{G12D}$;$Igf1R^{\Delta/\Delta}$ and $Kras^{G12D}$;$IR^{\Delta/\Delta}$ littermates revealed significantly less preneoplastic lesions or metaplasia and only some small fibrotic areas (Fig. 3.13). No other organs were altered in both genotypes. Only $Kras^{G12D}$;$Igf1R^{\Delta/\Delta}$;$IR^{\Delta/\Delta}$ double- knockout mice exhibited the expected restricted pancreas development. However, the remaining pancreatic tissue of 6 to 8 weeks old $Kras^{G12D}$;$Igf1R^{\Delta/\Delta}$;$IR^{\Delta/\Delta}$ mice showed normal acinar structures and a completely blocked lesion formation (Fig. 3.13). Consequently, the reduction of pancreatic weight was attributed to an impressive impairment of mADM/PanIN development and substantial reduction of adjacent stroma in $Kras^{G12D}$;$Igf1R^{\Delta/\Delta}$ and $Kras^{G12D}$;$IR^{\Delta/\Delta}$ mice compared to $Kras^{G12D}$;$Igf1R^{+/\Delta}$;$IR^{+/\Delta}$ and $Kras^{G12D}$ littermates.
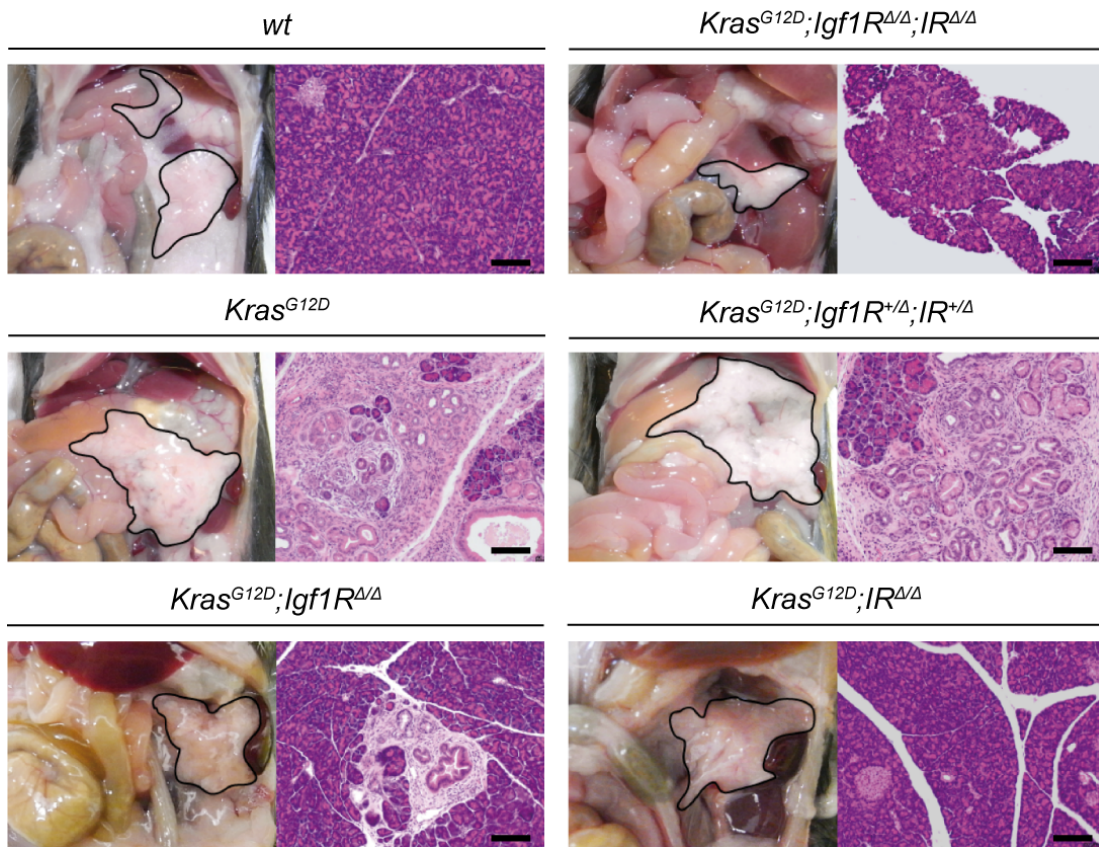
Figure 3.13: Loss of Igf1R and IR led to a substantial macroscopic and microscopic reduction of metaplastic processes in $Kras^{G12D}$ mice.
Macroscopic photographs of *wildtype*, $Kras^{G12D}$;$Igf1R^{\Delta/\Delta}$, $Kras^{G12D}$;$IR^{\Delta/\Delta}$, $Kras^{G12D}$;$Igf1R^{\Delta/\Delta}$;$IR^{\Delta/\Delta}$, $Kras^{G12D}$;$Igf1R^{+/\Delta}$;$IR^{+/\Delta}$ and $Kras^{G12D}$ pancreas at the age of 6 months. Note the wildtype like pancreas with a smaller size and the absence of visible cysts and stromal reaction in $Kras^{G12D}$;$Igf1R^{\Delta/\Delta}$ and $Kras^{G12D}$;$IR^{\Delta/\Delta}$ mice. Nearly no pancreatic tissue was detectable in $Kras^{G12D}$;$Igf1R^{\Delta/\Delta}$;$IR^{\Delta/\Delta}$ mice. The corresponding H&E stainings confirmed the macroscopic impression with a $Kras^{G12D}$ like phenotype of the heterozygous knockout mice, harbouring one remaining allel of each receptor and a wildtype like phenotype of the homozygous knockout mice with only rare focal PanIN lesions formation. The remaining pancreas of the double knockout mice exhibited normal acinar tissue without any lesion appearance. Scale bar = 50 µm.

To further substantiate the hypothesis of decreased PanIN formation in the knockout models, MUC5AC (marker specific for PanIN lesions) expression in the 6 months old $Kras^{G12D}$, $Kras^{G12D};Igf1R^{\Delta/\Delta}$ and $Kras^{G12D};IR^{\Delta/\Delta}$ mice was analysed (Fig. 3.14 A). Quantification of MUC5AC$^+$ lesions revealed significantly reduced PanIN formation in both knockout models in comparison to control animals. In double knockout mice PanIN formation was completely absent (Fig. 3.14 B). These observations led to the conclusion that complete genetic knockout of the $Igf1R$ or IR gene decreases metaplastic transdifferentiation but one remaining allele of those receptors is sufficient to support metaplastic processes.
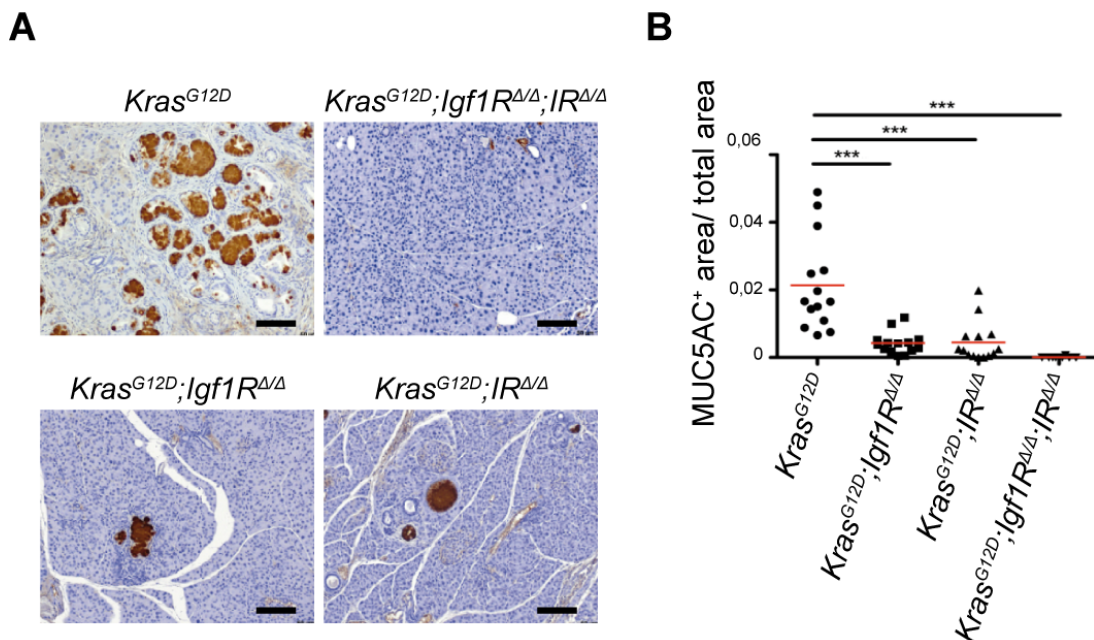
Figure 3.14: Less PanIN formation in $Kras^{G12D};Igf1R^{\Delta/\Delta}$ and $Kras^{G12D};IR^{\Delta/\Delta}$ mice.
(A) MUC5AC IHC stains specifically PanIN lesions in the different $Kras^{G12D}$ driven mouse models. Scale bar = 50 µm.
(B) Quantification of MUC5AC positive PanINs revealed a highly significant decrease in PanIN number for the 6 months old $Kras^{G12D};Igf1R^{\Delta/\Delta}$ and $Kras^{G12D};IR^{\Delta/\Delta}$ mice compared to $Kras^{G12D}$ littermates. Complete blockage of PanIN formation was seen in the 2 months old $Kras^{G12D};Igf1R^{\Delta/\Delta};IR^{\Delta/\Delta}$ mice (n = 8-10, *** p < 0.001).

3.3.3   Igf1R or IR ablation impairs PDAC development in $Kras^{G12D}$ mice

To detect whether the ablation of these receptors induced only a delay of PDAC initiation in this model an end-of-life analysis was used, in which a cohort of mice was followed for signs of disease progression until death. $Kras^{G12D}$ mice

have a median tumour onset of 12 months, but due to their human like heterogeneity in PDAC development the median survival is also 1 year. The majority of $Kras^{G12D}$;$Igf1R^{\Delta/\Delta}$ animals showed a significantly reduced life span comparable to $Igf1R^{\Delta/\Delta}$ mice (Fig.: 3.10). Nonetheless endpoint analyses of those mice were showing a wildtype pancreatic situation, consisting mostly of normal acinar tissue with only rare fibrotic areas and poor lesion formation, incomparable to the pancreatic situation of $Kras^{G12D}$ littermates. A minor group of $Kras^{G12D}$;$Igf1R^{\Delta/\Delta}$ mice and almost all $Kras^{G12D}$;$IR^{\Delta/\Delta}$ mice shared a significantly prolonged survival rate and developed, in contrast to their $Kras^{G12D}$ littermates, exceptionalness never PDAC (Fig. 3.15 B). Furthermore, $Kras^{G12D}$;$IR^{\Delta/\Delta}$ mice exhibited a median survival similar to that of $IR^{\Delta/\Delta}$ mice, emphasizing the survival prolonging effects of the pancreatic IR ablation. Histological end-point-analysis of both knockout models indicated high-grade fatty metaplasia of the acinar structures with a few remaining low grad PanINs and fibrotic areas embedded in adipose structures under the oppressive conditions of the oncogenic KRAS instead of progression to cancer (Fig. 3.15 A).

51

A

$Kras^{G12D}$ $Kras^{G12D};Igf1R^{\Delta/\Delta}$ $Kras^{G12D};IR^{\Delta/\Delta}$

B

Legend:
- $Kras^{G12D}$ (400 days)
- $Kras^{G12D};Igf1R^{\Delta/\Delta}$ (213 days)
- $Kras^{G12D};IR^{\Delta/\Delta}$ (673 days)
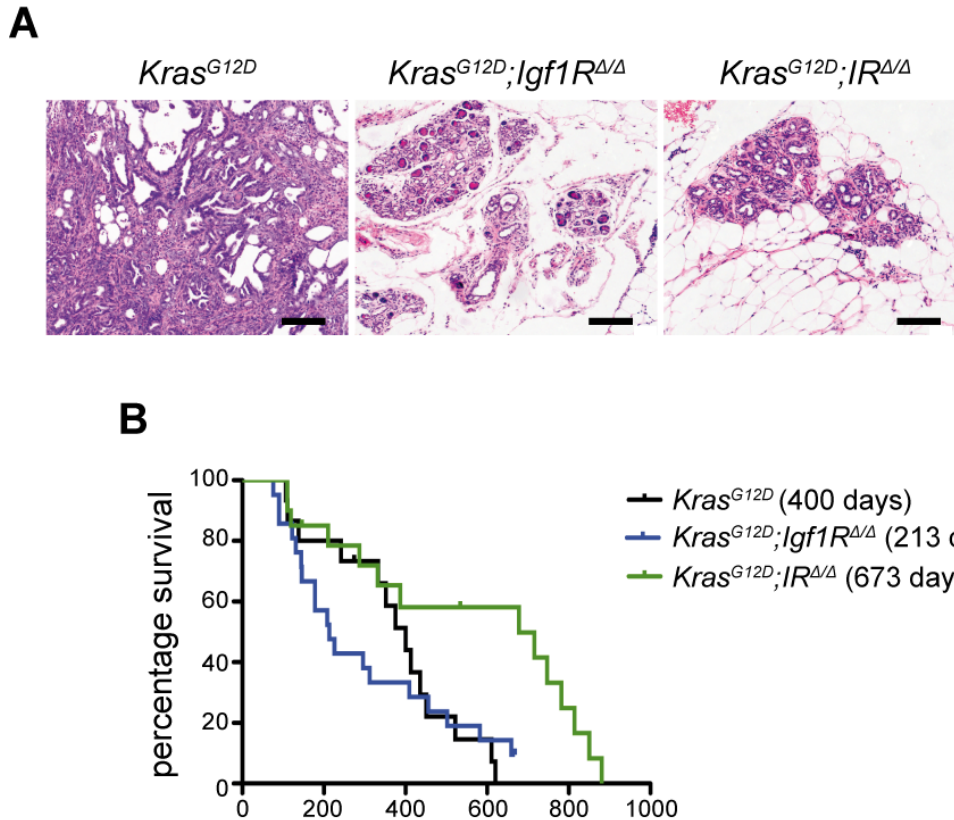
Figure 3.15: Loss of Igf1R or IR inhibited progression to PDAC in $Kras^{G12D}$ mice.
(A) Representative examples of end-point-histology (H&E staining) of pancreatic tissue from 24 months old $Kras^{G12D};Igf1R^{\Delta/\Delta}$ and $Kras^{G12D};IR^{\Delta/\Delta}$ mice compared to $Kras^{G12D}$ littermates. Left panel: well-differentiated murine PDAC, middle and right panel: adipose replacement of acinar structure with few non-malignant duct-like complexes. Scale bar = 50 µm.
(B) Survival analysis of $Kras^{G12D};Igf1R^{\Delta/\Delta}$ (n = 19, median 213 days, p = 0,0375 ($Kras^{G12D}$ vs. $Kras^{G12D};Igf1R^{\Delta/\Delta}$)) and $Kras^{G12D};IR^{\Delta/\Delta}$ mice (n = 14, median 673 days, p = 0,0158 ($Kras^{G12D}$ vs. $Kras^{G12D};IR^{\Delta/\Delta}$)) compared to $Kras^{G12D}$ littermates (n = 14, median 400 days).

To better understand the reasons for the reduced survival of $Igf1R^{\Delta/\Delta}$ and $Kras^{G12D};Igf1R^{\Delta/\Delta}$ mice, further blood analyses were performed next to the first metabolic investigations. Based on the finding of a disturbance in glucose uptake in $Igf1R^{\Delta/\Delta}$ mice, glucose levels and potentially thereof affected parameters have been measured. The haemogram of early diseased $Kras^{G12D};Igf1R^{\Delta/\Delta}$ mice showed elevated levels of glucose and GTP (glutamate pyruvate transaminase, indicator for liver damage), but no differences in CK (creatine kinase, indicator for energy metabolism) and LDH levels (lactate dehydrogenase, indicator for tissue damage) (Fig. 3.16 A). To further confirm liver damage as possible cause for the shortened life expectancy, glucose and GTP blood levels of healthy $Kras^{G12D}$, $Kras^{G12D};Igf1R^{\Delta/\Delta}$ and $Kras^{G12D};IR^{\Delta/\Delta}$ mice were determined. Elevated glucose levels as consequence of the disturbance in glucose uptake but not GTP levels were observed in 6 months old healthy $Kras^{G12D};Igf1R^{\Delta/\Delta}$ mice (Fig. 3.16 B). Thus, a possible explanation for the

reduced survival could be initially a hyperglycemia, leading to ketogenic, hyperglycemic acidosis and secondary liver problems.

In accordance with these findings the deletion of only one of those two receptors is sufficient to effectively block tumour development in a $Kras^{G12D}$ mediated background, despite initial steps are already present in the respective tissue.
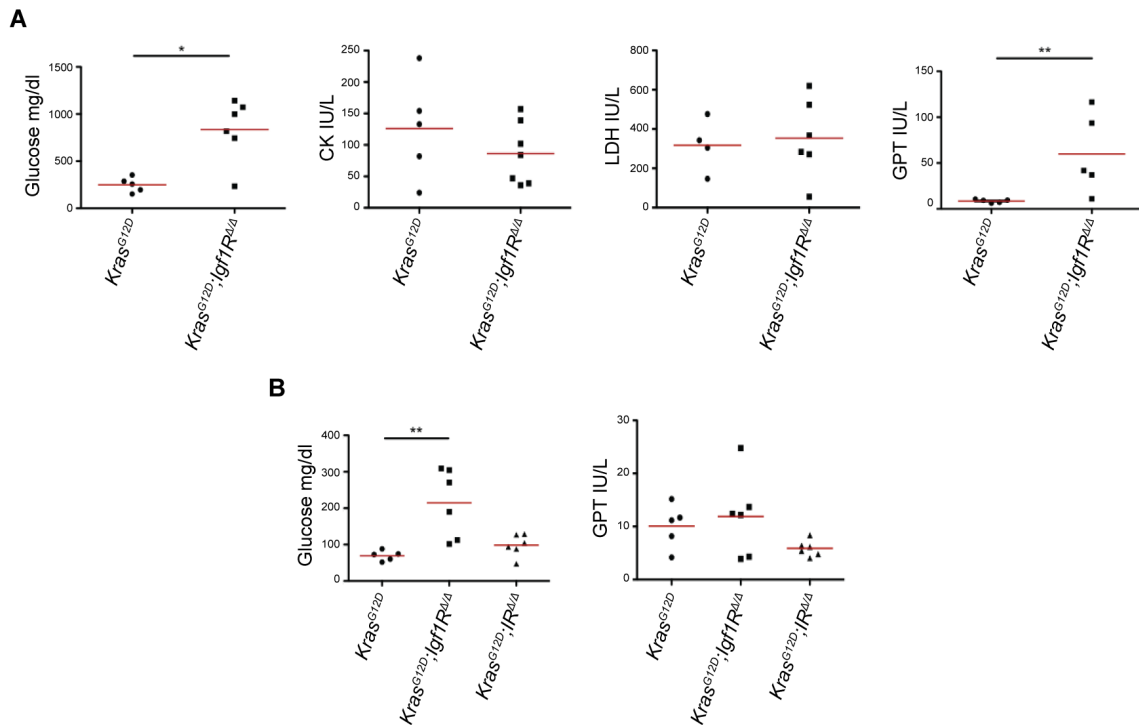
Figure 3.16: A disturbed glucose uptake and consequently elevated GTP levels as cause for the early dying of $Kras^{G12D};Igf1R^{\Delta/\Delta}$ mice.
(A) Early diseased $Kras^{G12D};Igf1R^{\Delta/\Delta}$ mice offered elevated glucose and GTP levels compared to $Kras^{G12D}$ animals of the same age (n = 4-6, * $p < 0.1$, ** $p < 0.01$).
(B) Healthy $Kras^{G12D};Igf1R^{\Delta/\Delta}$ mice exhibited only elevated blood glucose levels, blood GTP levels were comparable to $Kras^{G12D}$ and $Kras^{G12D};IR^{\Delta/\Delta}$ mice (n = 4-6, * $p < 0.1$, ** $p < 0.01$).

3.4 Igf1R/IR hybrid receptors are necessary for PanIN proliferation and progression to PDAC in $Kras^{G12D}$ mice

3.4.1 Loss of Igf1R or IR reduces proliferation of $Kras^{G12D}$ induced PanINs

To further clarify the aspect of reduced PanIN formation and subsequent impaired PDAC development through pancreatic deletion of Igf1R and IR in a $Kras^{G12D}$ mediated background, the proliferation rate of existing PanINs in

$Kras^{G12D}$, $Kras^{G12D};Igf1R^{\Delta/\Delta}$ and $Kras^{G12D};IR^{\Delta/\Delta}$ mice was assessed. Sequential slides of pancreatic tissue of the different 6-month-old knockout models and control animals were stained for Ki67 and MUC5AC to quantify proliferating cells only in MUC5AC positive PanINs. The Ki67 positive cells of the MUC5AC positive PanINs were counted and indeed, $Kras^{G12D};Igf1R^{\Delta/\Delta}$ and $Kras^{G12D};IR^{\Delta/\Delta}$ mice showed a significantly reduced proliferation of PanINs in comparison to $Kras^{G12D}$ control mice (Fig. 3.17 A and B). These results suggest that PanINs of $Kras^{G12D}$ mice are in need of these two receptors to proliferate and progress to higher-grade lesions and afterwards to PDAC. To further confirm this hypothesis immunohistochemical staining for Igf1R in human PDAC tissue was performed. A very high expression of Igf1R could be detected in PanIN1 lesion and no expression in ducts. Quantification and qualification of the Igf1R staining in human PanINs was showing high expression in early stages, and a decreased signal in higher grade PanINs. This outcome is additionally verifying the assumption of a need of this receptor in initial stages also in the human situation (Fig. 3.17 C). These results illustrate the requirement of the IR and the Igf1R for PanIN proliferation in a $Kras^{G12D}$ mediated background. For this very reason, deletion of one of those receptors resulted in less PanIN formation and blocked tumour development in $Kras^{G12D};Igf1R^{\Delta/\Delta}$ and $Kras^{G12D};IR^{\Delta/\Delta}$ mice.
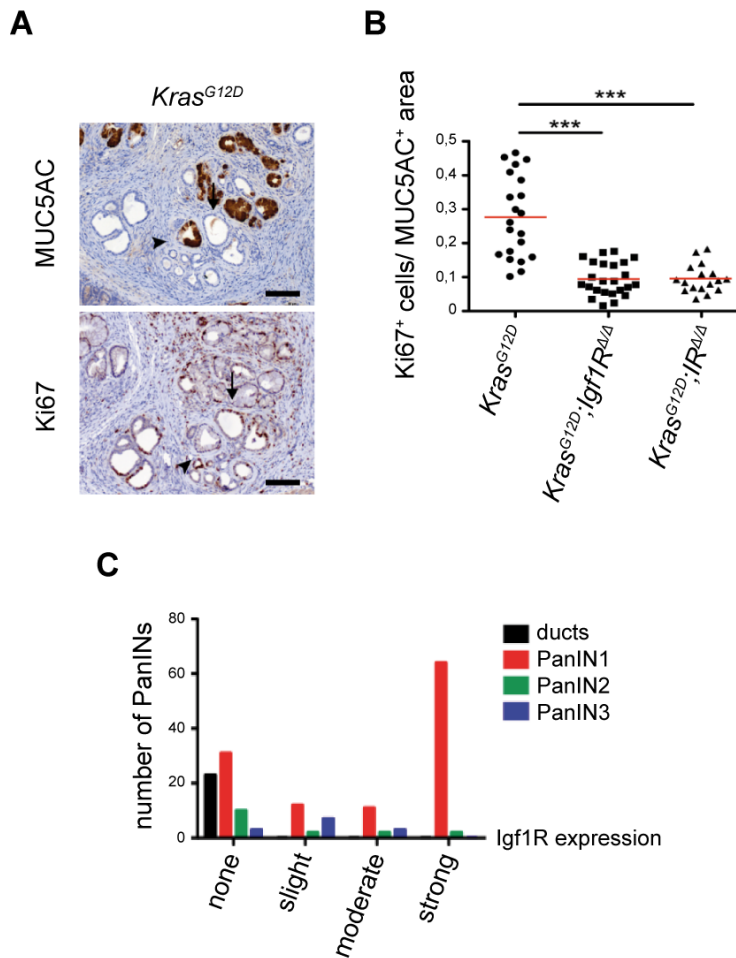
Figure 3.17: Early PanINs lesions require Igf1R and IR to proliferate and progress in higher grade PanINs and PDAC.
(A) Sequential slides of MUC5AC and Ki67 immunohistochemistry to count the proliferating cells only in PanINs. Scale bar = 50 µm.
(B) Quantification of proliferating Ki67 positive cells in MUC5AC positive PanINs showed a significant decrease of PanIN proliferation in $Kras^{G12D};Igf1R^{\Delta/\Delta}$ and $Kras^{G12D};IR^{\Delta/\Delta}$ mice compared to $Kras^{G12D}$ mice (n = 8-10, *** p < 0.001).
(C) Qualification and quantification of an Igf1R IHC of human tissue revealed a high Igf1R expression in early PanIN1 stages and less expression in higher grade PanINs and normal ducts.

3.4.2 Igf1R and IR hybrid receptors and not holoreceptors are the major players in PDAC formation

The similar phenotype caused by ablation of either Igf1R or IR in $Kras^{G12D}$ mice (Fig. 3.13 and 3.14) raised the possibility that these two receptors form predominantly heterodimers in pancreatic tumour cells, as hybrid receptors are very common in different cancers [94]. Furthermore, Western Blot analysis for Igf1R and IR of murine $Kras^{G12D}$ cell lines was showing a nearly identical expression pattern of the two receptors (Fig. 3.7 D). Also, qRT-PCR for mRNA expression of *Igf1R* and *IR* indicated an interplay of the two receptors by simultaneous down regulation of both receptors in both knockout models (Fig. 3.11 B). To elucidate this further, immunoprecipitation in three early-passaged tumour explants from $Kras^{G12D}$ mice was performed, Igf1R or IR were immunoprecipitated and blotted for IR or Igf1R, respectively. In each cell explant immunoprecipitated Igf1R exhibited a highly bound IR and *vice versa*

(Fig: 3.18). This analysis demonstrated a strong presence of Igf1R/IR hybrid receptors in murine PDAC. In summary, Igf1R and IR, in the conformation of hybrid receptors are required for the proliferation and progression of PanINs and to PDAC in a $Kras^{G12D}$ mediated background.
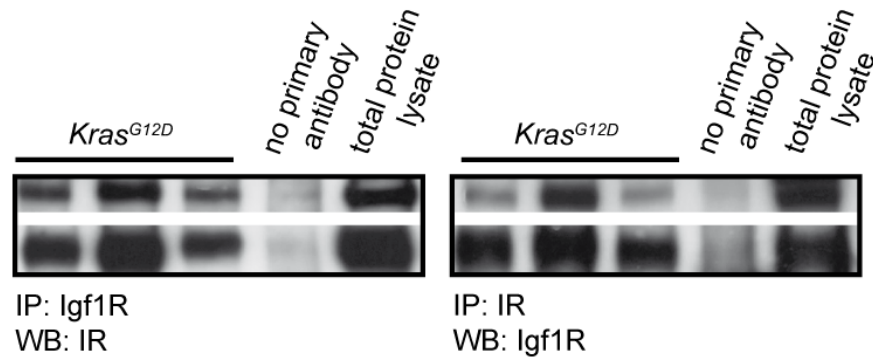
Figure 3.18: Igf1R/IR hybrid receptors and not holoreceptor predominate in the $Kras^{G12D}$ model.
Immunoprecipitation of Igf1R and blotted for IR and *vice versa* offered a strong expression of Igf1R/IR hybrid receptors in murine $Kras^{G12D}$ cells (upper band shows precursor protein, lower band the matured protein).

3.5 Igf1R and IR regulate the PI3K pathway and subsequential PDAC development

3.5.1 Loss of Igf1R and IR has no impact on the major EGFR-related pathways in a $Kras^{G12D}$ mediated background

Pancreatic tumourigenesis is dependent on several molecules that have been associated with EGFR signalling, including STAT3 activation [95] [96]. To analyse a possible connection of Igf1R and IR with this pathway, IHC for active phospho-STAT3 in $Kras^{G12D}$, $Kras^{G12D};Igf1R^{\Delta/\Delta}$ and $Kras^{G12D};IR^{\Delta/\Delta}$ mice was performed. In areas of lesion formation in pancreatic tissue of Igf1R and IR knockout mice phospho-STAT3 signal was present (Fig. 3.19 A). The significant difference in the quantification of phospho-STAT3 positive nuclei was due to the lower metaplastic processes in the two knockout models (Fig. 3.19 B). So this very dominant signalling pathway in PDAC was unaltered in $Kras^{G12D};Igf1R^{\Delta/\Delta}$ and $Kras^{G12D};IR^{\Delta/\Delta}$ mice compared to $Kras^{G12D}$ mice and consequently not reason for the decreased proliferation and formation of PanIN lesions.
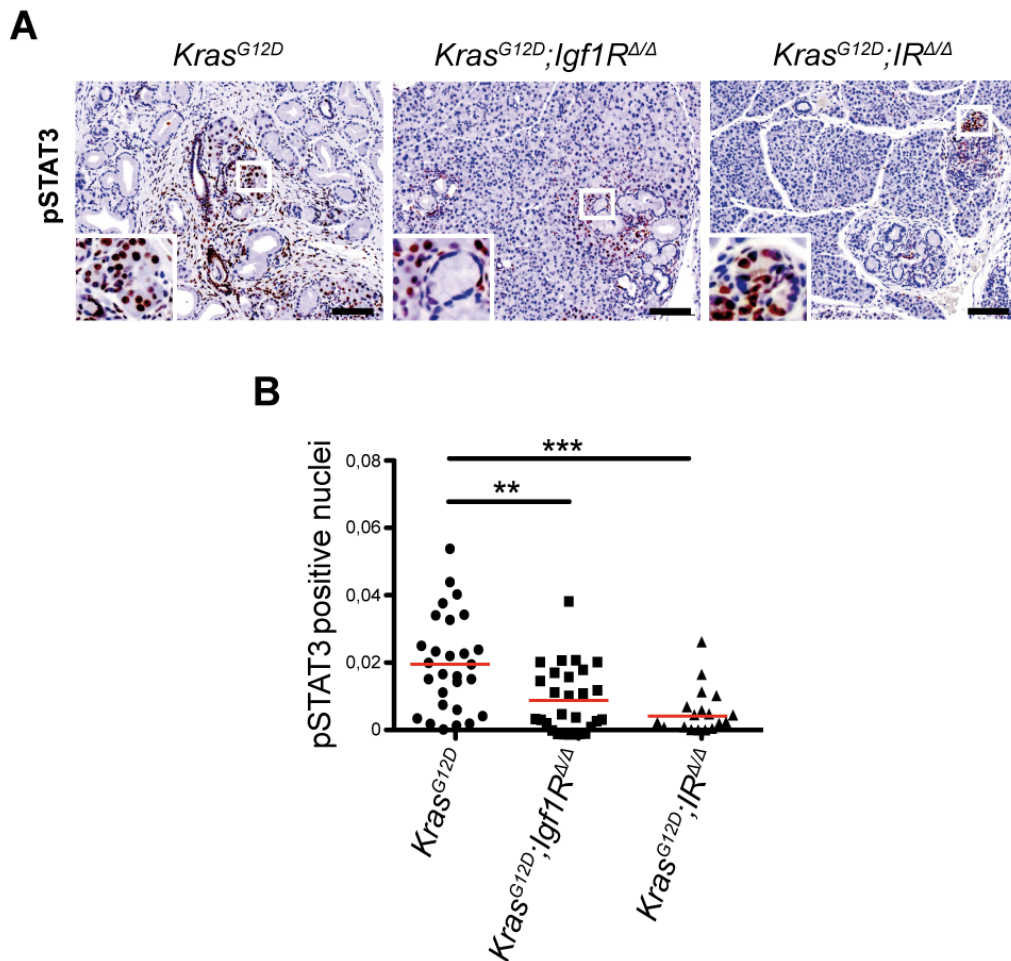
Figure 3.19: No differences of active phospho -STAT3 signalling in $Kras^{G12D};Igf1R^{\Delta/\Delta}$ and $Kras^{G12D};IR^{\Delta/\Delta}$ mice.
(A) Phospho-STAT3 IHC showed Stat3 activity in metaplastic areas in both knockout models, comparable to $Kras^{G12D}$ controls. Scale bar = 50 µm.
(B) Quantification of phospho-STAT3 positive nuclei revealed a significant decrease of the signal in $Kras^{G12D};Igf1R^{\Delta/\Delta}$ and $Kras^{G12D};IR^{\Delta/\Delta}$ mice, due to less fibrotic areas in those mice compared to $Kras^{G12D}$ littermates (n = 8-10, ** p < 0.01, *** p < 0.001).

3.5.2 Decreased active AKT but not ERK signalling in $Kras^{G12D};Igf1R^{\Delta/\Delta}$ and $Kras^{G12D};IR^{\Delta/\Delta}$ mice

Next I explored if the Igf1R and the IR regulate the activity levels of other pathways that contribute to the transforming potential of unregulated KRAS signalling. In PDAC the PI3K and MAPK signalling pathways are the two most deregulated signalling cascades [81] and the key actions of IRs and Igf1Rs are mainly performed via these two pathways [56]. Furthermore, it was already shown that despite the oncogenic activity of mutated KRAS this PDAC signalling network requires additional co-workers to achieve its invasiveness

[41]. To detect the explicit role of both receptors in this huge network, the expression of these two major Ras- dependent signalling modules was analysed. Notably, $Kras^{G12D};Igf1R^{\Delta/\Delta}$ and $Kras^{G12D};IR^{\Delta/\Delta}$ mice had no differences in the phosphorylation levels of some of the key contributor proteins, like ERK and STAT3 but showed a clear reduction of phosphorylated AKT (Fig. 3.20 A and B). Initial Western Blot analysis offered a slight decrease of phosphorylated ERK but a nearly absent phospho-AKT signal (Fig. 3.20 A). To further proof if the decreased activity signal of these two, in $Kras^{G12D}$ mice strongly up regulated pathways was ascribed to less lesion formation in the $Kras^{G12D};Igf1R^{\Delta/\Delta}$ and $Kras^{G12D};IR^{\Delta/\Delta}$ mice, IHC was performed. The Immunohistochemistry confirmed an active ERK signal in the remaining lesions of $Kras^{G12D};Igf1R^{\Delta/\Delta}$ and $Kras^{G12D};IR^{\Delta/\Delta}$ mice, but a decreased activity of AKT in these ADMs and PanINs compared to $Kras^{G12D}$ control animals (Fig. 3.20 B). Consequently, the reduced phospho-ERK signal in the Western Blot analysis was again due to reduced metaplastic activity in the knockout mice. Blockade of PI3K/AKT signalling may be the cause of the $Kras^{G12D};Igf1R^{\Delta/\Delta}$ and $Kras^{G12D};IR^{\Delta/\Delta}$ phenotype.
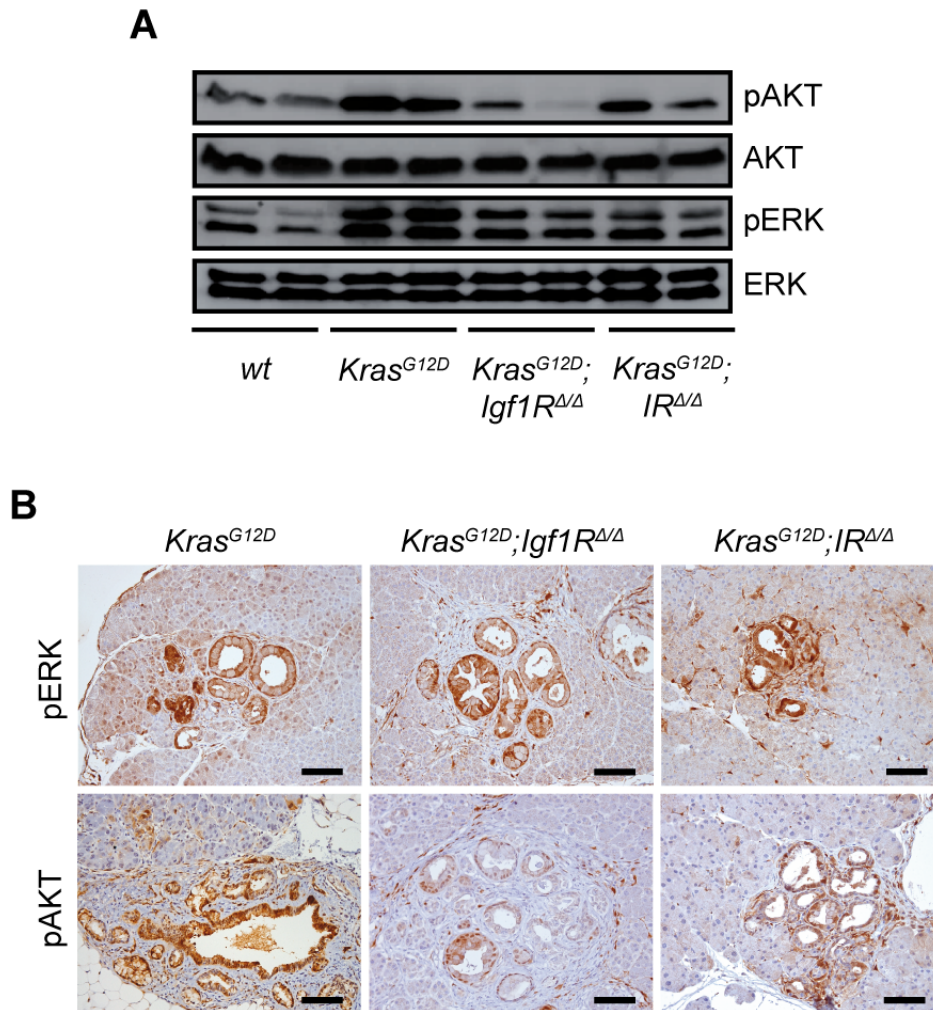
Figure 3.20 Decreased active phospho-AKT, but not phospho-ERK signalling in $Kras^{G12D};Igf1R^{\Delta/\Delta}$ and $Kras^{G12D};IR^{\Delta/\Delta}$ mice.
(A) Western Blot analysis was showing a slight decrease of active ERK signalling and a strong difference in phospho-AKT expression in the Igf1R and IR knockout mice.
(B) Immunohistochemistry for phospho-AKT and phospho-ERK offered only a reduced activity of AKT but not of ERK in the existing lesions of both knockout models. Scale bar = 50 µm.

3.5.3 Conditional activation of the PI3K, but not MAPK can reverse the $Kras^{G12D};Igf1R^{\Delta/\Delta}$ and $Kras^{G12D};IR^{\Delta/\Delta}$ phenotype

To confirm the reduced PI3K activity as molecular mechanism for decreased PanIN formation and inhibited progression to cancer in $Igf1R^{\Delta/\Delta}$ and $IR^{\Delta/\Delta}$ mice in a $Kras^{G12D}$ mediated background, mouse strains with pancreas-specific activation of MEK/ERK signalling (mouse strain with conditional activation of constitutively active MEK1-DD [49]) and conditional activation of PI3K (mouse strain with the constitutively active p110a^{H1047R} subunit of the PI3K; generated and collaboratively provided by D. Saur, TU Munich, [50]) were generated. For this approach $Ptf1a^{wt/Cre}$ lines were crossed to $Mek1^{wt/LSL-DD}$ and

$p110a^{wt/LSL-H1047R}$ mice. These GEMM show very similar pattern of ADM induction and PanIN progression and activation of the MAPK and PI3K pathways. To examine the hypothesis of less PI3K signalling as cause for blocked PanIN and PDAC development in $Kras^{G12D};Igf1R^{\Delta/\Delta}$ and $Kras^{G12D};IR^{\Delta/\Delta}$ mice, $Igf1R^{\Delta/\Delta}$ and $IR^{\Delta/\Delta}$ mice were crossed to $p110a^{H1047R}$ animals. If the absence of Igf1R and IR translates into diminished PI3K activity and consequently reduced PanIN formation and progression, a downstream reactivation of this pathway would overcome this blockage. Indeed the reappearance of an active PI3K cascade rescued the $Kras^{G12D};Igf1R^{\Delta/\Delta}$ and $Kras^{G12D};IR^{\Delta/\Delta}$ phenotype and induced lesion formation, as well as cancer development in $p110a^{H1047R};Igf1R^{\Delta/\Delta}$ and $p110a^{H1047R};IR^{\Delta/\Delta}$ mice comparable to $p110a^{H1047R}$ control animals. Immunohistochemical analysis of phospho-AKT and phospho-ERK expression showed similar amounts in knockout mice and $p110a^{H1047R}$ littermates, indicating the contributory presence of the two, in PDAC most dominant, cascades (Fig. 3.21 A). To further analyse this, $Mek1^{DD};Igf1R^{\Delta/\Delta}$ and $Mek1^{DD};IR^{\Delta/\Delta}$ mice were generated. If the PI3K regulation through Igf1R and IR is the relevant mechanism for the $Kras^{G12D};Igf1R^{\Delta/\Delta}$ and $Kras^{G12D};IR^{\Delta/\Delta}$ phenotype, upregulation of downstream components of the MAPK should not reverse the decreased PanIN formation and progression. Indeed, 3 months old $Mek1^{DD};Igf1R^{\Delta/\Delta}$ and $Mek1^{DD};IR^{\Delta/\Delta}$ mice offered a strongly depressed metaplastic situation compared to $Mek1^{DD}$ animals of the same age. Thus elevated MEK/ERK signalling, like it is the case in $Kras^{G12D}$ mice, is insufficient to promote PDAC in an Igf1R/IR deleted background. While phospho-ERK is comparably expressed in $Mek1^{DD};Igf1R^{\Delta/\Delta}$, $Mek1^{DD};IR^{\Delta/\Delta}$ and $Mek1^{DD}$ mice, the phospho-AKT signal decreases in the respective Igf1R and IR knockout mice (Fig. 3.21 B). In conclusion, an active MEK/ERK cascade requires an unlocked PI3K pathway to promote malignancy and Igf1Rs as well as IRs are the key regulators of the PI3K axis.
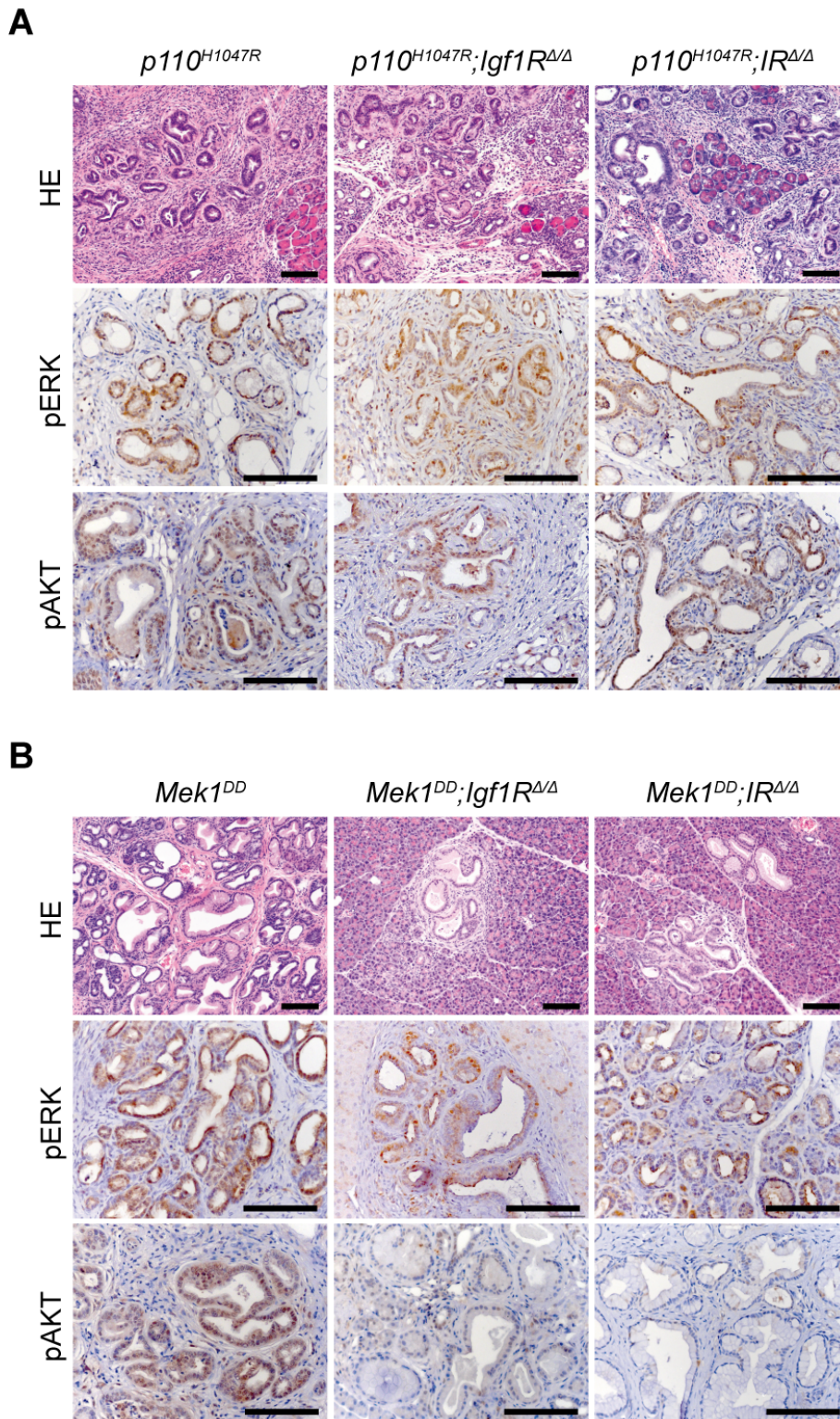
Figure 3.21 Conditional downstream activation of the PI3K but not the MAPK rescues the $Kras^{G12D};Igf1R^{\Delta/\Delta}$ and $Kras^{G12D};IR^{\Delta/\Delta}$ phenotype.

(A) $P110a^{H1047R};Igf1R^{\Delta/\Delta}$ and $p110a^{H1047R};IR^{\Delta/\Delta}$ mice at the age of 3 months were showing comparable ADM and lesion formation to $p110a^{H1047R}$ control animals. The dominant activation of the PI3K signalling in an Igf1R/IR deleted background reversed the inhibition of PanIN formation and progression in the $Kras^{G12D}$ model. The downstream ERK and AKT activity in both knockout models was comparable to the controls. Scale bar = 50 µm.

(B) A conditional activation of MEK signalling was insufficient to promote PanIN formation and progression when IR and Igf1R were lacking. 3 months old $Mek1^{DD};Igf1R^{\Delta/\Delta}$, $Mek1^{DD};IR^{\Delta/\Delta}$ mice were showing strongly reduced metaplastic processes compared to $Mek1^{DD}$ controls and a decreased phospho-AKT expression in the present lesions. Scale bar = 50 µm.

Furthermore, as expected from the $Igf1R^{\Delta/\Delta};IR^{\Delta/\Delta}$ and $Kras^{G12D};Igf1R^{\Delta/\Delta};IR^{\Delta/\Delta}$ mice, $Mek1^{DD};Igf1R^{\Delta/\Delta};IR^{\Delta/\Delta}$ animals offered a short lifespan of around 6 weeks. In all these three mouse models the simultaneous deletion of the Igf1R and IR led to a restricted pancreas and body development and a very short life expectancy. Surprisingly in the $p110a^{H1047R}$ background, the double knockout did not show this limited phenotype. $P110a^{H1047R};Igf1R^{\Delta/\Delta};IR^{\Delta/\Delta}$ mice showed normal body and pancreas development and were phenotypically completely comparable to $p110a^{H1047R}$ littermates. Survival analysis offered an extended lifespan of $p110a^{H1047R};Igf1R^{\Delta/\Delta};IR^{\Delta/\Delta}$ mice in contrast to all other double knockout animals (Fig. 3.22). This finding confirmed that reactivation of the AKT pathway rescues not only the blocked PDAC progression but also the restricted developmental phenotype, achieved through biallelic ablation of both receptors. Taken together, on one side AKT signalling is strongly regulated through Igf1R and IR and on the other side the PI3K pathways is relevant for both for PDAC formation as well as for normal development.
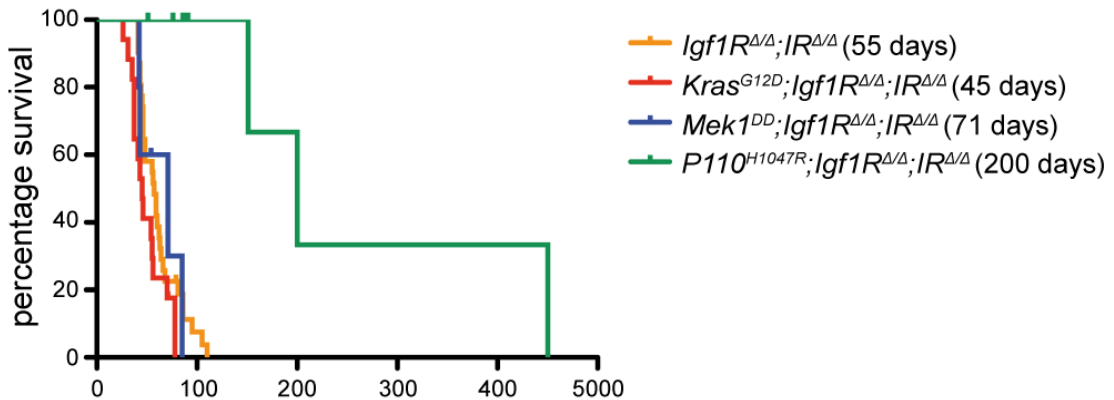
Figure 3.22: Survival analysis of $Igf1R^{\Delta/\Delta};IR^{\Delta/\Delta}$ mice.
Pancreas specific deletion of Igf1R together with IR led to a hypomorphic pancreas, a developmental impairment and a very short survival of around 6 weeks. Mice with an additional activating mutation of the $Kras^{G12D}$ or $Mek1^{DD}$ (n = 6, median 65 days) oncogene did not rescue this phenotype. Whereas $p110a^{H1047R};Igf1R^{\Delta/\Delta};IR^{\Delta/\Delta}$ mice showed normal body and pancreas development and had a median survival comparable to $p110a^{H1047R}$ littermates (n = 8, median 200 days, p < 0.0001 ($p110a^{H1047R};Igf1R^{\Delta/\Delta};IR^{\Delta/\Delta}$ vs. $Mek1^{DD};Igf1R^{\Delta/\Delta};IR^{\Delta/\Delta}$)).

3.6 Igf1R and IR ablation can block PDAC development in $Kras^{G12D}$ mice with additional mutation or deletion of p53

To emphasize the relevance of Igf1R and IR signalling for PDAC progression a

more aggressive GEMM for cancer development through additional modulation of p53 was generated: $Kras^{G12D};p53^{R172H};Igf1R^{\Delta/\Delta}$, $Kras^{G12D};p53^{R172H};IR^{\Delta/\Delta}$ and $Kras^{G12D};p53^{\Delta/\Delta};IR^{\Delta/\Delta}$ [31] [45]. $Kras^{G12D}$ mice with an additional activation of a dominant-negative R172H mutation of *p53* develop invasive and metastatic PDAC starting as early as 2.5 months, whereas a biallelic conditional loss of p53 induces a more aggressive phenotype with a tumour onset of 5 to 6 weeks [14]. Lack of Igf1R or IR signalling in these knockout mice resulted in strong ADM and PanIN development, but almost no progression to PDAC compared to controls of the same age (Fig. 3.23). Unfortunately, it was not possible to investigate later time points, since both PDAC models develop neurological disorders at a certain age resulting into earlier termination criteria. These results further strengthen the hypothesis that Igf1R and IR signalling is a crucial event for the progression of preneoplastic lesions to PDAC.
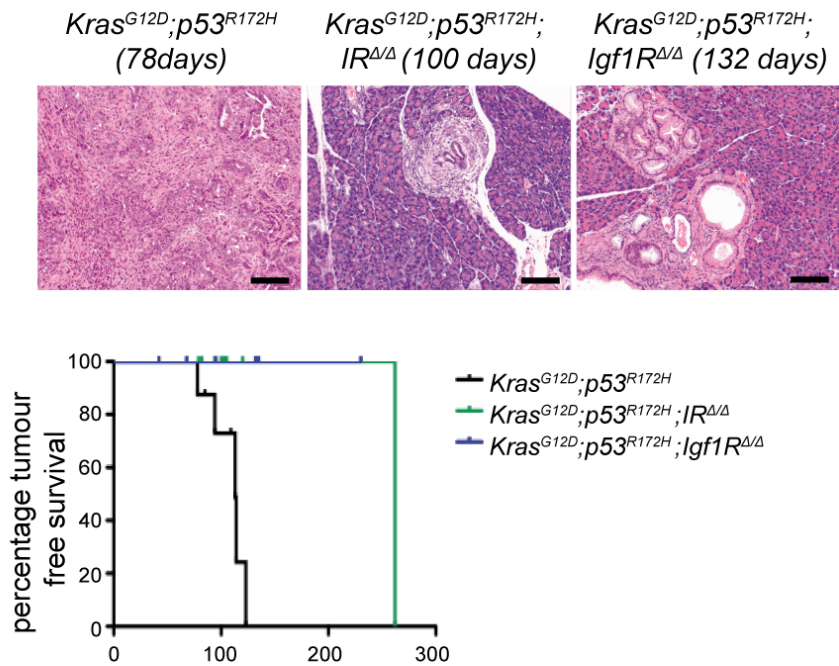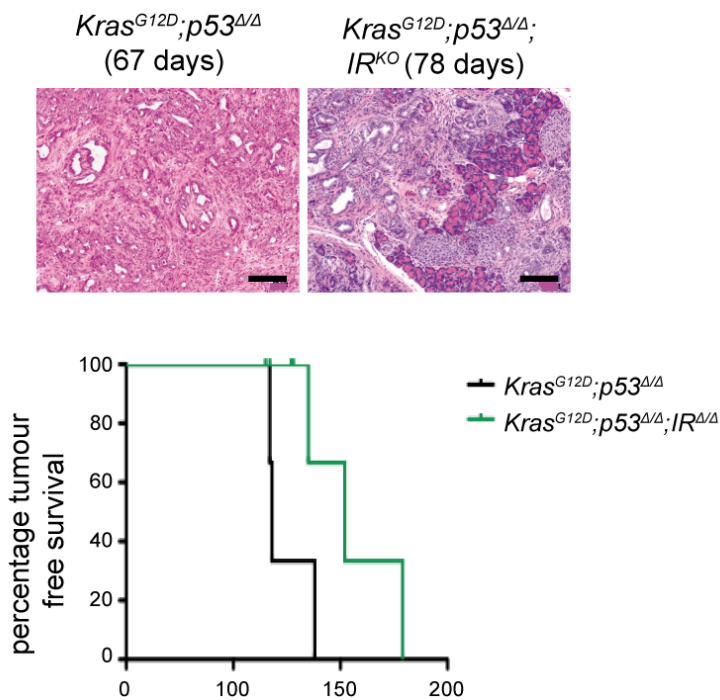
Figure 3.23 No progression to PDAC in *Kras^G12D* mice with additional p53 mutation or deletion through loss of Igf1R and IR.
(A) *Kras^G12D;p53^R172H* mice (n = 8, median tumour onset 113 days) developed tumours at around 10 weeks of age. At that time point only ADM and PanIN development, but no progression to PDAC could be observed in *Kras^G12D;p53^R172H;Igf1R^Δ/Δ* (n = 6, p = 0,0155 (*Kras^G12D;p53^R172H* vs. *Kras^G12D;p53^R172H;Igf1R^Δ/Δ*)) and *Kras^G12D;p53^R172H;IR^Δ/Δ* mice (n = 9, p = 0,0311 (*Kras^G12D;p53^R172H* vs. *Kras^G12D;p53^R172H;IR^Δ/Δ*)). Scale bar = 50 μm.
(B) *Kras^G12D* mice with an additional biallelic deletion of p53 resulted in a very aggressive PDAC model with tumour initiation as early as with around 5 weeks (n = 3, median tumour onset 68 days). This could be rescued through pancreatic deletion of the IR (n = 7, median tumour onset 102 days, p = 0,0367 (*Kras^G12D;p53^Δ/Δ* vs. *Kras^G12D;p53^Δ/Δ;IR^Δ/Δ*)). Scale bar = 50 μm.

3.7 Testing Igf1R and IR inhibitors for PDAC treatment

Based on the findings presented in the previous chapters it was hypothesized that depletion or inactivation of Igf1R and IR may inhibit pancreatic tumour growth. Subsequently, an available Igf1R/IR inhibitor was tested *in vitro*.

3.7.1 Blockage of Igf1R and IR activity by BMS-754807 inhibits survival of *Kras^{G12D}* cells in a dose dependent manner

BMS-754807 is a reversible small molecule tyrosine kinase inhibitor of Igf1R and IR. BMS-754807 has shown antitumour activity in a broad range of tumour types *in vitro* and *in vivo* [97] [98] [99]. First *in vitro* experiments with BMS-754807 affirmed reduced cell viability of several treated *Kras^{G12D}* cells but with different sensitivities to the inhibitor (Fig. 3.24 A). To address this heterogenic sensitivity pattern, the different *Kras^{G12D}* cell lines were analysed for their phospho-ERK and phospho-AKT expression (Fig. 3.24 B). Indeed, *Kras^{G12D}* cell lines with a higher phospho-AKT expression showed increased sensitivity to the inhibitor than cells with an additional strong ERK activation (Fig. 3.24 A). Thus, repression of Igf1R and IR by BMS-754807 induces growth inhibition in *Kras^{G12D}* driven pancreatic cancer cell lines. The different sensitivity of the drug, dependent on the distinct phospho-AKT and phospho-ERK expression of the cells, indicates a potential personalized treatment approach.
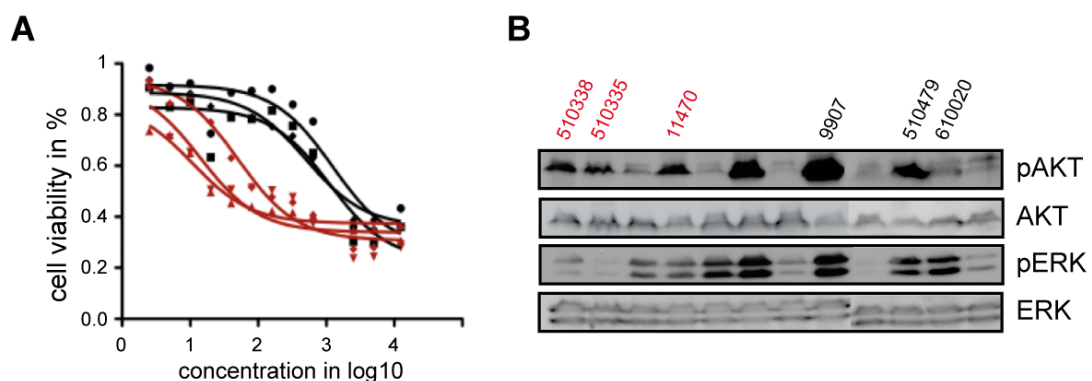
Figure 3.24 BMS-754807 inhibits cell viability with a higher sensitivity to *Kras^{G12D}* cells, showing strong phospho-AKT expression.
(A) Cell viability assay with BMS-754807, exhibiting a high sensitivity for *Kras^{G12D}* cells with a higher phospho-AKT than phospho-ERK expression.
(B) Expression of active ERK and AKT of the analysed *Kras^{G12D}* cell lines.

4. Discussion

In contrast to many other solid cancer types, treatment of pancreatic ductal adenocarcinoma (PDAC) over the last twenty years has been by far less successful. Consequently, despite its comparably low incidence, PDAC is the fourth leading cause of cancer-related deaths and is expected to be the second most cancer-related death in the western world by 2020. Although substantial research efforts in investigating pancreatic carcinogenesis have broadened our knowledge and many molecular mechanism essential for PDAC carcinogenesis have been described, efficient therapies are still missing and targeted therapies so far have been largely disappointing [14, 31]. However, an improved understanding of the multistep process that leads to malignancy through molecular profiling at the genetic and epigenetic level has revealed regulatory pathways, which drive tumour development, differentiation and growth. Because of their early and high prevalence, *Kras* mutations are considered a key determinant in the initiation of pancreatic carcinogenesis. Although conditional activation of just mutated oncogenic *Kras* specifically in the pancreas is necessary for the development of invasive and metastatic PDAC, it is not sufficient and the transformation of additional assistant molecules and pathways is required [41] [100]. It is of pivotal importance to improve our knowledge of every single aspect of this fatal disease to finally improve its treatment, also because pharmacologic targeting of activated RAS proteins has been unsuccessful to date. As a contribution to the overall goal, aim of this thesis was to unveil the contribution of Igf1R and IR signalling as an additional part of the complex signalling network, which is responsible for the progression of pancreatic tumourigenesis.

4.1 Progression to PDAC requires Igf1R and IR signalling

Insulin and insulin-like growth factors (IGFs) are potent mitogens, and the hypothesis that their receptors are important therapeutic targets in oncology has received considerable attention. Numerous clinical and epidemiological studies indicate a relation between circulating levels of insulin and IGFs and cancer risk [101] [102]. Furthermore, it has been shown that interfering in this signalling cascade had inhibitory effects on neoplastic behaviour and that a requirement for

presence of the Igf1R and IR for transforming activity of a variety of oncogenes exists [103]. Especially alterations in the IGF-I signalling pathway have been described over the years in multiple tumours, including osteosarcomas, gynaecological, gastrointestinal, prostate and lung cancers [104] [105]. Animal and human studies have demonstrated that IGF-I functions not only as an endocrine hormone but also as a paracrine and autocrine hormone, being produced by the tumour cells and interacting with the Igf1R, which is frequently overexpressed in tumours [72]. The link between insulin and cancer was created many years ago through epidemiological studies reporting that insulin therapy and insulin secretagogues may increase cancer risk [106] [107]. Obese individuals and those with type 2 diabetes were at a higher risk of dying from various cancers when compared with those with a normal body mass index and those without diabetes [108] [109]. Insulin resistance in metabolic tissues, such as muscle, liver, and adipose tissue, occurs in obesity and type 2 diabetes. In an attempt to overcome the peripheral insulin resistance, a compensatory hyperinsulinemia develops [110]. Some cancer cells have increased insulin receptor content, and in the setting of hyperinsulinemia, certain tumours may demonstrate increased activation of IR signalling pathways [111] [112]. The roles of the closely related IGF-I, IGF-II and their receptor interactions in cancer have also been extensively studied. Insulin indirectly increases hepatic IGF-I production [113]. In addition, hyperinsulinemia may increase the quantity of bioavailable IGF-I by directly or indirectly decreasing levels of IGF binding proteins [114, 115]. Lower levels of these binding proteins result in more unbound IGF-I that is free to interact with Igf1R. Additionally, many tumours overexpress IGF-II, which also signals through the Igf1R and the IR [116] [117] [118]. Notably different interactions between components of the highly related signalling pathways were observed in tumourigenesis, although functions of Igf1R and IR are rather distinct in normal, healthy tissue. In a metaplastic state receptors might lose these signalling distinctions and could start performing very similar actions. For example in human PDAC cell lines, increased expression and mitogenic signalling via high affinity IR has been reported [80]. This change in ratio of insulin receptor expression has been reported in cancer and is thought to profoundly influence the cellular response to insulin and IGFs. In addition to insulin, IR binds also IGF-II ligands and exposes the cell to strong growth promoting effects of IGFs [58]. Recent work in a mouse model of pancreatic neuroendocrine

cancer showed the IR indeed possesses functional redundancy with the Igf1R, thus conveying resistance to Igf1R targeted therapies [119]. The authors demonstrated that IR expression gradually increases from stage of hyperplastic lesions to tumour. Genetic ablation of IR led to impairment of tumour progression and sensitization of islet tumours to Igf1R targeted therapies. Notably, there is increasing evidence that IR is at least an as equal contributor as Igf1R in cancer signalling functions, but still parts of the whole picture are missing.

The predictably reproducible tumour onset and progression in the $Kras^{G12D}$ PDAC model has allowed to explore the *in vivo* functions of Igf1R and IR that affect the progression of preneoplastic lesions to PDAC. It was found that both human and murine preneoplastic lesions overexpress the Igf1R and the IR in early stages. The detection of the signal of both receptors decreases with higher stages but was still detectable in PDAC tissue and cells, indicating a requirement for these receptors rather in early stages of pancreatic tumourigenesis than in PDAC itself. Pancreatic ablation of one of the two receptors resulted in normal development of the mice, only the deletion of both receptors together showed an impaired phenotype with a hypomorphic pancreas and consequently digestion disturbance as cause for a restricted survival. Furthermore, not the lacking of the IR as supposed but that of Igf1R in the pancreas created glucose intolerance and secondary liver damage in the mouse models. Nevertheless it could be shown that $Kras^{G12D};Igf1R^{\Delta/\Delta}$ and $Kras^{G12D};IR^{\Delta/\Delta}$ mice have a clear reduction in PanIN formation compared to $Kras^{G12D}$ control animals. Surprisingly, the pancreas specific deletion of the Igf1R as well as of the IR resulted in a similar stop of PanIN progression in $Kras^{G12D}$ mice. The nearly absent proliferation of the existing PanINs in $Kras^{G12D};Igf1R^{\Delta/\Delta}$ and $Kras^{G12D};IR^{\Delta/\Delta}$ mice led not only to less PanIN formation in the pancreas of those animals but also to disruption of PDAC formation. Thus interference of the Igf1R or the IR signalling cascade in an oncogenic $Kras^{G12D}$ background could arrest PanIN formation and hinder the progression to PDAC through proliferation inhibition. An additional deletion or mutation of the tumour suppressor p53 could not reverse this phenotype as shown in $Kras^{G12D};p53^{R172H};Igf1R^{\Delta/\Delta}$, $Kras^{G12D};p53^{R172H};IR^{\Delta/\Delta}$ and $Kras^{G12D};p53^{\Delta/\Delta};IR^{\Delta/\Delta}$ mice. The similar results caused by the ablation of the Igf1R or the IR could be explained through a strong presence of Igf1R/IR hybrid receptors, detected in $Kras^{G12D}$ cells. These hybrid receptors are known to be highly overexpressed in

various tumour cells and specimens as a result of both Igf1R and IR overexpression [120] [121]. The lack of one receptor gene could impair the formation of those hybrid receptors and thus the proliferation and progression of PanINs in the respective mouse models. Taken as a whole, Igf1R and IR, most probably in a conformation of hybrid receptors are required for pancreatic tumourigenesis, which lies in their control of cellular proliferation of the neoplastic precursors.

## 4.2 Igf1R and IR signalling regulates activation of the PI3K/AKT pathway

Igf1R and IR signalling is mediated by a complex, highly integrated network that controls several processes. Despite their complete different functions in healthy cells, the downstream activation patterns of both receptors are of the same kind. When insulin, IGF-I or IGF-II bind to the extracellular α-chains of the Igf1R or IR, it results in homo or hetero dimerization of the receptor and auto phosphorylation of the intracellular juxta membrane tyrosine kinase domains, creating docking sites for adaptor proteins such as Insulin Receptor Substrate 1 (IRS1) and Src homology 2 domain containing (Shc) transforming protein [122]. IRS1 activates the p85 subunit of PI3K, which in turn phosphorylates membrane bound PIP_2 (Phosphatidylinositol 4,5-bisphosphate) to create PIP_3. PIP_3 recruits AKT to the membrane where it becomes activated to regulate cell metabolism, promote cell cycle progression, and inhibit pro-apoptotic signalling by impinging upon downstream targets including mTOR, BAD, and FOXO [123]. Shc recruits Grb2 and SOS proteins to activate RAS by stimulating GDP exchange for GTP [124]. Activated RAS triggers the classical MAPK pathway, characterized by the sequential activation of the kinases MEK and ERK. ERK activation leads to transcription of target genes necessary for cell proliferation, such as Cyclin D and Myc [125]. According to which of these pathways is just needed for the cell, they become activated by the two tyrosine kinases. Although a simple scheme of divergent cascades looks sufficient to explain Igf1R and IR signalling, the concept of critical nodes becomes apparent when one looks at the sheer number of gene and proteins that are involved for the different redundant actions.

Furthermore, these signalling pathways have recently shown to represent core-signalling drivers in pancreatic carcinogenesis and tumour maintenance [41, 92,

126]. Analysis of those downstream cascades revealed that $Kras^{G12D};Igf1R^{\Delta/\Delta}$ and $Kras^{G12D};IR^{\Delta/\Delta}$ mice had no differences in the phosphorylation levels of some of the major RAS-dependent signalling modules including phosphorylated ERK and STAT3 but showed a clear reduction of phosphorylated AKT. IHC analysis in $Kras^{G12D};Igf1R^{\Delta/\Delta}$ and $Kras^{G12D};IR^{\Delta/\Delta}$ mice showed preneoplastic lesions positive for phospho-ERK, but a decreased expression of phospho-AKT in these mice. The primary found decreased ERK activity in Western Blot analysis was due to less PanIN formation in these mouse models. Thus, blockade of PI3K/AKT signalling may be the responsible key event of the $Kras^{G12D};Igf1R^{\Delta/\Delta}$ and $Kras^{G12D};IR^{\Delta/\Delta}$ phenotype.

To functionally further address the role of MEK/ERK and PI3K/AKT as potential mediators of Igf1R/IR signalling, these downstream cascades were targeted using various transgenic mouse strains. These GEMMs with pancreas-specific activation of MEK/ERK signalling ($Mek1^{wt/LSL-DD}$ [49]) or conditional activation of the PI3K ($p110a^{wt/LSL-H1047R}$ [50]) show highly consistent development of PanIN and ADM lesions progressing to PDAC, comparable to the $Kras^{G12D}$ phenotype. Indeed the replacement of active oncogenic KRAS through a constitutively active PI3K in the pancreas of $Igf1R^{\Delta/\Delta}$ and $IR^{\Delta/\Delta}$ mice could reverse the halted PanIN formation and progression, observed in $Kras^{G12D};Igf1R^{\Delta/\Delta}$ and $Kras^{G12D};IR^{\Delta/\Delta}$ animals. Whereas the genetic activation of the MEK/ERK pathway resulted in the $Kras^{G12D}$ phenotype, the deletion of Igf1R or IR could reduce PanIN formation and progression in $Mek1^{wt/LSL-DD}$ animals. Subsequently only the downstream activation of the PI3K in $p110a^{H1047R};Igf1R^{\Delta/\Delta}$ and $p110a^{H1047R};IR^{\Delta/\Delta}$ mice was able to abolish the reduced phenotype caused by Igf1R and IR ablation. Additionally and most surprisingly $p110a^{H1047R};Igf1R^{\Delta/\Delta};IR^{\Delta/\Delta}$ mice were not showing a shortened lifespan, like it was the case for $Kras^{G12D};Igf1R^{\Delta/\Delta};IR^{\Delta/\Delta}$, $Igf1R^{\Delta/\Delta};IR^{\Delta/\Delta}$ and $Mek^{wt/LSL-DD};Igf1R^{\Delta/\Delta};IR^{\Delta/\Delta}$. The activation of the PI3K downstream of the Igf1R and IR is reversing the perturbed body and pancreas development of $Igf1R^{\Delta/\Delta};IR^{\Delta/\Delta}$ mice. These findings are showing the regulation of the PI3K pathway through the Igf1R/IR signalling and the necessity of this axis for PanIN formation and progression in GEMMs of PDAC. Another approach was showing the clear connection between EGFR and ERK activity, which presence was obligatory for the initiating events of the oncogenic $Kras^{G12D}$ activity [41]. Since there was already ADM and PanIN appearance in the $Kras^{G12D};Igf1R^{\Delta/\Delta}$ and $Kras^{G12D};IR^{\Delta/\Delta}$

mice, but no PDAC development in those mice, the Igf1R/IR-PI3K cascade could be more classified as progression pathway (Fig. 3.25). A dominant regulation of one pathway through one receptor does not exclude an interaction and activation of that with additive cascades. Moreover, activity pattern have to be considered more as networks than as single signalling cascades, with maybe special receptors being required for reaching a threshold of specific signal induction.
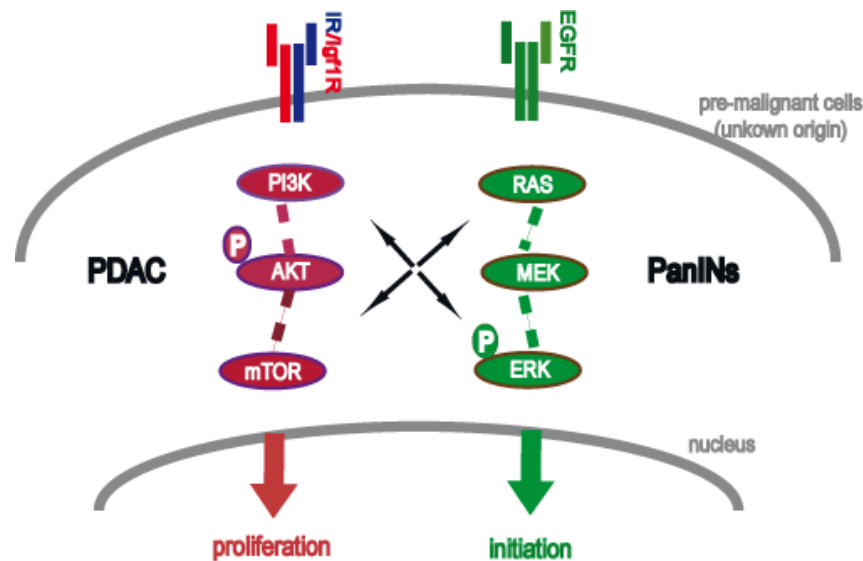
Figure 3.25 The Igf1R/IR-PI3K pathway is more responsible for the progression and the EGFR-MAPK cascade more for the initiation of *Kras*^{G12D} driven tumourigenesis.

4.3 Parallel inhibition of Igf1R and IR signalling reduces tumour cell survival

Recently, the rapid advances of molecular biology allowed an in-depth understanding of pancreatic carcinogenesis, and there are many attempts to modulate signal pathways using specific targeting agents. However, most of them have so far failed to improve survival significantly. The real challenge is now how these impressive advances of molecular biology could be successfully integrated into better clinical implications. For example although the data suggests that the Igf1R system might be important for PDAC, clinical trials performed with Igf1R blocking antibodies were largely disappointing [127]. Very recently the termination of a large Phase III clinical trial in patients with metastatic PDAC treated with the Igf1R blocking antibody ganitumab (AMG 479) in combination with standard of care chemotherapy gemcitabine was due to no significant improvement in the overall survival of patients [128]. One of the potential reasons for failure of Igf1R

targeted therapies is the co-existence of the structurally and functionally related IR in cancer. Another main cause could be the necessity of a personalized treatment approach, with the aim to distinguish between tumours being addicted to the targeted signalling. *In vitro* experiments with the Igf1R/IR inhibitor BMS-754807 affirmed reduced cell viability of several treated cell lines derived from *Kras*[G12D] mice, but with different sensitivities to the inhibitor. *Kras*[G12D] cells with a high phospho-AKT expression showed increased sensitivity to the inhibitor compared to cells with high expression of active ERK and AKT. In opposite, *Kras*[G12D] cells with high phospho-ERK expression were less sensitive to BMS-754807 compared to cells expressing high phospho-ERK levels. Consequently, PDACs with high AKT activity could be more sensitive to Igf1R/IR targeted therapies than tumours with a high phospho-ERK presence. An additional important factor could be the simultaneous blockage of the Igf1R and the IR, since previous therapeutic strategies avoid blocking the last one, worrying about a hyperglycaemia as a severe side effect [127]. But the data indicates more a metabolic impairment as result of the Igf1R deletion and not of the IR ablation. Consequently, the characterization of relevant pathways in the tumour and the additional inhibition of the highly homologous IR could improve Igf1R targeted therapies.

4.4 Conclusion

The aggressiveness of PDAC is mirrored in the complexity and redundancy of the molecular pathways activated during the carcinogenic and metastatic process. It is to be doubted that even a successful targeting of IR/Igf1R will be a magic bullet in PDAC therapy. Increasing evidence supports the contribution of insulin to pancreatic carcinogenesis. Insulin seems to be more significant than thought so far and should be considered with more attention. Further detailed work will be needed to define the clinical scenario, state of disease, and potential subgroups that may benefit from Igf1R/IR targeting. Suitable and sophisticated research approaches and identification of those disturbances that convert important metabolic regulators to malicious cancer promoting molecules remain a central task to the scientific field.

5. **Summary**

Aim of this thesis was to analyse the specific role of the (Insulin-like growth factor 1 receptors) Igf1R and the insulin receptor (IR), together with the involved signalling pathways in initiation and progression of pancreatic ductal adenocarcinoma (PDAC) using various genetically engineered mouse models (GEMM). PDAC is still one of the deadliest malignancies of the western world with a 5-year survival rate lower than 5%. Key factors include late diagnosis, early metastatic spread and especially a high intrinsic therapy resistance. To improve therapeutic strategies and thus prognosis of patients with PDAC new target structures have to been identified.

Receptor tyrosine kinases are playing a central role in pancreatic tumourigenesis. The Igf1R tyrosine kinase is the main mediator of the protumourigenic effects of IGF-I/II and inhibitors of the Igf1R signalling pathways are currently being tested in a number of therapeutic clinical trials, however with limited success. Furthermore, there is increasing evidence for an association of the highly homologous IR with tumourigenesis, such as hyperinsulinaemia as major risk factor. To closer characterize the function of both receptors in PDAC, GEMMs were generated with a pancreas specific deletion of Igf1R and/or IR. By use of well-established GEMMs, for example with pancreas specific activation of the *Kras* oncogene all stages of PDAC from early preneoplastic lesions to cancer in terminal stages could be examined. The genetic ablation of Igf1R and IR in the pancreas of $Kras^{G12D}$ mice induced an obvious reduction of preneoplastic lesion formation and no progression to invasive PDAC. The underlying cause is the necessity of these two receptors for the proliferation and progression of lesions in early stages of pancreatic tumourigenesis. Oncogenic *Kras* is activating a variety of signalling cascades, including the Raf/MEK/ERK and the PI3K/AKT pathway. Analysis of these downstream signalling cascades and expression studies revealed a strong regulation of the PI3K by Igf1R/IR hybrid receptors. Additional studies with different GEM models confirmed the dependency of the PI3K/AKT pathway from both Igf1R and IR for precursor lesion progression to PDAC, whereas the Raf/MEK/ERK pathway seems rather responsible for the initiation. The upstream Igf1- and insulin receptors could represent a necessary connection of these cascades. This study thus adds further insight into the different relevant signalling pathways of PDAC working in a close network rather than a linear activity pattern, which may have therapeutic consequences.

6. References

1. Bardeesy, N. and R.A. DePinho, *Pancreatic cancer biology and genetics.* Nat Rev Cancer, 2002. **2**(12): p. 897-909.

2. Edlund, H., *Pancreatic organogenesis--developmental mechanisms and implications for therapy.* Nat Rev Genet, 2002. **3**(7): p. 524-32.

3. Slack, J.M., *Developmental biology of the pancreas.* Development, 1995. **121**(6): p. 1569-80.

4. Offield, M.F., et al., *PDX-1 is required for pancreatic outgrowth and differentiation of the rostral duodenum.* Development, 1996. **122**(3): p. 983-95.

5. Krapp, A., et al., *The bHLH protein PTF1-p48 is essential for the formation of the exocrine and the correct spatial organization of the endocrine pancreas.* Genes Dev, 1998. **12**(23): p. 3752-63.

6. Pan, F.C. and C. Wright, *Pancreas organogenesis: from bud to plexus to gland.* Dev Dyn, 2011. **240**(3): p. 530-65.

7. Mulkeen, A.L., P.S. Yoo, and C. Cha, *Less common neoplasms of the pancreas.* World J Gastroenterol, 2006. **12**(20): p. 3180-5.

8. Toll, A.D., R.H. Hruban, and S.Z. Ali, *Acinar cell carcinoma of the pancreas: clinical and cytomorphologic characteristics.* Korean J Pathol, 2013. **47**(2): p. 93-9.

9. Jemal, A., et al., *Cancer statistics, 2009.* CA Cancer J Clin, 2009. **59**(4): p. 225-49.

10. Hidalgo, M., *Pancreatic cancer.* N Engl J Med, 2010. **362**(17): p. 1605-17.

11. Neoptolemos, J.P., et al., *Adjuvant chemotherapy with fluorouracil plus folinic acid vs gemcitabine following pancreatic cancer resection: a randomized controlled trial.* JAMA, 2010. **304**(10): p. 1073-81.

12. Siegel, R., D. Naishadham, and A. Jemal, *Cancer statistics, 2012.* CA Cancer J Clin, 2012. **62**(1): p. 10-29.

13. Siveke, J.T. and R.M. Schmid, *Chromosomal instability in mouse metastatic pancreatic cancer--it's Kras and Tp53 after all.* Cancer Cell, 2005. **7**(5): p. 405-7.

14.   Mazur, P.K. and J.T. Siveke, *Genetically engineered mouse models of pancreatic cancer: unravelling tumour biology and progressing translational oncology.* Gut, 2012. **61**(10): p. 1488-500.

15.   Hezel, A.F., et al., *Genetics and biology of pancreatic ductal adenocarcinoma.* Genes Dev, 2006. **20**(10): p. 1218-49.

16.   Morris, J.P.t., S.C. Wang, and M. Hebrok, *KRAS, Hedgehog, Wnt and the twisted developmental biology of pancreatic ductal adenocarcinoma.* Nat Rev Cancer, 2010. **10**(10): p. 683-95.

17.   Brugge, W.R., et al., *Diagnosis of pancreatic cystic neoplasms: a report of the cooperative pancreatic cyst study.* Gastroenterology, 2004. **126**(5): p. 1330-6.

18.   Maitra, A., et al., *Precursors to invasive pancreatic cancer.* Adv Anat Pathol, 2005. **12**(2): p. 81-91.

19.   Aichler, M., et al., *Origin of pancreatic ductal adenocarcinoma from atypical flat lesions: a comparative study in transgenic mice and human tissues.* J Pathol, 2012. **226**(5): p. 723-34.

20.   Carriere, C., et al., *The Nestin progenitor lineage is the compartment of origin for pancreatic intraepithelial neoplasia.* Proc Natl Acad Sci U S A, 2007. **104**(11): p. 4437-42.

21.   De La, O.J., et al., *Notch and Kras reprogram pancreatic acinar cells to ductal intraepithelial neoplasia.* Proc Natl Acad Sci U S A, 2008. **105**(48): p. 18907-12.

22.   Takaori, K., et al., *Current topics on precursors to pancreatic cancer.* Adv Med Sci, 2006. **51**: p. 23-30.

23.   Hruban, R.H., et al., *Pancreatic intraepithelial neoplasia: a new nomenclature and classification system for pancreatic duct lesions.* Am J Surg Pathol, 2001. **25**(5): p. 579-86.

24.   Wagner, M., et al., *Curative resection is the single most important factor determining outcome in patients with pancreatic adenocarcinoma.* Br J Surg, 2004. **91**(5): p. 586-94.

25.   Burris, H.A., 3rd, et al., *Improvements in survival and clinical benefit with gemcitabine as first-line therapy for patients with advanced pancreas cancer: a randomized trial.* J Clin Oncol, 1997. **15**(6): p. 2403-13.

26.   Trouilloud, I., et al., *Medical treatment of pancreatic cancer: new hopes after 10 years of gemcitabine.* Clin Res Hepatol Gastroenterol, 2011. **35**(5): p. 364-74.

27. Schneider, G., et al., *Molecular biology of pancreatic cancer--new aspects and targets.* Anticancer Res, 2008. **28**(3A): p. 1541-50.

28. Hustinx, S.R., et al., *Concordant loss of MTAP and p16/CDKN2A expression in pancreatic intraepithelial neoplasia: evidence of homozygous deletion in a noninvasive precursor lesion.* Mod Pathol, 2005. **18**(7): p. 959-63.

29. Aguirre, A.J., et al., *Activated Kras and Ink4a/Arf deficiency cooperate to produce metastatic pancreatic ductal adenocarcinoma.* Genes Dev, 2003. **17**(24): p. 3112-26.

30. Rozenblum, E., et al., *Tumor-suppressive pathways in pancreatic carcinoma.* Cancer Res, 1997. **57**(9): p. 1731-4.

31. Hingorani, S.R., et al., *Trp53R172H and KrasG12D cooperate to promote chromosomal instability and widely metastatic pancreatic ductal adenocarcinoma in mice.* Cancer Cell, 2005. **7**(5): p. 469-83.

32. Hahn, S.A., et al., *DPC4, a candidate tumor suppressor gene at human chromosome 18q21.1.* Science, 1996. **271**(5247): p. 350-3.

33. Miyazono, K., *TGF-beta/SMAD signaling and its involvement in tumor progression.* Biol Pharm Bull, 2000. **23**(10): p. 1125-30.

34. Zavadil, J. and E.P. Bottinger, *TGF-beta and epithelial-to-mesenchymal transitions.* Oncogene, 2005. **24**(37): p. 5764-74.

35. Fleming, J.B., et al., *Molecular consequences of silencing mutant K-ras in pancreatic cancer cells: justification for K-ras-directed therapy.* Mol Cancer Res, 2005. **3**(7): p. 413-23.

36. Malumbres, M. and M. Barbacid, *RAS oncogenes: the first 30 years.* Nat Rev Cancer, 2003. **3**(6): p. 459-65.

37. Shaw, R.J. and L.C. Cantley, *Ras, PI(3)K and mTOR signalling controls tumour cell growth.* Nature, 2006. **441**(7092): p. 424-30.

38. Kolibaba, K.S. and B.J. Druker, *Protein tyrosine kinases and cancer.* Biochim Biophys Acta, 1997. **1333**(3): p. F217-48.

39. Giroux, V., J.C. Dagorn, and J.L. Iovanna, *A review of kinases implicated in pancreatic cancer.* Pancreatology, 2009. **9**(6): p. 738-54.

40. Takeuchi, K. and F. Ito, *Receptor tyrosine kinases and targeted cancer therapeutics.* Biol Pharm Bull, 2011. **34**(12): p. 1774-80.

41. Ardito, C.M., et al., *EGF receptor is required for KRAS-induced pancreatic tumorigenesis.* Cancer Cell, 2012. **22**(3): p. 304-17.

42. Moore, M.J., et al., *Erlotinib plus gemcitabine compared with gemcitabine alone in patients with advanced pancreatic cancer: a phase III trial of the National Cancer Institute of Canada Clinical Trials Group.* J Clin Oncol, 2007. **25**(15): p. 1960-6.

43. Hingorani, S.R., et al., *Preinvasive and invasive ductal pancreatic cancer and its early detection in the mouse.* Cancer Cell, 2003. **4**(6): p. 437-50.

44. Mazur, P.K., et al., *Identification of epidermal Pdx1 expression discloses different roles of Notch1 and Notch2 in murine Kras(G12D)-induced skin carcinogenesis in vivo.* PLoS One, 2010. **5**(10): p. e13578.

45. Bardeesy, N., et al., *Both p16(Ink4a) and the p19(Arf)-p53 pathway constrain progression of pancreatic adenocarcinoma in the mouse.* Proc Natl Acad Sci U S A, 2006. **103**(15): p. 5947-52.

46. Bardeesy, N., et al., *Smad4 is dispensable for normal pancreas development yet critical in progression and tumor biology of pancreas cancer.* Genes Dev, 2006. **20**(22): p. 3130-46.

47. Kojima, K., et al., *Inactivation of Smad4 accelerates Kras(G12D)-mediated pancreatic neoplasia.* Cancer Res, 2007. **67**(17): p. 8121-30.

48. Castellano, E. and J. Downward, *RAS Interaction with PI3K: More Than Just Another Effector Pathway.* Genes Cancer, 2011. **2**(3): p. 261-74.

49. Srinivasan, L., et al., *PI3 Kinase Signals BCR-Dependent Mature B Cell Survival.* Cell, 2009. **139**(3): p. 573-586.

50. Eser, S., et al., *Selective requirement of PI3K/PDK1 signaling for Kras oncogene-driven pancreatic cell plasticity and cancer.* Cancer Cell, 2013. **23**(3): p. 406-20.

51. Hankinson, S.E., et al., *Circulating concentrations of insulin-like growth factor-I and risk of breast cancer.* Lancet, 1998. **351**(9113): p. 1393-6.

52. Chan, K. and E.M. Spencer, *Megakaryocytes endocytose insulin-like growth factor (IGF) I and IGF-binding protein-3: a novel mechanism directing them into alpha granules of platelets.* Endocrinology, 1998. **139**(2): p. 559-65.

53. Belfiore, A., et al., *Insulin receptor isoforms and insulin receptor/insulin-like growth factor receptor hybrids in physiology and disease.* Endocr Rev, 2009. **30**(6): p. 586-623.

54. Pollak, M., *The insulin and insulin-like growth factor receptor family in neoplasia: an update.* Nat Rev Cancer, 2012. **12**(3): p. 159-69.

55. Pollak, M., *The insulin receptor/insulin-like growth factor receptor family as a therapeutic target in oncology.* Clin Cancer Res, 2012. **18**(1): p. 40-50.

56. Gallagher, E.J. and D. LeRoith, *Minireview: IGF, Insulin, and Cancer.* Endocrinology, 2011. **152**(7): p. 2546-51.

57. Yee, D., *Insulin-like growth factor receptor inhibitors: baby or the bathwater?* J Natl Cancer Inst, 2012. **104**(13): p. 975-81.

58. Frasca, F., et al., *Insulin receptor isoform A, a newly recognized, high-affinity insulin-like growth factor II receptor in fetal and cancer cells.* Mol Cell Biol, 1999. **19**(5): p. 3278-88.

59. Trajkovic-Arsic, M., E. Kalideris, and J.T. Siveke, *The role of insulin and IGF system in pancreatic cancer.* J Mol Endocrinol, 2013. **50**(3): p. R67-74.

60. Brogiolo, W., et al., *An evolutionarily conserved function of the Drosophila insulin receptor and insulin-like peptides in growth control.* Curr Biol, 2001. **11**(4): p. 213-21.

61. Belfiore, A., *The role of insulin receptor isoforms and hybrid insulin/IGF-I receptors in human cancer.* Curr Pharm Des, 2007. **13**(7): p. 671-86.

62. Pollak, M., *Insulin, insulin-like growth factors and neoplasia.* Best Pract Res Clin Endocrinol Metab, 2008. **22**(4): p. 625-38.

63. Brogiolo, G., J. Flammer, and I.O. Haefliger, *Latanoprost is a vasoconstrictor in isolated porcine ciliary arteries.* Klin Monbl Augenheilkd, 2001. **218**(5): p. 373-5.

64. Ohlsson, C., et al., *The role of liver-derived insulin-like growth factor-I.* Endocr Rev, 2009. **30**(5): p. 494-535.

65. Yu, H. and T. Rohan, *Role of the insulin-like growth factor family in cancer development and progression.* J Natl Cancer Inst, 2000. **92**(18): p. 1472-89.

66. Kulkarni, R.N., et al., *Tissue-specific knockout of the insulin receptor in pancreatic beta cells creates an insulin secretory defect similar to that in type 2 diabetes.* Cell, 1999. **96**(3): p. 329-39.

67. Bao, Y., et al., *Dietary insulin load, dietary insulin index, and risk of pancreatic cancer.* Am J Clin Nutr, 2011. **94**(3): p. 862-8.

68.	Cui, Y. and D.K. Andersen, *Diabetes and pancreatic cancer.* Endocr Relat Cancer, 2012. **19**(5): p. F9-F26.

69.	Hakam, A., et al., *Coexpression of IGF-1R and c-Src proteins in human pancreatic ductal adenocarcinoma.* Dig Dis Sci, 2003. **48**(10): p. 1972-8.

70.	Valsecchi, M.E., et al., *Epidermal growth factor receptor and insulinlike growth factor 1 receptor expression predict poor survival in pancreatic ductal adenocarcinoma.* Cancer, 2012. **118**(14): p. 3484-93.

71.	Karna, E., et al., *Serum and tissue level of insulin-like growth factor-I (IGF-I) and IGF-I binding proteins as an index of pancreatitis and pancreatic cancer.* Int J Exp Pathol, 2002. **83**(5): p. 239-45.

72.	Dong, X., et al., *Insulin-like growth factor axis gene polymorphisms modify risk of pancreatic cancer.* Cancer Epidemiol, 2012. **36**(2): p. 206-11.

73.	Bergmann, U., et al., *Insulin-like growth factor I overexpression in human pancreatic cancer: evidence for autocrine and paracrine roles.* Cancer Res, 1995. **55**(10): p. 2007-11.

74.	Tomizawa, M., et al., *Insulin-like growth factor-I receptor in proliferation and motility of pancreatic cancer.* World J Gastroenterol, 2010. **16**(15): p. 1854-8.

75.	Williams, J.A. and I.D. Goldfine, *The insulin-pancreatic acinar axis.* Diabetes, 1985. **34**(10): p. 980-6.

76.	Barreto, S.G., et al., *The islet-acinar axis of the pancreas: more than just insulin.* Am J Physiol Gastrointest Liver Physiol, 2010. **299**(1): p. G10-22.

77.	Butler, A.E., et al., *Adaptive changes in pancreatic beta cell fractional area and beta cell turnover in human pregnancy.* Diabetologia, 2010. **53**(10): p. 2167-76.

78.	Asano, T., et al., *Insulin receptor substrate is a mediator of phosphoinositide 3-kinase activation in quiescent pancreatic cancer cells.* Cancer Res, 2005. **65**(20): p. 9164-8.

79.	Rozengurt, E., J. Sinnett-Smith, and K. Kisfalvi, *Crosstalk between insulin/insulin-like growth factor-1 receptors and G protein-coupled receptor signaling systems: a novel target for the antidiabetic drug metformin in pancreatic cancer.* Clin Cancer Res, 2010. **16**(9): p. 2505-11.

80.	Fisher, W.E., L.G. Boros, and W.J. Schirmer, *Insulin promotes pancreatic cancer: evidence for endocrine influence on exocrine pancreatic tumors.* J Surg Res, 1996. **63**(1): p. 310-3.

81.   Appleman, V.A., et al., *KRAS(G12D)- and BRAF(V600E)-induced transformation of murine pancreatic epithelial cells requires MEK/ERK-stimulated IGF1R signaling.* Mol Cancer Res, 2012. **10**(9): p. 1228-39.

82.   Tanno, S., et al., *AKT activation up-regulates insulin-like growth factor I receptor expression and promotes invasiveness of human pancreatic cancer cells.* Cancer Res, 2001. **61**(2): p. 589-93.

83.   Weroha, S.J. and P. Haluska, *IGF-1 receptor inhibitors in clinical trials--early lessons.* J Mammary Gland Biol Neoplasia, 2008. **13**(4): p. 471-83.

84.   Malaguarnera, R. and A. Belfiore, *The insulin receptor: a new target for cancer therapy.* Front Endocrinol (Lausanne), 2011. **2**: p. 93.

85.   Kawaguchi, Y., et al., *The role of the transcriptional regulator Ptf1a in converting intestinal to pancreatic progenitors.* Nat Genet, 2002. **32**(1): p. 128-34.

86.   Olive, K.P., et al., *Mutant p53 gain of function in two mouse models of Li-Fraumeni syndrome.* Cell, 2004. **119**(6): p. 847-60.

87.   Marino, S., et al., *Induction of medulloblastomas in p53-null mutant mice by somatic inactivation of Rb in the external granular layer cells of the cerebellum.* Genes Dev, 2000. **14**(8): p. 994-1004.

88.   Kloting, N., et al., *Autocrine IGF-1 action in adipocytes controls systemic IGF-1 concentrations and growth.* Diabetes, 2008. **57**(8): p. 2074-82.

89.   Bruning, J.C., et al., *A muscle-specific insulin receptor knockout exhibits features of the metabolic syndrome of NIDDM without altering glucose tolerance.* Mol Cell, 1998. **2**(5): p. 559-69.

90.   Srinivasan, L., et al., *PI3 kinase signals BCR-dependent mature B cell survival.* Cell, 2009. **139**(3): p. 573-86.

91.   Malaguarnera, R., et al., *Insulin receptor isoforms and insulin-like growth factor receptor in human follicular cell precursors from papillary thyroid cancer and normal thyroid.* J Clin Endocrinol Metab, 2011. **96**(3): p. 766-74.

92.   Siveke, J.T., et al., *Concomitant pancreatic activation of Kras(G12D) and Tgfa results in cystic papillary neoplasms reminiscent of human IPMN.* Cancer Cell, 2007. **12**(3): p. 266-79.

93.   Baker, J., et al., *Role of insulin-like growth factors in embryonic and postnatal growth.* Cell, 1993. **75**(1): p. 73-82.

94.   Belfiore, A. and R. Malaguarnera, *Insulin receptor and cancer.* Endocr Relat Cancer, 2011. **18**(4): p. R125-47.

95.   Lesina, M., et al., *Stat3/Socs3 activation by IL-6 transsignaling promotes progression of pancreatic intraepithelial neoplasia and development of pancreatic cancer.* Cancer Cell, 2011. **19**(4): p. 456-69.

96.   Fukuda, A., et al., *Stat3 and MMP7 contribute to pancreatic ductal adenocarcinoma initiation and progression.* Cancer Cell, 2011. **19**(4): p. 441-55.

97.   Munshi, S., et al., *Structure of apo, unactivated insulin-like growth factor-1 receptor kinase at 1.5 A resolution.* Acta Crystallogr D Biol Crystallogr, 2003. **59**(Pt 10): p. 1725-30.

98.   Carboni, J.M., et al., *BMS-754807, a small molecule inhibitor of insulin-like growth factor-1R/IR.* Mol Cancer Ther, 2009. **8**(12): p. 3341-9.

99.   Kolb, E.A., et al., *Initial testing (stage 1) of the IGF-1 receptor inhibitor BMS-754807 by the pediatric preclinical testing program.* Pediatr Blood Cancer, 2011. **56**(4): p. 595-603.

100.   Heid, I., et al., *Early requirement of Rac1 in a mouse model of pancreatic cancer.* Gastroenterology, 2011. **141**(2): p. 719-30, 730 e1-7.

101.   Chan, J.M., et al., *Plasma insulin-like growth factor-I and prostate cancer risk: a prospective study.* Science, 1998. **279**(5350): p. 563-6.

102.   Ma, J., et al., *Prediagnostic body-mass index, plasma C-peptide concentration, and prostate cancer-specific mortality in men with prostate cancer: a long-term survival analysis.* Lancet Oncol, 2008. **9**(11): p. 1039-47.

103.   Sell, C., et al., *IGF-1 receptor levels and the proliferation of young and senescent human fibroblasts.* Biochem Biophys Res Commun, 1993. **194**(1): p. 259-65.

104.   de Ostrovich, K.K., et al., *Paracrine overexpression of insulin-like growth factor-1 enhances mammary tumorigenesis in vivo.* Am J Pathol, 2008. **173**(3): p. 824-34.

105.   Huang, Y.F., et al., *Clinical implications of insulin-like growth factor 1 system in early-stage cervical cancer.* Br J Cancer, 2008. **99**(7): p. 1096-102.

106.   Hemkens, L.G., et al., *Risk of malignancies in patients with diabetes treated with human insulin or insulin analogues: a cohort study.* Diabetologia, 2009. **52**(9): p. 1732-44.

107. Currie, C.J., C.D. Poole, and E.A. Gale, *The influence of glucose-lowering therapies on cancer risk in type 2 diabetes.* Diabetologia, 2009. **52**(9): p. 1766-77.

108. Calle, E.E., et al., *Overweight, obesity, and mortality from cancer in a prospectively studied cohort of U.S. adults.* N Engl J Med, 2003. **348**(17): p. 1625-38.

109. Coughlin, S.S., et al., *Diabetes mellitus as a predictor of cancer mortality in a large cohort of US adults.* Am J Epidemiol, 2004. **159**(12): p. 1160-7.

110. Reaven, G.M., *Pathophysiology of insulin resistance in human disease.* Physiol Rev, 1995. **75**(3): p. 473-86.

111. Novosyadlyy, R., et al., *Insulin-mediated acceleration of breast cancer development and progression in a nonobese model of type 2 diabetes.* Cancer Res, 2010. **70**(2): p. 741-51.

112. Papa, V., et al., *Elevated insulin receptor content in human breast cancer.* J Clin Invest, 1990. **86**(5): p. 1503-10.

113. Amiel, S.A., et al., *Effect of diabetes and its control on insulin-like growth factors in the young subject with type I diabetes.* Diabetes, 1984. **33**(12): p. 1175-9.

114. Leung, K.C., et al., *Insulin regulation of human hepatic growth hormone receptors: divergent effects on biosynthesis and surface translocation.* J Clin Endocrinol Metab, 2000. **85**(12): p. 4712-20.

115. Frystyk, J., et al., *Free insulin-like growth factors in human obesity.* Metabolism, 1995. **44**(10 Suppl 4): p. 37-44.

116. Wu, H.K., et al., *Relaxation of imprinting of human insulin-like growth factor II gene, IGF2, in sporadic breast carcinomas.* Biochem Biophys Res Commun, 1997. **235**(1): p. 123-9.

117. Zhao, R., et al., *Loss of imprinting of the insulin-like growth factor II (IGF2) gene in esophageal normal and adenocarcinoma tissues.* Carcinogenesis, 2009. **30**(12): p. 2117-22.

118. Murphy, S.K., et al., *Frequent IGF2/H19 domain epigenetic alterations and elevated IGF2 expression in epithelial ovarian cancer.* Mol Cancer Res, 2006. **4**(4): p. 283-92.

119. Ulanet, D.B., et al., *Insulin receptor functionally enhances multistage tumor progression and conveys intrinsic resistance to IGF-1R targeted therapy.* Proc Natl Acad Sci U S A, 2010. **107**(24): p. 10791-8.

120. Kim, J.G., et al., *Heterodimerization of glycosylated insulin-like growth factor-1 receptors and insulin receptors in cancer cells sensitive to anti-IGF1R antibody.* PLoS One, 2012. **7**(3): p. e33322.

121. Belfiore, A., et al., *Insulin/IGF-I hybrid receptors play a major role in IGF-I signaling in thyroid cancer.* Biochimie, 1999. **81**(4): p. 403-7.

122. Samani, A.A., et al., *The role of the IGF system in cancer growth and metastasis: overview and recent insights.* Endocr Rev, 2007. **28**(1): p. 20-47.

123. Kooijman, R., *Regulation of apoptosis by insulin-like growth factor (IGF)-I.* Cytokine Growth Factor Rev, 2006. **17**(4): p. 305-23.

124. Ryan, P.D. and P.E. Goss, *The emerging role of the insulin-like growth factor pathway as a therapeutic target in cancer.* Oncologist, 2008. **13**(1): p. 16-24.

125. Pratilas, C.A. and D.B. Solit, *Targeting the mitogen-activated protein kinase pathway: physiological feedback and drug response.* Clin Cancer Res, 2010. **16**(13): p. 3329-34.

126. Mazur, P.K., et al., *Notch2 is required for progression of pancreatic intraepithelial neoplasia and development of pancreatic ductal adenocarcinoma.* Proc Natl Acad Sci U S A, 2010. **107**(30): p. 13438-43.

127. Rieder, S., et al., *Insulin-like growth factor signaling as a therapeutic target in pancreatic cancer.* Anticancer Agents Med Chem, 2011. **11**(5): p. 427-33.

128. Kindler, H.L., et al., *A randomized, placebo-controlled phase 2 study of ganitumab (AMG 479) or conatumumab (AMG 655) in combination with gemcitabine in patients with metastatic pancreatic cancer.* Ann Oncol, 2012. **23**(11): p. 2834-42.

7. **Appendix**

ADM	Acinar ductal metaplasia
AKT	V-akt murine thymoma viral oncogene homolog
BAD	Bcl-2 Associated Death
Bp	Base pairs
CK	Creatine kinase
DMEM	Dulbecco's Modified Eagle's Medium
EDTA	Ethylendiamintetraacetat
EGFR	Epidermal growth factor receptor
EGF	Epidermal growth factor
ELISA	Enzyme Linked Immunosorbent Assay
EMT	Epidermal to mesenchymal transmission
ERK	Extracellular signal-related protein kinase
FCS	Fetal calf serum
FFPE	Formalin-fixed, paraffin- embedded
FOXO	Forkhead box class O
GEMM	Genetically engineered mouse model
GDP	Guanosine diphosphate
GTP	Glutamate pyruvate transaminase
H & E	Hematoxylin and eosin
Igf1R	Insulin-like growth factor 1 receptor
IGF	Insulin-like growth factor
IR	Insulin receptor
IRS1	Insulin receptor substrate 1
IHC	Immunohistochemistry
IPMN	Intraductal papillary mucinous neoplasia
KRAS	Kirsten-Ras
LDH	Lactate dehydrogenase
LSL	Lox-Stop-Lox
MAPK	Mitogen activated protein kinase

MCN	Mucinous cystic neoplasia
MEK	Mitogen activated protein kinase kinase
MDM2	Mouse double minute 2 homolog
mTOR	Mammalian target of Rapamycin
NDLB	Non denaturating lysis buffer
NF-κB	Nuclear factor 'kappa-light-chain-enhancer' of activated B - cells
PanIN	Pancreatic intraepithelial neoplasia
PBS	Phosphate buffered saline
PDAC	Pancreatic ductal adenocarcinoma
PDVF	Polyvinylidene difluoride
Pdx1	Pancreatic and duodenal homeobox 1
PET	Pancreatic endocrine tumour
PI3K	Phosphoinositid-3-Kinase
PIP	Phosphatidylinositol phosphate
Ptf1a	Pancreas specific transcription factor, 1a
RAF	Rat fibrosarcoma
RAS	Rat sarcoma
Rb	Retinoblastoma
RTK	Receptor tyrosine kinase
RT-PCR	Reverse transcription-Polymerase-chain reaction
SDS-PAGE	Sodium dodecyl sulfate polyacrylamide gel electrophoresis
SOS	Son of sevenless
STAT3	Signal transducer and activator of transcription 3
TBS-T	Mixture of Tris-Buffered Saline and Tween 20
TGF-β	Transforming growth factor β

7.2 Acknowledgements - Danksagungen